Two Leucine-rich receptor kinases mediate signaling linking cell wall biosynthesis and ACC synthase in Arabidopsis and possible downstream elements in the pathway

Shouling Xu

A dissertation submitted to the faculty of the University of North Carolina at Chapel Hill in partial fulfillment of the requirements for the degree of Doctor of Philosophy in the Department of Biology.

Chapel Hill
2008

Approved by

Advisor: Joseph J. Kieber

Jeff Dangl

Sarah Liljegren

Jason Reed

Gregory Copenhaver

ABSTRACT

Shouling Xu: Two Leucine-rich receptor kinases mediate signaling linking cell wall biosynthesis and ACC synthase in Arabidopsis and possible downstream elements in the pathway

(Under the direction Dr. Joseph J. Kieber)

The cell wall is essential for plants. In an elongating cell, the cellulose microfibrils are wrapped transversely around the cell, thus allowing longitudinal expansion but restricting lateral expansion. The signaling pathways that regulate cell wall biosynthesis in response to developmental and environmental cues are still poorly understood. I describe the cloning and characterization of two *Arabidopsis thaliana* LRR receptor-like kinases, FEI1 and FEI2, that act as positive regulators of cell wall biosynthesis. Mutations in *FEI1* and *FEI2* disrupt anisotropic expansion and the synthesis of cell wall polymers, and act additively with inhibitors or mutations disrupting cellulose biosynthesis. In addition, I demonstrate that FEI1 is an active protein kinase; however, a kinase-inactive version of FEI1 was able to fully complement the *fei1 fei2* mutant, suggesting intrinsic kinase activity is not required for FEI function in roots. The expansion defect in *fei1 fei2* roots was suppressed by inhibition of ACC synthase, an enzyme that converts Ado-Met to ACC in ethylene biosynthesis, but not by disruption of the ethylene response pathway. Furthermore, the FEI proteins interact directly with ACC synthase. These results suggest that the FEI proteins define a novel signaling pathway that regulates cell wall function, likely via an ACC-mediated signal. To further our understanding of the FEI pathway in

mediating cell wall biosynthesis, a suppressor screen was carried out and nine suppressors (*shou1-shou8*) which represent mutation in eight different genes or complementation groups have been identified. Two suppressors have been further studied. *shou1* was mapped to bottom arm of chromosome 5 and found to encode a pentatricopeptide repeat protein. In addition, two alleles of *shou2* have been identified and mapped to a 47kb region on the upper arm of chromosome 1. Paradoxically, *shou2* also inhibits root hair elongation. These studies have uncovered a novel signaling pathway regulating cell wall biosynthesis.

Dedicated to my husband, Weimin, and to my parents, for their unconditional love and support

Acknowledgement

Looking back on my Ph.D journey, I feel that I have been extremely fortunate. I love my projects, my colleagues, my advisor, and Chapel Hill, a second hometown in my heart. I am deeply indebted to the following people. Without them, I would never have been able to finish this dissertation.

First and foremost I thank my husband, Weimin, who has provided so much love and support during these years. Thank you for all your patience and tolerance. This dissertation is our achievement. We have been apart for so long and I am blessed that we are still together. I am looking forward to moving with you and spending every day with you all my life!

To Cris, thank you for all your help, advice, time, and love. Although we have had small discrepancies, we have much more in common. I really enjoyed getting to know you over the years. Thank you for your support.

To Wenjing, Gyeongmee, Blaire and Tracy. It has been so much fun spending time with you in the office. You girls made my life much happier. Blaire, thank you for helping me with the thesis.

To Fer, Jason, Monica, Maureen, and Chaiyi. Fer and Jason, thank you for not only helping me with experiments, but also with all the small tasks that move my experiments forward, such as opening the lids of the bottles. Monica, thank you for ordering equipment for me and organizing the lab. Maureen, you are such a unique person. Thank you for your insightful writing suggestions. I have learned a lot from you. Chaiyi, I love your cooking. Thank you for your company in the later hours whenever everyone is gone home.

To Bridey, Veronica, Claire, Aaron, Jenn, Hyunsook, Jean and Jennifer. Bridey, you always impress me with your style and your wit. Veronica, thank you for all the kindness and help when I joined the lab. Claire, whenever I read Jane Austin's stories, I cannot help thinking about you. Aaron, it was a lot of fun sitting next to you listening to your jokes and humor. You are such a nice guy and an optimistic person. Jenn, I have always been impressed by your discipline and intelligence. Thank you for all the suggestions and help. Hyunsook, you are such an organized person and I have learned a lot from you. Jean, thank you for your help and your good looks. Jennifer, thank you for your help with everything.

To Mike and Alicia. Mike, you are such a super undergraduate. I was extremely lucky to have you work with me. Thank you for tolerating me during my little tyranny. By training you, I have learned a lot. You were so fun to work with. Alicia, you were a great undergraduate to work with and a great technician in the lab.

There are too many people to mention personally but I must, however, mention a few special people. First, I have to mention Fredrick, who helped me to start in the Kieber lab. I also want to thank Paul and Sarah in the Reed lab for suggestions on genetic mapping and tissue fixing, respectively. I would like to thank Zhiyong, Aijuan, David, Eui Hwan, and Yijian in the Dangl lab for help and advice in protein interactions. I also want to thank Yujin for his expertise in flower development. In addition, I would like to thank Jingui, Jirong and Yashwanti in Jones lab for their help. I would like to thank Mike and Jon for making soil. Jon, thank you for your plants and vegetables.

I would like to thank a lot of my friends who have fed me, comforted me, and helped me in the last six years. To Shun, Ying, Youjun, Keqi and Liyan, I love you girls so much! I would also like to thank my host family, Carol, Ross, and Rachel, who have given me love and support.

I also have to thank my committee members Jeff Dangl, Jason Reed, Greg Copenhaver and Sarah Liljegren. You have provided me enthusiasm, support and focus. Thank you for helping me get through this process.

Lastly and most importantly, I could not have done any of this if it wasn't for Joe Kieber. Thank you for your guidance, inspiration, patience and support over the years. I am extremely grateful to have you as an advisor. You have been a great advisor and a great person to work with. You always cheered me up when I felt down. You let me express ideas, disagree with you, and tolerate my "little" temper. Thank you for your numerous

efforts in training me to perform experiments well, be a good lab citizen, and improve my writing. I will always remember what you told me, “The more you work, the more luck you will get.”

TABLE OF CONTENTS

LIST OF TABLES

LIST OF FIGURES

LIST OF ABBREVIATIONS

ACC	1-aminocyclopropane-1-carboxylic acid
ACR4	Arabidopsis homolog of CRINKLY4
ACS	ACC synthase
acw1	*altered cell wall 1*
Ado-Met	S-adenosylmethionine
AGP	arabinogalactan protein
AIB	α-aminoisobutyric acid
AOA	aminnooxy-acetic acid
AtCSLD	Arabidopsis cellulose synthase-like (subfamily D)
Basta	glufosinate-ammonium
CAPS	cleaved amplified polymorphic sequence
cDNA	Complementary DNA
CDPK	Calcium-dependent protein kinase
CESA	cellulose synthase
cev1	*constitutive expression of VSP1*
cob	*cobra*
Col-0	Columbia
CR4	CRINKLY4
CrRLK1L	*Catharanthus roseus* protein-kinase-1-like
Dex	Dexamethasone
ein2	*ethylene insensitive 2*

eld1	*elongation defective 1*
eli1	*ecotopic lignin1*
EMS	ethyl methanesulfonate
EST	expressed *sequence* tag
eto	*ethylene overproduction*
etr1	*ethylene response 1*
fra2	*fragile fiber2*
gDNA	genomic DNA
GFP	green fluorescent protein
gl1	*glabrous1*
Gluc	5-Br-Cl-3-indolyl-β-D-glucuronic acid
GPI	glycosylphosphatidylinositol
GST	glutathione S-transferase
gun1	*genome-uncoupled 1*
HRGP	hydroxyproline-rich glycoproteins
irx2	*isoxaben resistant*
JA	jasmonic acid
K	lysine
kob1	*kobito1*
kor	*korrigan*
KSR	kinase suppressor of Ras
L	Liter
LecRK	lectin receptor protein kinases

Ler	Arabidopsis ecotype Landsberg
lit	*lion's tail*
LRR	leucine rich repeat
LRX	LRR-extensin
lue	*LUC-super-expressors*
MAP	mitogen activated protein kinase
MBP	myelin basic protein
MCP	1-methylcyclopropen
mor1	*microtubule organization 1*
MS	Murashige and Skoog salts
MYC	C-myc derived epitope tag
PCR	polymerase chain reaction
PPR	pentatricopeptide repeat protein
prc1	*procuste1*
R	arginine
RLK	receptor-like kinase
rsw2	*radial swelling2*
SE	standard error
sos	*salt over sensitive*
sub	*strubbelig*
T-DNA	transferred DNA
the1	*theseus1*
ton2	*tonneu2*

TUA1	ALPHA-1 TUBULIN
UTR	untranslated region
VR1	variable region
WAK	Wall-Associated Kinase
WT	wild-type
X-Gal	5-bromo-4-chloro-3-indolyl-β-D-galactopyranoside
Zn	zinc-binding domain

Chapter 1

Cellulose biosynthesis and cell wall signaling in higher plants

Abstract

The plant cell wall is a dynamic and responsive structure. For proper cell growth, plant must coordinate cell wall loosening, deposition of new wall materials, and subsequent rigidification in response to developmental and environmental cues. Cellulose is a major component and the primary load-bearing element of plant cell walls. Monitoring cell wall integrity and constant adjustment of cell wall biosynthesis are crucial for the ability of plants to response to mechanical stress or pathogen attack. Here, I will review recent current knowledge about the regulation of cellulose biosynthesis and cell wall signaling.

Introduction

The cell wall is essential for plants. It provides rigidity and protection against mechanical stress. It also defines the size and shape of the cell, and provides a barrier to infection by pathogens. The cell wall is a diverse and highly dynamic structure that responds to developmental and environmental cues (reviewed by Pilling and Höfte, 2003; Somerville et al., 2004).

Plant cell walls are composite structures, made up of polysaccharides, proteins, phenolic compounds, and other materials (Cosgrove, 2005). Polysaccharides are the most abundant polymers in the cell wall. They are divided into three groups: cellulose microfibrils, hemicellulose (e.g. xyloglucan, xylans, and mannans) and pectins. Cellulose microfibrils are insoluble cable-like structures composed of β-1-4-linked glucan chains. Because of its strength, cellulose microfibrils are the major load-bearing component in the cell wall. Hemicellulose coats the surface of cellulose and crosslinks cellulose microfibrils, which, together with the pectin matrix, form a network that is sufficient to resist turgor pressure.

There are two kinds of cell wall: primary and secondary cell walls. The primary cell wall is a network that is deposited in cells that are still expanding. In some cells types, such as fiber cells in wood or xylem cells in vascular tissues, a secondary cell wall is laid down inside the primary cell wall after the cells have finished dividing and are fully expanded. Both primary and secondary cell walls contain cellulose and hemicelluloses. However, primary cell walls also contain many enzymes and structural proteins, as well as pectin, whereas secondary walls contain lignin, but with little pectin or protein (Lerouxel et al., 2006).

The plant cell wall has a dynamic structure, subject to constant remodeling during cell expansion or in response to pathogen attack or other stresses. The remodeling of the cell wall must be performed in a highly regulated manner to ensure the cell wall is loosened sufficiently, but not so much that the cell ruptures. The cell achieves this coordination via a wall sensing, signaling and feedback system (Humphrey et al., 2007).

In this chapter, I will focus on recent studies addressing the major components involved in the regulation of cellulose biosynthesis in the primary cell wall, and how these elements regulate cell expansion. The mutants in my thesis project have cell expansion defects as a result of deficiency in primary cell wall biosynthesis and thus, I will focus on primary cell walls. Secondary cell wall biosynthesis has been covered in several excellent recent reviews (Mellerowicz and Sundberg, 2008; York and O'Neill, 2008; Zhong and Ye, 2007). In addition, I will also discuss components that have been recently discovered that play a role in sensing and monitoring cell wall integrity.

The importance of cellulose and cellulose synthase

Cellulose microfibrils are the core load-bearing component of the cell wall, and the orientation of cellulose microfibrils determines the direction of cell expansion. Cellulose microfibrils are insoluble, cable-like fibers that consist of 36 hydrogen-bonded chains of β-1-4-linked glucose molecules. In rapidly expanding cells, the cellulose microfibrils are deposited predominantly perpendicular to the axis of expansion, wound in hoops, which facilitates anisotropic (unequal) cell growth (Green, 1980; Taiz, 1984). Treatment with cellulose biosynthesis inhibitors, such as isoxaben, results in a rapid loss of growth anisotropy (Scheible et al., 2003). Consistent with inhibitor studies, cellulose-deficient

mutants, such as *radial swelling 1* (*rsw1*)(Cellulose synthase 1/CESA1) (Arioli et al., 1998; Williamson et al., 2001) and *procuste/quill* (Cellulose synthase 6/CESA6) (Fagard et al., 2000), display reduced or no anisotropic growth, generally accompanied by cell swelling. Severe cellulose-deficient mutants, such as null allele of *CESA1*, result in embryo lethality (Williamson et al., 2001).

The Arabidopsis genome contains ten plasma-localized Cellulose Synthase (*CESA*) genes that share a conserved structure. The proteins are about 1000 amino acids in length and have eight putative transmembrane domains. The N-terminal region of each protein has a zinc-binding domain (Zn) followed by a variable region 1 (VR1). The Zn domain is involved in CESA protein dimerization (Kurek et al., 2002). The central, cytosolic catalytic domain contains the D,D,D,Q/RXXRW motif that is required for glycosyltransferase activity (Somerville, 2006). Cellulose synthases form an enzyme complex that has a hexameric rosette structure (terminal complexes) of approximately 25-30 nm in diameter, which is present at the plasma membrane. It has been hypothesized that each hexameric rosette is comprised of six rosette subunits and each rosette subunit contains six CESA proteins, and thus, a total of thirty-six CESA proteins form a single rosette, which synthesize 36 β-1-4-linked glucan chains simultaneously (Somerville, 2006).

A combination of expression analyses, genetic studies, and co-immunoprecipation experiments has defined roles for the various *CESA* genes. CESA1, CESA3 and CESA6 interact with each other to form a class of rosettes that function in primary cell wall biosynthesis. CESA2, CESA5 and CESA9 are partially redundant with CESA6 in different stages of growth. CESA4, CESA7 and CESA8 comprise distinct rosettes that function in

secondary cell wall biosynthesis (Desprez et al., 2007; Persson et al., 2007; Persson et al., 2005).

How is the orientation of cellulose microfibrils achieved?

One of the key features of cellulose biosynthesis is that microfibrils are deposited predominantly transversely to the axis of cellular expansion. How do the cells achieve this? Evidence suggests that cytoplasmic microtubules are involved in the control of the orientation of microfibrils. It has been hypothesized that microtubules constrain rosette movement by serving as a template for the cellulose synthase rosettes, similar to a track (Giddings and Staehelin, 1991). Important evidence for this model comes from the observation that in elongating cells, cortical microtubules form arrays that also are oriented transversely to the axis of elongation and are mostly co-aligned with the cellulose microfibrils in the primary cell wall. Moreover, disruption of microtubules results in anisotropic defects. The cortical array of root epidermal cells remain transverse as cells move through the elongation zone, with some cells displaying obliquely oriented cortical arrays just before root hair emergence, which marks the point where elongation decreases (Baskin et al., 2004; Dolan et al., 1994).

Several mutants with either disorganized or severely disrupted cortical microtubules have been identified and these mutants are correlated with defective anisotropic growth. These mutants include: *tonneau1 and ton2/fass* (Camilleri et al., 2002; McClinton and Sung, 1997; Traas et al., 1995), *lue1/ botero1/fra2* (Bichet et al., 2001; Bouquin et al., 2003; Burk and Ye, 2002; Burk et al., 2001) and *microtubule organization1* (Sugimoto et al., 2003; Whittington et al., 2001).

How cortical microtubules control the orientation of cellulose microfibrils is still not understood. One confounding observation is that the *mor1* mutant appears to have a normal alignment of cellulose microfibrils, despite a significant disruption of the cortical microtubule arrays (Sugimoto et al., 2003). This raises the possibility that the microtubules might control anisotropy by a mechanism other than by directly controlling the alignment of microfibrils.

However, recent co-localization of both CESA6 (one cellulose synthase component) and the microtubule protein TUA1 (tubulin) in Arabidopsis, revealed that the synthase moves along the plasma membrane in tracks that largely coincided with cortical microtubules (Paredez et al., 2006). Inhibition of microtubule polymerization changed the fine-scale distribution and pattern of moving CESA complexes in the membrane, indicating a relatively direct mechanism for guidance of cellulose deposition by the cytoskeleton.

COBRA has been identified as a potential candidate that might mediate the microtubule-controlled orientation of microfibrils. The *cobra* mutant displays radial expansion in the elongation zone of the root, and this is correlated to a disorganization of microfibrils and a reduction in the level of crystalline cellulose. A weak *cobra* allele has mild phenotype, and only displays swollen roots on high sucrose plates (Schindelman et al., 2001). However, null *cob* mutants are extremely deficient in cellulose and are strongly dwarfed (Roudier et al., 2005). *COBRA* encodes a putative GPI-anchored extracelluar protein that is localized to the longitudinal sides of root cells. Interestingly, COBRA is distributed in a banding pattern transverse to the longitudinal axis via a microtubule-dependent mechanism. This suggests that COBRA might mediate the microtubule-controlled orientation of

microfibrils. However, the precise role of COBRA remains unclear. It will be interesting to determine how CESA6 and TUA1 localize in *cobra* mutants.

Mutations in other genes affecting cellulose

In addition to CESA proteins, other proteins have been identified that are involved in regulating cellulose biosynthesis directly, including *KORRIGAN* and *KOBITO*. The *KOR* gene encodes a β-1-4 glucanase (Nicol et al., 1998). *korrigan* is allelic to *lions tail* (*lit*), *radial swelling 2* (*rsw2)*, *isoxaben resistant 2* (*irx2*), and *altered cell wall 1* (*acw1*) (Hauser et al., 1995; Lane et al., 2001; Mølhøj et al., 2002; Sato et al., 2001; Szyjanowicz et al., 2004). The weakest allele, *acw1,* reduces cellulose specifically in secondary cell wall biosynthesis, but strong alleles of *KOR* cause defects in cytokinesis (Zuo et al., 2000). KOR is predicted to be membrane localized; however, KOR-GFP fusion protein studies are as yet inconclusive (reviewed by Taylor, 2008). The soluble domain of a KOR-like protein from Brassica has been shown to have cellulase activity. KOR is hypothesized to interact with CESA proteins in the membrane to remove noncrystalline glucan chains, but the exact role of KOR is yet to be determined. *kobito*, which is allelic to *elongation defective 1* (*eld1*) and *ABA insensitive 8* (*abi8*), encodes a membrane protein of unknown function (Suzuki et al., 2003). In the elongation zone of *kob1* mutant roots, microfibrils are randomly oriented, resembling those of the *rsw1* mutant at restrictive temperatures.

Sensing and feedback signaling in cell wall function

The plant cell wall is a dynamic structure, and mediates responses to external stimuli and stresses, such as pathogen attack and wounding. The cell wall is constantly remodeled in

response to development and environmental inputs. How does the plant accomplish this remodeling? While expansins and extensins have been shown to be involved in cell wall loosening and rigidification respectively, the system to sense the cell wall integrity in plants is largely unknown (Humphrey et al., 2007). Ectopic lignin deposition or pectin composition changes have been observed in various cellulose-deficient mutants, indicating that the cell senses the wall defects and that there is a feedback system to compensate and maintain cell wall integrity (Caño-Delgado et al., 2003; His et al., 2001). But what is the sensor(s) and signal transduction pathway(s) mediating this response?

Plant receptor kinases that have the ability to bind polymers in the cell wall are good candidates; such kinases include the WAKs and LecRKs. The WAKs are proteins that are localized in the plasma membrane and have an N-terminal domain that binds extremely tightly to pectin in the cell wall. In *wak2* mutants, root elongation was reduced (Kohorn et al., 2006). LecRKs contain an extracellular lectin-like domain which may bind carbohydrates, which is consistent with a role as a cell wall sensor; however, there is no experimental data to support this hypothesis.

Recently, a suppressor screen of *prc1* has been identified *THESEUS1* as a potential cell wall sensor (Humphrey et al., 2007). *the1* partially restores hypocotyl elongation and suppresses the ectopic lignin accumulation of the *prc* mutant. However, surprisingly, *the1* does not restore cellulose biosynthesis in *prc1 the1*, suggesting that the inhibition of elongation in the *prc1* mutant is an active response to cell wall defects. In addition, disruption of THE1 in a *prc1* background deceases ectopic lignification, while overexpression of THE1 results in increased lignification, further confirming that THE1 is involved in signaling the cell wall integrity. *THE1* encodes a receptor-like kinases (RLK)

belonging to the CrRLK1L (*Catharanthus roseus* protein-kinase-1-like) family. It has been proposed that THE1 acts as a receptor kinase that monitors cell wall integrity.

Conclusions

Much progress has been made towards our understanding of the function and regulation of cellulose biosynthesis. Several candidates have been identified that play a role in the regulation of cellulose biosynthesis, including KORRIGAN and COBRA. How these proteins function and interact to regulate plant cell biosynthesis is an exciting area of future research. Furthermore, plants have a system to monitor the cell wall integrity, and proteins such as THE1 play an important role in this process, but much remains to be learned regarding this process.

References

Arioli, T., Peng, L., Betzner, A., Burn, J., Wittke, W., Herth, W., Camilleri, C., Höfte, H., Plazinski, J., Birch, R., *et al.* (1998). Molecular analysis of cellulose biosynthesis in Arabidopsis. Science **279**, 717-720.

Baskin, T., Beemster, G., Judy-March, J., and Marga, F. (2004). Disorganization of cortical microtubules stimulates tangential expansion and reduces the uniformity of cellulose microfibril alignment among cells in the root of Arabidopsis. Plant Physiol Biochem **135**, 2279-2290.

Bichet, A., Desnos, T., Turner, S., Grandjean, O., and Hofte, H. (2001). *BOTERO1* is required for normal orientation of cortical microtubules and anisotropic cell expansion in *Arabidopsis*. Plant J **25**, 137-148.

Bouquin, T., Mattsson, O., Naested, H., Foster, R., and Mundy, J. (2003). The *Arabidopsis lue1* mutant defines a katanin p60 ortholog involved in hormonal control of microtubule orientation during cell growth. J Cell Sci **116**, 791-801.

Burk, D., and Ye, Z. (2002). Alteration of oriented deposition of cellulose microfibrils by mutation of a katanin-like microtubule-severing protein. Plant Cell **14**, 2145-2160.

Burk, D. H., Liu, B., Zhong, R., Morrison, W. H., and Ye, Z.-H. (2001). A Katanin-like Protein Regulates Normal Cell Wall Biosynthesis and Cell Elongation. Plant Cell **13**, 807-828.

Camilleri, C., Azimzadeh, J., Pastugila, M., Bellini, C., Grandjean, O., and Bouchez, D. (2002). The *Arabidopsis TONNEAU2* gene encodes a putative novel protein phosphatase 2A regulatory subunit essential for the control of the cortical cytoskeleton. Plant Cell **14**, 833-845.

Caño-Delgado, A., Penfield, S., Smith, C., Catley, M., and Bevan, M. (2003). Reduced cellulose synthesis invokes lignification and defense responses in Arabidopsis thaliana. Plant J **34**, 351-362.

Cosgrove, D. J. (2005). Growth of the plant cell wall. Nat Rev Mol Cell Biol **6**, 850-861.

Desprez, T., Juraniec, M., Crowell, E., Jouy, H., Pochylova, Z., Parcy, F., Höfte, H., Gonneau, M., and Vernhettes, S. (2007). Organization of cellulose synthase complexes involved in primary cell wall synthesis in Arabidopsis thaliana. Proc Natl Acad Sci U S A **104**, 15572-15577.

Dolan, L., Duckett, C., Grierson, C., Linstead, P., Schneider, K., Lawson, E., Dean, C., and Roberts, K. (1994). Clonal relationships and cell patterning in the root epidermis of *Arabidopsis*. Development **120**, 2465-2474.

Fagard, M., Desnos, T., Desprez, T., Goubet, F., Refregier, G., Mouille, G., McCann, M., Rayon, C., Vernhettes, S., and Hofte, H. (2000). *PROCUSTE1* encodes a cellulose synthase required for normal cell elongation specifically in roots and dark-grown hypocotyls of Arabidopsis. Plant Cell **12**, 2409-2424.

Giddings, T. H. J., and Staehelin, L. A. (1991). Microtubule-mediated control of microfibril deposition: A re-examination of the hypothesis. In The Cytoskeletal Basis of Plant Growth and Form, C. W. Lloyd, ed. (London, Academic Press), pp. 85–99.

Hauser, M., Morikami, A., and Benfey, P. (1995). Conditional root expansion mutants of Arabidopsis. Development **121**, 1237-1252.

His, I., Driouich, A., Nicol, F., Jauneau, A., and Höfte, H. (2001). Altered pectin composition in primary cell walls of korrigan, a dwarf mutant of Arabidopsis deficient in a membrane-bound endo-1,4-beta-glucanase. Planta **212**, 348-358.

Humphrey, T. V., Bonetta, D. T., and Goring, D. R. (2007). Sentinels at the wall: cell wall receptors and sensors. New Phytol **176**, 7-21.

Kohorn, B. D., Kobayashi, M., Johansen, S., Riese, J., Huang, L. F., Koch, K., Fu, S., Dotson, A., and Byers, N. R. (2006). An Arabidopsis cell wall-associated kinase required for invertase activity and cell growth. Plant J **46**, 307-316.

Kurek, I., Kawagoe, Y., Jacob-Wilk, D., Doblin, M., and Delmer, D. (2002). Dimerization of cotton fiber cellulose synthase catalytic subunits occurs via oxidation of the zinc-binding domains. Proc Natl Acad Sci U S A **99**, 11109-11114.

Lane, D. R., Wiedemeier, A., Peng, L., Hofte, H., Vernhettes, S., Desprez, T., Hocart, C. H., Birch, R. J., Baskin, T. I., Burn, J. E., *et al.* (2001). Temperature-sensitive alleles of RSW2 link the KORRIGAN Endo-1,4-β-glucanase to cellulose synthesis and cytokinesis in Arabidopsis. Plant Physiol **126**, 278-288.

Lerouxel, O., Cavalier, D., Liepman, A., and Keegstra, K. (2006). Biosynthesis of plant cell wall polysaccharides - a complex process. Curr Opin Plant Biol **9**, 621-630.

McClinton, R., and Sung, Z. (1997). Organization of cortical microtubules at the plasma membrane in Arabidopsis. Planta **201**, 252-260.

Mellerowicz, E., and Sundberg, B. (2008). Wood cell walls: biosynthesis, developmental dynamics and their implications for wood properties. Curr Opin Plant Biol **11**, 293-300.

Mølhøj, M., Pagant, S., and Höfte, H. (2002). Towards understanding the role of membrane-bound endo-beta-1,4-glucanases in cellulose biosynthesis. Plant Cell Physiol **43**, 1399-1406.

Nicol, F., His, I., Jauneau, A., Vernhettes, S., Canut, H., and Höfte, H. (1998). A plasma membrane-bound putative endo-1,4-beta-D-glucanase is required for normal wall assembly and cell elongation in Arabidopsis. EMBO J **17**, 5563-5576.

Paredez, A. R., Somerville, C. R., and Ehrhardt, D. W. (2006). Visualization of cellulose synthase demonstrates functional association with microtubules. Science ***312***, 1491-1495.

Persson, S., Paredez, A., Carroll, A., Palsdottir, H., Doblin, M., Poindexter, P., Khitrov, N., Auer, M., and Somerville, C. (2007). Genetic evidence for three unique components in primary cell-wall cellulose synthase complexes in Arabidopsis. Proc Natl Acad Sci U S A **104**, 15566-15571.

Persson, S., Wei, H., Milne, J., Page, G., and Somerville, C. (2005). Identification of genes required for cellulose synthesis by regression analysis of public microarray data sets. Proc Natl Acad Sci U S A **102**, 8633-8638.

Pilling, E., and Höfte, H. (2003). Feedback from the wall. Curr Opin Plant Biol **6**, 611-616.

Roudier, F., Fernandez, A., Fujita, M., Himmelspach, R., Borner, G., Schindelman, G., Song, S., Baskin, T., Dupree, P., Wasteneys, G., and Benfey, P. (2005). COBRA, an Arabidopsis Extracellular Glycosylphosphatidylinositol-Anchored Protein, Specifically Controls Highly Anisotropic Expansion through Its Involvement in Cellulose Microfibril Orientation. Plant Cell. **17**, 1749-1763.

Sato, S., Kato, T., Kakegawa, K., Ishii, T., Liu, Y.-G., Awano, T., Takabe, K., Nishiyama, Y., Kuga, S., Sato, S., *et al.* (2001). Role of the putative membrane-bound endo-1,4-β-gucanase KORRIGAN in cell elongation and cellulose synthesis in *Arabidopsis thaliana*. Plant Cell Physiol **42**, 251-263.

Schindelman, G., Morikami, A., Jung, J., Baskin, T. I., Carpita, N. C., Derbyshire, P., McCann, M. C., and Benfey, P. N. (2001). COBRA encodes a putative GPI-anchored protein, which is polarly localized and necessary for oriented cell expansion in Arabidopsis. Genes Dev **15**, 1115-1127.

Somerville, C. (2006). Cellulose synthesis in higher plants. Annu Rev Cell Dev Biol **22**, 53-78.

Somerville, C., Bauer, S., Brininstool, G., Facette, M., Hamann, T., Milne, J., Osborne, E., Paredez, A., Persson, S., Raab, T., *et al.* (2004). Toward a systems approach to understanding plant cell walls. Science **306**, 2206-2211.

Sugimoto, K., Himmelspach, R., Williamson, R. E., and Wasteneys, G. O. (2003). Mutation or drug-dependent microtubule disruption causes radial swelling without

altering parallel cellulose microfibril deposition in Arabidopsis root cells. Plant Cell **15**, 1414-1429.

Suzuki, Y., Saso, K., Fujioka, S., Yoshida, S., Nitasaka, E., Nagata, S., Nagasawa, H., Takatsuto, S., and Yamaguchi, I. (2003). A dwarf mutant strain of Pharbitis nil, Uzukobito (kobito), has defective brassinosteroid biosynthesis. Plant J **36**, 401-410.

Szyjanowicz, P., McKinnon, I., Taylor, N., Gardiner, J., Jarvis, M., and Turner, S. (2004). The irregular xylem 2 mutant is an allele of korrigan that affects the secondary cell wall of Arabidopsis thaliana. Plant J **37**, 730-740.

Taylor, N. G. (2008). Cellulose biosynthesis and deposition in higher plants. New Phytol **178**, 239-252.

Traas, J., Bellini, C., Nacry, P., Kronenberger, J., Bouchez, D., and M, C. (1995). Normal differentiation patterns in plants lacking microtubular preprophase bands. . Science **375**, 676-677.

Whittington, A. T., Vugrek, O., Wei, K. J., Hasenbein, N. G., Sugimoto, K., Rashbrooke, M. C., and Wasteneys, G. O. (2001). MOR1 is essential for organizing cortical microtubules in plants. Nature **411**, 610-613.

Williamson, R. E., Burn, J. E., Birch, R., Baskin, T. I., Arioli, T., Betzner, A. S., and Cork, A. (2001). Morphology of *rsw1*, a cellulose-deficient mutant of *Arabidopsis thaliana*. Protoplasma **215**, 116-127.

York, W., and O'Neill, M. (2008). Biochemical control of xylan biosynthesis - which end is up? Curr Opin Plant Biol **11**, 258-265.

Zhong, R., and Ye, Z. (2007). Regulation of cell wall biosynthesis. Curr Opin Plant Biol **10**, 564-572.

Zuo, J., Niu, Q., Nishizawa, N., Wu, Y., Kost, B., and Chua, N. (2000). KORRIGAN, an Arabidopsis endo-1,4-beta-glucanase, localizes to the cell plate by polarized targeting and is essential for cytokinesis. Plant Cell **12**, 1137-1152.

Chapter 2

Two leucine-rich repeat receptor kinases mediate signaling linking cell wall biosynthesis and ACC synthase in *Arabidopsis*

Preface

The following chapter is published as Shou-Ling, Xu, Abidur Rahman, Tobias I. Baskin and Joseph J. Kieber. " Two leucine-rich repeat receptor kinases mediate signaling linking cell wall biosynthesis and ACC synthase in Arabidopsis" in *Plant Cell*, Volume 20, on November 18, 2008; 10.1105/tpc.108.063354.

Abstract

The plant cell wall is a dynamic structure that changes in response to developmental and environmental cues through poorly understood signaling pathways. We identified two LRR receptor-like kinases in Arabidopsis that play a role in regulating cell wall function. Mutations in these *FEI1* and *FEI2* genes disrupt anisotropic expansion and the synthesis of cell wall polymers, and act additively with inhibitors or mutations disrupting cellulose biosynthesis. While FEI1 is an active protein kinase, a kinase-inactive version of FEI1 was able to fully complement the *fei1 fei2* mutant. The expansion defect in *fei1 fei2* roots was suppressed by inhibition of ACC synthase, an enzyme that converts Ado-Met to ACC in ethylene biosynthesis, but not by disruption of the ethylene response pathway. Furthermore, the FEI proteins interact directly with ACC synthase. These results suggest that the FEI proteins define a novel signaling pathway that regulates cell wall function, likely via an ACC-mediated signal.

Introduction

The regulation of cell expansion plays a fundamental role in plant growth and development. Despite this critical role, the regulatory inputs that control this process are poorly understood. Cell expansion is regulated primarily by turgor pressure and by the properties of the plant cell wall, which is composed of a polysaccharide network of cellulose microfibrils crosslinked by hemicelluloses in a pectin matrix, along with numerous proteins (Somerville, 2006). The primary load bearing elements of the cell wall are the cellulose microfibrils, and their orientation and crosslinking are key factors that determine both the direction and extent of cell expansion (Darley et al., 2001). In longitudinally expanding cells, the cellulose microfibrils are deposited primarily in an orientation perpendicular to the axis of expansion, thus constricting radial expansion (Green, 1980; Taiz, 1984; Baskin, 2005). Consistent with this, disruption of cellulose biosynthesis by treatment with various chemical inhibitors results in a rapid loss of growth anisotropy (Scheible et al., 2001; Desprez et al., 2002).

Cellulose microfibrils are synthesized by cellulose synthase, an enzyme that is present at the plasma membrane as a hexameric protein complex called the rosette (reviewed in: Somerville, 2006). Genetic analysis and inhibitor studies indicate that cytoplasmic microtubules play an important role in guiding the orientation of the deposition of cellulose microfibrils (reviewed in: Baskin, 2001), and the cellulose synthase rosette was found to move along the plasma membrane in tracks that largely coincided with the cortical microtubules (Paredez et al., 2006).

Additional components involved in regulating cell wall biosynthesis have been identified in genetic screens for mutations that alter root or hypocotyl elongation in Arabidopsis. The *cobra* mutant displays radial expansion in the elongation zone of the root,

and this is correlated to a disorganization of microfibrils and a reduction in the level of crystalline cellulose in cells in the root elongation zone. *COBRA* encodes a putative glycosylphosphatidylinositol (GPI)-anchored extracellular protein that is localized to the longitudinal sides of root cells in a banding pattern transverse to the longitudinal axis (Schindelman et al., 2001). The *sos5* mutant is a conditional mutant that displays arrested root growth and a swollen root phenotype in the presence of salt stress (Shi et al., 2003). *SOS5* encodes a GPI-anchored extracellular protein with two arabinogalactan protein-like and fascilin-like domains that has been hypothesized to play a role in cell adhesion.

Several members of the receptor-like Ser/Thr protein kinase (RLK) family in Arabidopsis have been implicated in regulating cell growth in different contexts (Hématy and Höfte, 2008). The RLKs are a large, diverse family of transmembrane signaling elements in plants, only a few of which have been functionally characterized (Morillo and Tax, 2006). The Arabidopsis protein THE1, which belongs to the CrRLK1L (*Catharanthus roseus* protein-kinase-1-like) subfamily, has been hypothesized to sense cell wall integrity (Hématy et al., 2007). A second group of RLKs, the WAKs, are tightly bound to the cell wall and likely play an important role in regulating its function (He et al., 1996; Anderson et al., 2001). Here, we describe two Arabidopsis leucine-rich repeat RLKs (LRR-RLKs) in a distinct RLK clade whose disruption results in defects in cell expansion primarily in roots. Further analysis links ACC synthase to this pathway, as well as SOS5, which together define a novel pathway regulating cell wall biosynthesis.

Results

Disruption of *FEI1* and *FEI2* alters cell expansion

The Arabidopsis genome encodes over 200 predicted LRR-RLKs, most of which have unknown functions (Morillo and Tax, 2006). We identified two highly similar LRR-RLKs (82% amino acid identity; Figure 2.1A and Figure S2.1 online) that when both disrupted caused a swollen root phenotype (Figures 2.1 and 2.2). We named these kinases FEI, after the Chinese word for fat. FEI1 (At1g31420) and FEI2 (At2g35620) are in the same RLK subfamily XIII as ERECTA (Shiu and Bleecker, 2001), which is distinct from the THE1 and WAK subfamilies. The insertions in *fei1*, *fei2-1 and fei2-2* (Figure 2.1B) result in the elimination of the corresponding full-length transcript (Figure 2.1E). In the case of *fei1*, there is a truncated transcript present in the mutant plants corresponding to the region of the gene upstream of the T-DNA insertion site (Figure 2. 1E). The single *fei1* or *fei2* mutants were indistinguishable from the wild type in all aspects of growth and development (Figure 2. 1). The double *fei1 fei2* mutant was nearly indistinguishable from wild type on 1% ("low") sucrose media (Figures 2.1C and 2.1F), but in the presence of 4.5% (“high”) sucrose, the *fei1 fei2* double mutant displayed short, radially swollen roots (Figures 2.1D and 2.1F and Figure 2.2). Root elongation is reduced in the *fei1 fei2* mutant two days after transfer as compared to wild-type seedlings (Figure 2. 1G), and swelling is visible three days after transfer (Figure S2. 2). Four days after transfer to non-permissive conditions, the diameter of the mutant root was greater than two-fold larger as compared to the wild type (wild-type root: 163 ± 11 μm, n = 8; *fei1 fei2*: 316 ± 68 μm, n = 8). The F_2 of a cross between *fei1/fei1* and *fei2/fei2* segregated seedlings displaying the mutant phenotype in a ratio consistent with two recessive loci (653 wild type: 39 swollen roots, $\chi^2 = 0.45$ for the expected 15:1 ratio). A genomic copy of *FEI1* or *FEI2* fused with a C-myc epitope tag (FEI1-myc or FEI2-myc) was able to fully

complement the root swelling phenotype of *fei1 fei2* (Figures 2.3B and 2.3C), confirming that the phenotype was the result of disruption of these genes.

Wild-type Arabidopsis root cells undergo primarily longitudinal expansion. The increased diameter and reduced elongation observed in *fei1 fei2* double mutant roots suggests that anisotropic expansion is defective in mutant root cells. Consistent with this, examination of transverse sections of root apices revealed that the *fei1 fei2* epidermal cells, and to a lesser extent cells in the inner layers, displayed a high degree of radial swelling (Figure 2. 2). The root cells of the single *fei* mutants appeared indistinguishable from wild-type root cells (Figure S2. 3). The number of cells in each of the layers of the root was not appreciably altered in the *fei1 fei2* mutants (i.e. there were 23-26 (n=5) epidermal cells in *fei1 fei2* vs. 20-27 (n=5) for wild type). We conclude that the *fei1 fei2* mutations cause the cells in the elongation zone to undergo a shift in expansion from longitudinal to isotropic. The *fei1 fei2* mutants also displayed swollen roots on media that contains an elevated concentration of NaCl (Figure S2. 4B). However, *fei1 fei2* roots do not swell in the presence of 1 to 6% mannitol or sorbitol (Figure S2. 5), indicating that the effect of sucrose and NaCl was not the result of a response to elevated osmolarity.

Intrinsic kinase activity is not required for FEI function

The sequences of the C-terminal domains of FEI1 and FEI2 have all the features of a Ser/Thr protein kinase catalytic domain, including all the 11 conserved subdomains of eukaryotic protein kinases (Figure S2. 1) (Hanks et al., 1988). To test if the FEI1 kinase has intrinsic protein kinase activity, we expressed the kinase domain of FEI1 in *E. coli* as a GST-fusion protein. Purified recombinant FEI1 was active in *in vitro* protein kinase assays; it was

able to autophosphorylate and to phosphorylate myelin basic protein (Figure 2. 3A). Substitution of the invariant Lys residue in subdomain II in FEI1 with Arg ($FEI1^{K334R}$) resulted in a complete loss of kinase activity (Figure 2. 3A), as has been observed in other protein kinases. Interestingly, this kinase-inactive version of FEI1 (or FEI2) was able to complement a *fei1 fei2* mutant (Figures 2. 3B and 2.3C), although complementation was not as consistent as that observed with the WT *FEI1* or *FEI2* gene: 10/10 independent transformants displayed full complementation when transformed with wild-type *FEI1* or *FEI2*, whereas 3/10 and 2/10 independent transformants were fully complemented with the respective mutant versions. This indicates that kinase activity is not essential for FEI function *in vivo*, though it contributes to optimal FEI function.

FEI is localized to the plasma membrane and is broadly expressed

Analysis of the deduced amino acid sequence of FEI1 and FEI2 predicts a single transmembrane domain, similar to other RLKs. Consistent with this, both a FEI1-myc and FEI2-myc fusion proteins were present in a microsome fraction (Figure 2. 4I). Furthermore, a FEI2-GFP fusion protein, which was able to complement the *fei1 fei2* mutant (Figure S2. 6), localized to the periphery of the cell in a pattern consistent with a plasma membrane localization (Figure 2. 4J).

Both *FEI1* and *FEI2* are most highly expressed in the root meristem and elongation zone as revealed by promoter-GUS fusions (Figure 2. 4). Published microarray analysis revealed that *FEI1* and *FEI2* are expressed at approximately equal levels in the different radial layers of the root tip, including the epidermis (Birnbaum et al., 2003). Extended staining of *FEI* promoter-GUS lines revealed a broader staining pattern for these two genes

(Figure 2. 4), similar to the pattern obtained from publicly available array data (Zimmermann et al., 2005).

FEI1 and FEI2 function in hypocotyls and flowers

FEI1 and *FEI2* both are expressed in the hypocotyls of etiolated seedlings (Figures 2.4B and 2.4F), which, like roots, are composed of cells that undergo primarily longitudinal expansion. Thus, we examined if the *fei1 fei2* double mutant had defects in hypocotyl growth. The hypocotyls of etiolated seedlings of *fei1 fei2* were significantly fatter than those of wild-type or single *fei* mutants (Figures 2.4K, 2.4L and 2.4M). However, contrary to the root phenotype of *fei1 fei2*, this was not accompanied by a decrease in the overall length of the hypocotyl (Figure S2. 7), and this occurred in either low or high sucrose. This swollen hypocotyl phenotype was complemented by transgenes containing genomic copies of either *FEI1* or *FEI2*. The modest increase in the diameter of the *fei1 fei2* mutant hypocotyls (Figure 2. 4M) was substantially less than the increased width observed in the mutant roots. Examination of transverse sections of WT and mutant etiolated seedlings revealed that the increased diameter of the *fei1 fei2* hypocotyls was associated with an increase in cell size, not cell number (Figure 2. 4L). We did not observe a significant change from the wild type in the level or spatial distribution of lignin in the *fei1 fei2* etiolated hypocotyls as revealed by phloroglucinol staining (Figure S2. 8). There was not obvious swelling in any other tissues of the *fei1 fei2* mutant. However, the *fei1 fei2 cob* triple mutant (see below), but neither *fei1 fei2* nor *cob*, had shortened stamen filaments and this triple mutant was partially infertile (Figure 2. 4N), indicating a role for the FEI kinases in these tissues. Consistent with this, analysis of

the promoter-GUS fusions reveals expression of both *FEI1* and *FEI2* in stamen filaments (Figure 2. 4D and 2.4H).

The *fei1 fei2* mutant is defective in cellulose biosynthesis

The altered pattern of cell expansion in the *fei1 fei2* mutants suggests a defect in cell wall function. As cortical microtubules have been implicated in regulating anisotropic growth, we examined their arrangement in epidermal cells of wild-type and *fei1 fei2* roots using an anti-α-tubulin antibody. In both wild-type and *fei1 fei2* double mutant root cells, the microtubules in the elongation zone were aligned primarily transversely to the axis of growth three days after transfer to non-permissive conditions (Figure S2. 9). This indicates that growth anisotropy in the *fei1 fei2* mutants is not the result of disruption of the pattern of microtubules.

To begin to assess if the properties of the cell wall are altered in the mutant, we examined the effect of isoxaben, an inhibitor of cellulose synthase, on *fei1 fei2*. Growth in the presence of high sucrose rendered wild-type roots hypersensitive to isoxaben (Figure 2. 5A), which indicates that elevated sucrose sensitizes roots to perturbations in cellulose synthesis. In the presence of low sucrose, both the *prc1* mutant, which disrupts a catalytic subunit of cellulose synthase (CESA6) (Fagard et al., 2000), and *fei1 fei2* displayed increased sensitivity to isoxaben (Figure 2. 5C). This suggests that *fei1 fei2* perturbs the biosynthesis or function of cellulose. Consistent with this, the roots of *fei1 fei2* seedlings grown in non-permissive conditions produce ectopic lignin (Figure 2. 1H), which is generally correlated with a decreased level of crystalline cellulose (Humphrey et al., 2007). We further analyzed cellulose synthesis by measuring incorporation of ^{14}C-glucose into crystalline and non-

crystalline cellulosic cell wall fractions of excised root tips. In permissive conditions, *fei1 fei2* roots were similar to the wild-type. However, in non-permissive conditions, *fei1 fei2* mutant roots displayed a striking defect in cellulose biosynthesis, as measured by incorporation of labeled glucose into acid-insoluble (crystalline cellulose; Peng et al., 2000) and acid-soluble material (non-crystalline cellulose and other wall polymers; Heim et al., 1998) (Figure 2. 5D).

When viewed with a transmission electron microscope, the walls from the swollen root cells of the *fei1 fei2* mutant were not appreciably altered in thickness as compared to the WT. However, the size of the intercellular spaces in the outer cell layer layers of the *fei1 fei2* mutant roots were reduced in non-permissive conditions (Figure 2. 5B), similar to the *sos5* and *rsw1-20* mutants (Shi et al., 2003; Beeckman et al., 2002).

The *COBRA* (*COB*) gene encodes a GPI-anchored plant-specific protein of unknown function. Null *cob* mutants are extremely deficient in cellulose, are strongly dwarfed and are sterile (Roudier et al., 2005). However, weak *cob* alleles, including the *cob-1* allele used in this study, result in fertile plants that display a sucrose-dependent swollen root phenotype (Figure 2. 6). *prc1-1*, which is a likely null allele of *CESA6*, also displays a sucrose-dependent swollen root phenotype (Figure 2. 6). We examined the genetic interactions of *fei1 fei2* with *cob* and *prc1*. The *fei1 fei2 cob* and *fei1 fei2 prc1* triple mutants display an enhanced root phenotype as compared to the parental lines; the triple mutant roots were significantly shorter and more swollen in non-permissive conditions (Figures 2.6B and 2.6C). Moreover, the *fei1 fei2 cob* and *fei1 fei2 prc1* displayed swollen roots even in permissive conditions, in which the single or double mutants do not display significant swelling (Figures

2.6A and 2.6C). These synergistic interactions suggest that FEI1 and FEI2 act in a pathway independent from COB or PRC1 to regulate cell wall function.

salt-overly-sensitive5 (*sos5*) was isolated as a mutant that displayed a swollen root tip in the presence of moderately high salt (Shi et al., 2003). The *SOS5* gene encodes a putative cell surface adhesion protein with AGP-like and fasciclin-like domains. As the phenotype of *sos5* is similar to that of the *fei1 fei2* double mutant, we tested the effect of high sucrose on *sos5* seedlings. Similar to *fei1 fei2*, growth of *sos5-2* (a novel T-DNA insertion allele that is a transcript null; Figure S2. 4) in the presence of high sucrose also resulted in a swollen root phenotype (Figure 2. 6B). In contrast, we did not observe a swollen root phenotype in other *sos* mutants (*sos1*, *sos2*, *sos3*, *sos4*) in response to elevated sucrose (Figure S2. 10). Furthermore, etiolated *sos5-2* seedlings displayed swollen hypocotyls similar to *fei1 fei2* (Figure 2. 4M). The roots of the *sos5-2 fei1 fei2* triple mutant were indistinguishable from the *fei1 fei2* double mutant in their response to increasing levels of NaCl (Figure 2. 6). Likewise, the hypocotyl width of the *sos5-2 fei1 fei2* triple mutant etiolated seedlings was comparable to that of the *fei1 fei2* double mutant (Figure 2. 4M). The non-additive nature of *sos5-2* and *fei1 fei2* suggests that these gene products act in a linear pathway to regulate cell elongation.

ACC Synthase plays a role in FEI1/FEI2 mediated cell expansion

Ethylene plays an important role in regulating expansion in many plant cells, and inhibition of ethylene biosynthesis or perception can partially revert the swollen phenotypes of certain root morphology mutants, such as *sabre* (Aeschbacher et al., 1995) and *cev1* (Ellis et al., 2002). We determined the effect of blocking ethylene biosynthesis on the *fei1 fei2* swollen root phenotype. α-aminoisobutyric acid (AIB), which is a structural analog of ACC

that blocks ACC oxidase activity by acting as a competitive inhibitor, reverted *fei1 fei2* mutant roots grown in the presence of high sucrose or elevated NaCl to a nearly wild-type morphology (Figure 2. 7A and 2.7B; Table 1; Figure S2. 4B). AIB also reverted the defect in cellulose synthesis in *fei1 fei2* (Figure 2. 5E). However, AIB did not revert the hypocotyl phenotype of *fei1 fei2*. Aminooxy-acetic acid (AOA), which inhibits enzymes that require pyroxidal phosphate, including ACC synthase (ACS), reverted the *fei1 fei2* swollen root phenotype (Figure 2. 7A and 2.7B; Table 2.1). As AOA and AIB block ethylene biosynthesis by distinct mechanisms, it is unlikely that this phenotypic reversion of *fei1 fei2* is due to off-target effects. Furthermore, this is not a general effect of AIB as it did not revert root swelling phenotype of the *cob* mutant (Figure S2. 11), even at higher concentrations (data not shown). Surprisingly, neither 1-methylcyclopropene (1-MCP) nor silver ion (silver thiosulfate), both of which block ethylene perception, had any appreciable effect on the root phenotype of *fei1 fei2* mutants (Table 2.1). Likewise, neither *etr1,* which disrupts an ethylene receptor, nor *ein2*, a strong ethylene-insensitive mutant that acts downstream of ETR1, suppressed the *fei1 fei2* root phenotype (Figure 2. 7A; Table 2.1).

Consistent with the other similarities to the *fei1 fei2* mutant, root swelling in *sos5-2* seedlings grown in the presence of either high sucrose or elevated NaCl was reversed by AIB and AOA, but not by blocking the response to ethylene (Figure 2. 7A and 2.7B; Table 2.1; Figure S2. 4). This suggests that either swelling in the absence of FEI depends on a hitherto undiscovered pathway for ethylene perception, or that ACC itself is acting as a signaling molecule.

We tested if the FEIs interacted with ACS using a yeast two-hybrid assay. The kinase domain of both FEI1 and FEI2 interacted with both ACS5 and ACS9, two type-2 ACS

proteins (Chae and Kieber, 2005). In contrast, neither FEI1 nor FEI2 interacted with ACS2 (Figure 2. 7C), which belongs to a distinct subclade of ACS proteins (type-1) that have divergent C-terminal domains (Chae and Kieber, 2005). Likewise, the *eto2* and *eto3* mutations, which alter the C-terminal domains of ACS5 and ACS9 respectively and which block the rapid degradation of these proteins *in vivo*, disrupted the interaction with FEI1 and FEI2 in the yeast two-hybrid interaction (Figure 2. 7C). Disruption of the kinase activity did not affect the interaction with ACS, as both $FEI1^{K334R}$ and $FEI2^{K332R}$ interacted with ACS5. In contrast, the ERECTA kinase domain did not interact with ACS5 in a yeast two-hybrid assay, indicating that there is specificity in the interaction with ACS5. We failed to detect an interaction between FEI1 and FEI2 with either themselves or with each other in a yeast two-hybrid assay.

We next tested the ability of FEI1 to phosphorylate purified ACS5. We were not able to detect phosphorylation of ACS5 *in vitro* by purified, catalytically-active FEI1 (Figure 2. 7D). The purified ACS5 used in this analysis was enzymatically active and could be phosphorylated in our conditions by a partially purified soybean CDPK (data not shown), which had been shown previously to phosphorylate ACC synthase (Tatsuki and Mori, 2001; Sebastià et al., 2004). Thus, the lack of phosphorylation of ACS5 by FEI1 in this analysis is not likely the result of mis-folding of ACS5.

Measurements of ethylene production revealed that root tissues from wild-type and *fei1 fei2* mutant seedlings grown on low or high sucrose in the light made comparable amounts of ethylene (8.9±0.8 pl•1 cm root segment^{-1}•day^{-1} for wild type vs. 11.9±0.2 pl•1 cm root segment^{-1}•day^{-1} for *fei1 fei2*). Likewise, ethylene production in dark-grown *fei1 fei2* seedlings was similar to wild type (5.6±0.3 pl•seedling^{-1}•day $^{-1}$ for wild-type seedlings vs.

5.8±0.7 pl•seedling^{-1}•day^{-1} for *fei1 fei2*). Thus, the FEIs do not appear to affect the overall level or catalytic activity of ACC synthase.

Discussion

FEIs are required for anisotropic growth in the root

We show that the FEI1 and FEI2 LRR-RLKs are necessary for anisotropic cell expansion in Arabidopsis root cells, and also play a role in cell expansion in stamen filaments and the hypocotyls of etiolated seedlings. Biochemical studies and genetic analyses with other cellulose-deficient mutants reveal that these FEI kinases modulate cell wall function, including positively regulating the biosynthesis of cellulose, a wall component necessary for anisotropic expansion. Two other divergent RLKs have been implicated in cell wall function: the WAK and THE1 kinases. The WAK kinases are involved in cell expansion in various Arabidopsis tissues and their extracellular domains are tightly linked to the cell wall (Anderson et al., 2001; Wagner and Kohorn, 2001). Interestingly, *wak2* mutants display reduced cell expansion that is sensitive to the level of sugar and salt in the media (Kohorn et al., 2006). However, in contrast to *fei1 fei2*, high sugar levels suppress the cell expansion defect in *wak2*, and it is the extent, not the orientation, of cell expansion that is altered in *wak2*. THE1 has been hypothesized to be involved in monitoring the cell wall integrity, as *the1* mutations suppress the short hypocotyl, but not the cellulose deficient phenotype of *prc1* (Hématy et al., 2007). This is distinct from the FEIs, as the *fei1 fei2* double mutant significantly impairs cellulose biosynthesis. The *the1* mutation also suppresses some, but not all, other mutants affecting cell expansion. Alteration of *THE1* function does not have an effect in a wild-type background, suggesting perhaps genetic redundancy, or that it plays a role only in conditions in which cell wall integrity is compromised. While it would be interesting to determine the interaction between *the1* and *fei1 fei2*, the lack of suppression of

the root elongation phenotype of *prc1* by *the1* may render this genetic interaction non-informative.

Similar to THE1, the FEIs may also sense cell wall signals and in turn provide feedback to the cellulose biosynthesis machinery. One potential ligand for the FEIs is the extracellular protein SOS5. SOS5 encodes a putative cell surface adhesion protein that is required for normal cell expansion (Shi et al., 2003). Several lines of evidence suggest that SOS5 functions in a linear pathway with the FEIs: 1) *sos5* mutants have a very similar root elongation phenotype to *fei1 fei2,* including the dependence on sucrose and salt; 2) The root swelling phenotypes of both *fei1 fei2* and *sos5-2* are suppressed by AIB and AOA, but not by blocking the known ethylene response pathway; 3) Both *fei1 fei2* and *sos5-2* display a thickened hypocotyl phenotype; 4) The *fei1 fei2* and *sos5-2* mutations show a non-additive genetic interaction; and 5) The patterns of expression of the *FEIs* and *SOS5* are largely overlapping (Figure 2. 4 and Shi et al., 2003). Thus, SOS5 acts on the same pathway as the FEIs to mediate the function of the cell wall. As *SOS5* encodes an extracellular protein, it is possible that it acts as, or is involved in the production or presentation of, a FEI ligand.

In addition to *fei1 fei2* and *sos5-2*, the *cob* and *prc1* mutants also display root swelling that is dependent on the concentration of sucrose in the media (Figure 2. 6). It has been proposed that this conditional phenotype reflects defects that are apparent only at high rates of cell elongation, such as in the presence of sucrose (Benfey et al., 1993). However, our data does not support this hypothesis as increasing sucrose above 1% actually leads to a slight decrease in the rate of root elongation, at least in our growth conditions, but the root swelling phenotype of both *fei1 fei2* and *sos5-2* continues to intensify. Furthermore, low levels of NaCl, which reduce the rate of root elongation, also caused swelling in the *sos5-2*

and *fei1 fei2* mutants. The effect of sucrose/salt on *fei1 fei2* mutants is not the result of increased osmotic potential of the media as high levels of sorbitol or mannitol do not induce the phenotype. Our results indicate that wild-type plants are more susceptible to perturbation of cellulose biosynthesis in the presence of high sucrose or salt. How these conditions affect the function of the cell wall remains to be determined.

Kinase activity is dispensable for FEI function

Consistent with their sequences, the FEIs have intrinsic kinase activity; however, kinase activity is not essential for FEI function, at least for the phenotypes that we observed. There are many examples of so-called pseudokinases (reviewed in: Kroiher et al., 2001; Boudeau et al., 2006), which display clear homology to kinases, but which lack conservation of one or more of the catalytic residues in the kinase core. Pseudokinases are especially prevalent in plant genomes, and it has been estimated that approximately 20% of Arabidopsis RLKs are kinase-deficient (Castells and Casacuberta, 2007). For example, STRUBBELIG (SUB), which is a member of the LRR-RLKs (class V) that is involved in the development of multiple organs, includes two alterations in residues that are highly conserved in functional kinases, and genetic and biochemical analyses indicate that the SUB kinase domain is catalytically inactive (Chevalier et al., 2005). The *ACR4* (Arabidopsis homologue of *CR4*) RLK encodes an active kinase, but disruption of the kinase catalytic domain by site-directed mutagenesis does not disrupt its function *in vivo* (Gifford et al., 2005), similar to what we observe for FEI1 and FEI2. One model for how the FEIs and other kinase-deficient RLKs signal is that they heterodimerize with, and are then transphosphorylated by, a kinase-active member of the same protein family. An alternative possibility it that the FEI signaling does not involve phosphorylation, but rather

the proteins act as scaffolds to localize other components in a protein complex or to a particular place in the cell. An example of this is the human KSR (Kinase Suppressor of Ras) protein, which is similar in sequence to protein kinases, but which acts as a scaffold protein that coordinates the assembly of a multiprotein MAP kinase complex at the membrane (Claperon and Therrien, 2007). In any case, the kinase activity of the FEIs, while not essential, is clearly required for optimal function as only a subset of the *fei1 fei2* double mutant transformants harboring the catalytically-inactive version of the FEIs were fully complemented. As kinase activity is not required for function, it is possible that the *fei1* allele used in this study is not a functional null as there is a truncated *FEI1* transcript present. The similarity in the strength of the phenotype of *fei1 fei2* to *sos5-2*, a null allele in a gene acting on the same pathway as the FEIs, argues somewhat against this.

Role of ACS5 in SOS5/FEI pathway

What role do ACS5 and other type-2 ACS enzymes play in regulating cell wall function in the root? ACS5 has been shown to be an enzymatically active ACC synthase (Yamagami et al., 2003), the product of which is ACC, the immediate precursor for ethylene. Ethylene has been shown to play a role in regulating anisotropic growth. In hypocotyls, ethylene inhibits elongation primarily by altering the orientation of cell elongation, which is correlated with a change in the orientation of the microtubules (Steen and Chadwick, 1981; Lang et al., 1982; Roberts et al., 1985; Takahashi et al., 2003). In the root, ethylene strongly inhibits root elongation, but radial expansion is only modestly increased and microtubules appear to be unaffected (Baskin and Williamson, 1992). Thus, in the root, ethylene appears to primarily inhibit the overall amount of cell expansion, not its orientation. One potential

mechanism for this is the elevation of ROS levels in the elongation zone of Arabidopsis roots in response to ACC, which leads to the crosslinking of hydroxyproline-rich glycoproteins (HRGPs) and callose deposition in the cell wall, both of which may contribute to reduced cell expansion (De Cnodder et al., 2005).

There are several mutants that affect growth anisotropy in the root that are linked to ethylene, including *sabre*, *cev1* and *lue1* (Aeschbacher et al., 1995; Ellis et al., 2002; Bouquin et al., 2003). *cev1*, a mutation in the cellulose synthase *CesA3* gene, produces elevated levels of ethylene, and its phenotype is partially suppressed by mutations that disrupt ethylene signaling (Ellis et al., 2002). Similar to *fei1 fei2*, the swollen root phenotype of the *sabre* mutant can be partially rescued by blocking ethylene action through use of ethylene biosynthesis inhibitors, and the *sabre* mutant does not display an increase in ethylene biosynthesis (Aeschbacher et al., 1995). However, in contrast to *fei1 fei2*, *sabre* also can be rescued by inhibition of ethylene perception or by *etr1*. The authors propose that ethylene and SABRE counteract with each other to regulate the degree of radial expansion of root cells. However, neither ethylene-overproducing mutants nor constitutive ethylene signaling mutants have such a dramatic root swollen phenotype, which would be predicted from such a model.

The interaction of type-2 ACSs with the FEIs, and the reversion of the *fei1 fei2* mutant by inhibitors of ethylene biosynthesis strongly suggest a link between ACS function and altered cell wall function in *fei* mutant roots. However, several lines of evidence indicate that this is not the result of altered ethylene levels: 1) Mutants that increase or decrease ethylene biosynthesis do not show a root swelling phenotype (e.g. Vogel et al., 1998); 2) The *fei* phenotype cannot be reversed by blocking ethylene perception; 3) In non-permissive

conditions, ethylene production is not substantially altered in *fei1 fei2* mutant roots. Thus, we conclude that the FEIs do not alter ACS activity or levels, and that the FEIs do not act via ethylene. How then does ACC synthase function in the FEI pathway, and how do the FEIs affect ACC synthase function?

One possibility is that the ACS protein may perform a function distinct from the production of ACC. There are multiple examples of such so-called moonlighting proteins (Moore, 2004). However, if this were the case, it would not explain the reversion of *fei1 fei2* by AIB, which is a structural analog of ACC that should not directly affect ACS function. A second model is that perhaps *fei1 fei2* alter ethylene biosynthesis in a small number of critical cells, which may not be detectable in our analysis, and this elevated ethylene may be perceived by a second, independent ethylene response pathway that functions in this developmental context. This model is possible, but two lines of evidence argue somewhat against it: First, it would not explain the lack of root swelling in various ethylene biosynthesis mutants; Second, it is probable that, similar to ETR1 and its paralogs, any additional ethylene receptor would be blocked by silver ion (Burg and Burg, 1967), and thus silver should, but does not, revert the *fei1 fei2* phenotype. A final model that is consistent with the data is that ACC itself, rather than ethylene, acts as a signaling molecule to regulate cell expansion in the FEI/SOS5 pathway. In such a scenario, AIB, which is a structural analog of ACC, would act as a competitive inhibitor to block binding to a hypothetical ACC receptor. Disruption of ethylene binding would not affect this response, and there would be no alteration in ethylene levels in the mutant. The data are most consistent with this model in which ACC acts as a signal, but additional studies are required to confirm this.

What is the nature of the interaction of the FEI and ACS proteins? The FEI proteins do not appear to phosphorylate ACS5, which is consistent with the lack of requirement for kinase activity for FEI function. Furthermore, ethylene levels are not altered in *fei1 fei2* mutants, suggesting that there is no change in ACS levels or activity. One model consistent with the data is that the FEIs act as a scaffold to localize a fraction of ACS protein to a subdomain of the plasma membrane, and/or to assemble ACS into a protein complex. This would be similar to KSR, a protein kinase that acts as a scaffold in a MAP kinase cascade. This localized ACS would then generate a localized signal to regulate cell wall biosynthesis.

We propose that the FEI kinases play a role in regulating cell wall architecture, possibly mediating interactions between the cell wall and intracellular signaling pathways. The FEI RLKs may act as a scaffold to localize ACS, or may complex ACS with other proteins. The extracellular SOS5 protein also feeds into this pathway. Exactly how ACS functions in this pathway, and how this pathway interacts with the biosynthetic machinery of the cell wall and with other regulatory inputs into cell wall function are important questions for the future.

Methods

Plant material

The Columbia (Col-0) ecotype was used in this study. The *fei1* insertion (SALK_080073)(Alonso et al., 2003) was localized to position +2599 (relative to the translational start site). The *fei2-1* insertion was isolated by PCR screening (using primers FEI2-S5, FEI1-A5, and T-DNA left border primer; See Table S2.1) of a T-DNA insertion library made in a Col *gl1* line (http://www.dartmouth.edu/~tjack/et.html). The *fei2-1* insertion was localized to position +2012. The *fei2-2* insertion (SALK_044226)(Alonso et al., 2003) was localized to position +3386. The insertions sites all were confirmed by DNA sequencing of PCR amplified products using gene-specific and left border primers (Table S2.1) from the respective lines. The *fei1 fei2-1* double mutant line was used all experiments, unless otherwise noted. The *sos5-2* (SALK_125874)(Alonso et al., 2003) and *ein2-50* (SALK_106282)(Alonso et al., 2003) alleles were obtained from the SALK T-DNA insertion collection. The *cob-1* and *prc1-1* alleles were used in this study and were obtained from the Arabidopsis Stock Center. The *eto2* (Kieber et al., 1993) and *etr1-3* (Chang et al, 1993) mutants have been previously described.

Growth conditions and measurement

For growth in soil, plants were grown at 23°C in ~75 μE constant light. For growth *in vitro*, seeds were surface sterilized and cold treated at 4°C for 3 days in the dark and then treated with white light for 3 h. Seedlings were grown on vertical plates containing 1X Murashige and Skoog salts (MS) 1% sucrose, 0.6% phytagel (Sigma) at 22°C in ~100 μE constant light.

For measurements of root elongation, seedlings were grown for 4 days on vertical plates containing no sucrose or in some cases 1% sucrose as noted in legends and then transferred to MS media supplemented with the indicated additions. For the ethylene inhibitor studies, α-aminoisobutyric acid (AIB) (1 mM) and aminooxyacetic acid (AOA) (0.375 mM), 1-methylcyclopropene (MCP) (20 mg Ethylbloc; Floralife, Inc. Walterboro, SC) were added to a 6 L container or silver thiosulfate (0.02 mM) was added to the high sucrose MS agar.

RT-PCR

Total RNA was isolated from seven-day-old seedlings using an RNeasy kit (Qiagen Inc, Valencia, CA). First-strand cDNA was synthesized from 1 μg of the total RNA pretreated with RNase-free DNAase (Promega, Madison, WI) using a SuperScript II kit (Invitrogen Corporation, Carlsbad, CA) with random hexamers according to the manufacturer's instruction. Quantitative RT-PCR was performed with SYBR premix ex-Taq according to the manufacturer's instructions (Takara Bio Inc., Shiga, Japan) using gene-specific primers (See: Table S2.1).

FEI constructs and transgenic plants

Genomic fragments comprising the entire coding region of *FEI1* or *FEI2* and 1 kb of the respective 5' flanking DNA were amplified from BAC T8E3 and T20F21 DNA respectively by PCR (primers: FEI1-S7 and FEI1-A3; FEI2-S7 and FEI2-A4; see: Table S2.1) using Pfu DNA polymerase as described by the manufacturer (Stratagene; La Jolla, CA) and the fragments cloned into pENTR-TOPO-D (Invitrogen Corporation, Carlsbad, CA). The resultant entry plasmid was used in an LR reaction (as described by the manufacturer;

Invitrogen Corporation, Carlsbad, CA) to introduce the respective genes into the binary pGWB16 (Nakagawa et al., 2007) vector for complementation. The kinase domain of *FEI1* were amplified from cDNA by RT-PCR using first strand cDNA generated from wild-type Col RNA and gene-specific primers (FEI1-C2 and FEI1-A5; Table S2.1). Kinase deficient versions of *FEI1* or *FEI2* were obtained by site-directed mutagenesis using primers containing the desired point mutation (FEI1-M2F and FEI1-M2R; FEI2-M2F and FEI2-M2R; see Table S2.1). For expression of a GFP fusion protein, a *FEI2* genomic fragment (amplified using primers FEI2-S8 and FEI2-A4; see Table S2.1) was cloned into pENTR-TOPO-D (Invitrogen Corporation, Carlsbad, CA) and then introduced into the binary vector pGWB5 (Nakagawa et al., 2007). For promoter-GUS fusions, genomic fragments comprising 3 kb of 5' flanking DNA of *FEI1* or *FEI2* were amplified from WT genomic DNA (using primers FEI1-PROM-F1 and FEI1-PROM-R1; and FEI2-PROM-F2 and FEI2-PROM-R2; see Table S2.1), cloned into pENTR4 vector and then introduced into the binary vector pGWB2 (Nakagawa et al., 2007). All clones were confirmed by DNA sequencing. The resulting plasmids were transformed into *Agrobacterium tumefaciens*, strain GV3101. Transgenic plants were generated by the floral dip method (Clough and Bent, 1998) and selected on MS medium containing 50 mg/l kanamycin and 30 mg/l hygromycin. All destination binary vectors were kindly provided by Dr. Tsuyoshi Nakagawa from the Research Institute of Molecular Genetics, Matsue, Japan.

Protein kinase assays

The FEI1 and FEI1^{K334R} kinase domains in pENTR-TOPO-D (see above) were introduced into the plasmid pDEST15 by Gateway cloning (Invitrogen Corporation, Carlsbad, CA). The

respective GST-fusion proteins were isolated using Glutathione Sepharose™ 4 Fast Flow media according to manufacturer's directions (Amersham Biosciences, Piscataway, NJ). ACS5 was purified as described (Chae et al., 2003). Myelin basic protein was purchased from Sigma-Aldrich (St. Louis, MO). The *in vitro* kinase assays were performed in kinase reaction buffer: 50 mM Tris-HCl, pH 7.5, 10 mM $MgCl_2$, 10 mM $MnCl_2$, 10 mM DTT, 10 μM ATP and 5 μCi of [γ-^{32}P] ATP (2 mCi/ml; PerkinElmer Life Science, Waltham, MA). The reaction was incubated at RT for 1 hr and then terminated by adding 10 μl 6× SDS sample buffer. The reaction was then incubated at 97° C for 5 min and then run on 12% SDS-PAGE. The gel was stained with Coomassie Brilliant Blue G-250, dried and subject to autoradiography.

Phloroglucinol staining

Phloroglucinol staining was performed as described (Cano Delgado et al., 2000). Seedlings were fixed in a solution of 3 part ethanol to 1 parts acetic acid, and then cleared in a solution of chloral hydrate:glycerol:water (8:1:2). The seedlings were then stained lignin in a 2% pholorglucinol-HCl solution.

Analysis of FEI expression patterns

Tissue from transgenic lines harboring the *FEI1* or *FEI2* promoter GUS fusions was stained in 100 mM sodium phosphate buffer pH 7.0, with 10 mM EDTA (pH 8.0), 0.5 mM potassium ferricyanide, 0.5 mM potassium ferrocyanide, 1 mM X-Gluc, 0.1% Triton X-100. The tissue was stained either 1 hr or overnight at 37°C as indicated. Chlorophyll was

removed with 95% ethanol. Ten independent transgenic lines were analyzed and a representative line photographed.

Localization of *FEI2-GFP*

Root apices from seven-day-old transgenic plants harboring 35S:*FEI2*-GFP were used for confocal analyses. A Zeiss LSM510 confocal microscope filtered with FITC10 set (excitation 488 nm with emissions 505-530 nm and 530-560 nm) was used for this analysis. 0.8 M mannitol was applied to the root tip on the slides for plasmolysis.

Membrane fractionation of FEI1-myc fusion proteins

FEI1-myc and *FEI2*-myc homozygous transgenic lines were grown on 1% sucrose MS plates for 7 days. Membrane proteins were fractionated by grinding 200 mg of root tissue per 500 µl of buffer (20 mM Tris [pH 8.0], 0.33 M sucrose, 1 mM EDTA, and plant protease inhibitor cocktail (Roche Applied Science, Indianapolis, IN)) and insoluble debris pelleted by centrifugation at 2,000 g for 10 min at 4°C. The supernatant of the spin was designated the total fraction. 150 µl of the total fraction was further centrifuged at 20,000 g for 45 min at 4°C. The supernatant of this spin was designated as the soluble fraction and the pellet was resuspended in 100 µl of buffer to form the microsome fraction. Proteins were separated on a 12% SDS-PAGE and analyzed by western blotting. The anti-myc antibody was obtained from Roche Applied Science (Indianapolis, IN). Anti-Hsc antibody was used as a loading control was obtained from Stressgen (Ann Arbor, MI) and chicken α-mouse secondary antibody was obtained from Santa Cruz (Santa Cruz, CA).

Cellulose synthesis assays

Cellulose synthesis was determined by ^{14}C-glucose labeling as described (Fagard et al., 2000) with the following modifications. Seedlings were grown on 0% sucrose MS plates for 4 days and then transferred to MS media containing various supplements (as indicated in the Figure 2. legends) for 3 days. 1.5 cm root tips were cut and washed 3X with 3 ml of glucose-free MS media. 40 root tips were then incubated in 1 ml MS media containing ^{14}C-glucose (NEN Research, Boston, MA), 0.1 $\mu Ci.ml^{-1}$ for 1 hr in the dark at 22°C in glass tubes. After treatment, the roots were washed three times with 3 ml of glucose-free MS medium. Next, the roots were extracted 3X with 3 ml of boiling absolute ethanol for 20 min, and total aliquots were collected ("ethanol-soluble fraction"). Roots were then resuspended in 3 ml of chloroform/methanol (1:1 v/v), extracted for 20 min at 45°C, and finally resuspended in 3 ml of acetone for 15 min at room temperature with gentle shaking. The remaining material was resuspended in 500 µl of an acetic acid/nitric acid/water solution (8:1:2 v/v/v), for 1 hr in a boiling water bath. Acid-soluble material and acid-insoluble material were separated by glass microfiber filters (GF/A; 2.5cm diameter; Whatman, Maidstone, UK) after which the filters were washed with 5 ml of water. The acid wash and water wash constitute the acid-soluble fraction. The filters yield the acid-insoluble fraction. The amount of label in each fraction was determined by scintillation counting using liquid scintillation fluid (Scintiverse^{TM} BD cocktail, Fisher SX 18-4). The percentage of label incorporation was expressed as 100X the ratio of the amount of label in each fraction to the total amount of label (ethanol plus acid-soluble plus acid-insoluble fractions). Experiments were repeated four times with comparable results.

Microscopy

Arabidopsis root tips were fixed in 2% paraformaldehyde/2.5% glutaraldehyde in phosphate buffer (0.1M sodium phosphate, pH 7.4). After rinsing with phosphate buffer, the samples were post-fixed with 1% osmium tetroxide in sodium phosphate buffer for 30 min. Samples were dehydrated through an increasing ethanol series followed by propylene oxide, and infiltrated and embedded in Polybed 812 epoxy resin (Polysciences, Inc., Warrington, PA). For light microscopy, 1 μm cross-sections of the root tips were cut using a glass knife and a Leica Ultracut S ultramicrotome (Leica Microsystems, Inc., Bannockburn, IL), mounted on glass slides and stained with 1% toluidine blue in 1% borax. For transmission electron microscopy, selected blocks were further trimmed and ultrathin sections (70 nm) were cut using a diamond knife. Ultrathin sections were mounted on 200 mesh copper grids and stained with 4% uranyl acetate and Reynolds' lead citrate. Sections were examined using a LEO EM-910 transmission electron microscope operating at 80kV (Carl Zeiss SMT, Peabody, MA), and digital images were taken using an Orius SC1000 CCD Camera (Gatan, Inc., Pleasanton, CA).

Whole root tips were visualized by first fixing in an ethanol/acid (9:1) solution overnight, followed by two washes in 90% and 70% ethanol. Roots were then cleared with a chloral hydrate/glycerol/water solution (8:1:2) and the tips were visualized using Nomarski optics using a Nikon Eclipse 80i Microscope.

Analysis of microtubules

Seedlings were grown for 5 days on 1% sucrose and then transferred onto plates containing 1% sucrose, 4.5% sucrose or 1% sucrose plus 50 mM NaCl for 3 days. Seedlings were fixed, stained for microtubules, and imaged, all as described (Bannigan et al., 2006). Briefly, the

fixative contained 4% paraformaldehyde, 1% glutaraldehyde, 50 mM Pipes, and 1 mM $CaCl_2$. Seedlings were permeablized by mild digestion of pectin and brief incubation in ice-cold methanol. After rehydration in PBS, roots were incubated with 1/1000 mouse monoclonal α-tubulin antibody (Sigma, St Louis, MO, USA) at 37° C overnight. The secondary antibody used was CY3-conjugated goat anti-mouse (1/200, Jackson Immuno Research, West Chester, PA, USA). The imaging of whole roots was carried out using a Zeiss confocal microscope (Zeiss, 510 Meta; Carl Zeiss) equipped with a 63x oil-immersion objective. Projections were assembled using Zeiss software.

Measurement of ethylene production

Approximately 30 seedlings were grown on 1% sucrose MS plates for three days and then transferred to 4.5% sucrose plates for three days. 1 cm root tips were excised and placed in 22-ml gas chromatography vials that contained 3 ml of 4.5% liquid MS medium. The vials were capped and incubated for 24 hours at 23°C in the dark and the accumulated ethylene measured as as described by Vogel et al. (1998). For etiolated tissue, seedlings (about 40 per vial) were grown in 22 ml gas chromatography vials containing 3 ml of MS medium in the dark for 4 days. The accumulated ethylene was measured by gas chromatography as described (Vogel et al., 1998)

Yeast two–hybrid analysis

The open reading frames corresponding to the various tested genes were cloned into the bait plasmid (pEG202) or prey plasmid (pJG4-5) by Gateway cloning from the respective entry

clones made with the primers shown in Table S2.1 online. The plasmids were transformation into the yeast strain EGY48 via LiOAc transformation as described (Chen et al. 1992).

Reference

Aeschbacher, R., Hauser, M.-T., Feldmann, K.A., and Benfey, P.N. (1995). The *SABRE* gene is required for normal cell expansion in *Arabidopsis*. Gene Dev. **9,** 330-340.

Alonso, J.M., Stepanova, A.N., Leisse, T.J., Kim, C.J., Chen, H., Shinn, P., Stevenson, D.K., Zimmerman, J., Barajas, P., Cheuk, R., Gadrinab, C., Heller, C., Jeske, A., Koesema, E., Meyers, C.C., Parker, H., Prednis, L., Ansari, Y., Choy, N., Deen, H., Geralt, M., Hazari, N., Hom, E., Karnes, M., Mulholland, C., Ndubaku, R., Schmidt, I., Guzman, P., Aguilar-Henonin, L., Schmid, M., Weigel, D., Carter, D.E., Marchand, T., Risseeuw, E., Brogden, D., Zeko, A., Crosby, W.L., Berry, C.C., and Ecker, J.R. (2003). Genome-wide insertional mutagenesis of *Arabidopsis thaliana*. Science **301,** 653-657.

Anderson, C.M., Wagner, T.A., Perret, M., He, Z.H., He, D., and Kohorn, B.D. (2001). WAKs: cell wall-associated kinases linking the cytoplasm to the extracellular matrix. Plant Mol. Biol. **47,** 197-206.

Bannigan, A., Wiedemeier, A.M.D., Williamson, R.E., Overall, R.L., and Baskin, T.I. (2006). Cortical microtubule arrays lose uniform alignment between cells and are oryzalin resistant in the Arabidopsis mutant, *radially swollen 6*. Plant Cell Physiol. **47,** 949-958.

Baskin, T.I. (2001). On the alignment of cellulose microfibrils by cortical microtubules: A review and a model. Protoplasma **215,** 150-171.

Baskin, T.I. (2005). Anisotropic expansion of the plant cell wall. Annu. Rev. Cell Dev. Biol. **21,** 203-222.

Baskin, T.I., and Williamson, R.E. (1992). Ethylene, microtubules and root morphology in wild-type and mutant *Arabidopsis* seedlings. Curr. Top. Plant Biochem. Physiol. **11,** 118-130.

Beeckman, T., Przemeck, G.K.H., Stamatiou, G., Lau, R., Terryn, N., De Rycke, R., Inze, D., and Berleth, T. (2002). Genetic complexity of cellulose synthase A gene function in Arabidopsis embryogenesis. Plant Physiol. **130,** 1883-1893.

Benfey, P.N., Linstead, P.J., Roberts, K., Schiefelbein, J.W., Hauser, M.-T., and Aeschbacher, R. (1993). Root development in Arabidopsis: four mutants with dramatically altered root morphogenesis. Development **119,** 57-70.

Birnbaum, K., Shasha, D.E., Wang, J.Y., Jung, J.W., Lambert, G.M., Galbraith, D.W., and Benfey, P.N. (2003). A gene expression map of the Arabidopsis root. Science **302,** 1956-1960.

Boudeau, J., Miranda-Saavedra, D., Barton, G.J., and Alessi, D.R. (2006). Emerging roles of pseudokinases. Trends Cell Biol. **16,** 443-452.

Bouquin, T., Mattsson, O., Naested, H., Foster, R., and Mundy, J. (2003). The *Arabidopsis lue1* mutant defines a katanin p60 ortholog involved in hormonal control of microtubule orientation during cell growth. J Cell Sci. **116,** 791-801.

Burg, S., and Burg, E. (1967). Molecular requirements for the biological activity of ethylene. Plant Physiol. **42,** 144-152.

Caño-Delgado, A., Penfield, S., Smith, C., Catley, M., and Bevan, M. (2003) Reduced cellulose synthesis invokes lignification and defense responses in *Arabidopsis thaliana*. Plant J. **34**,351-362.

Castells, E., and Casacuberta, J.M. (2007). Signalling through kinase-defective domains: the prevalence of atypical receptor-like kinases in plants. J. Exp. Bot. **58,** 3503-3511.

Chae, H.S., Faure, F., and Kieber, J.J. (2003)The *eto1*, *eto2*, and *eto3* mutations and cytokinin treatment increase ethylene biosynthesis in Arabidopsis by increasing the stability of ACS protein.Plant Cell.**15**, 545-559.

Chae, H.S., and Kieber, J.J. (2005). Eto Brute? The role of ACS turnover in regulating ethylene biosynthesis. Trend Plant Sci. **10,** 291-296.

Chang, C., Kwok, S.F., Bleecker, A.B., and Meyerowitz, E.M. (1993)Arabidopsis ethylene-response gene ETR1: similarity of product to two-component regulators. Science. **262**,539-544.

Chen, D.C.. Yang, B.C., and Kuo, T.T. (1992) One-step transformation of yeast in stationary phase. Curr. Genet. **21**, 83-84.

Chevalier, D., Batoux, M., Fulton, L., Pfister, K., Yadav, R.K., Schellenberg, M., and Schneitz, K. (2005). STRUBBELIG defines a receptor kinase-mediated signaling pathway regulating organ development in Arabidopsis. Proc. Natl. Acad. Sci. USA **102**, 9074-9079.

Claperon, A., and Therrien, M. (2007). KSR and CNK: two scaffolds regulating RAS-mediated RAF activation. Oncogene **26,** 3143-3158.

Clough, S.J., and Bent, A.F. (1998). Floral dip: a simplified method for Agrobacterium-mediated transformation of *Arabidopsis thaliana*. Plant J. **16,** 735-743.

Darley, C.P., Forrester, A.M., and McQueen-Mason, S.J. (2001). The molecular basis of plant cell wall extension. Plant Mol Biol. **47,** 179-195.

De Cnodder, T., Vissenberg, K., Van Der Straeten, D., and Verbelen, J.P. (2005). Regulation of cell length in the *Arabidopsis thaliana* root by the ethylene precursor 1-

aminocyclopropane- 1-carboxylic acid: a matter of apoplastic reactions New Phytol. **168,** 541-550.

Desprez, T., Vernhettes, S., Fagard, M., Refrégier, G., Desnos, T., Aletti, E., Py, N., Pelletier, S., and Höfte, H. (2002). Resistance against herbicide isoxaben and cellulose deficiency caused by distinct mutations in same cellulose synthase isoform CESA6. Plant Physiol. **128,** 482-490.

Ellis, C., Karafyllidis, I., Wasternack, C., and Turner, J.G. (2002). The Arabidopsis mutant *cev1* links cell wall signaling to jasmonate and ethylene responses. Plant Cell **14,** 1557-1566.

Fagard, M., Desnos, T., Desprez, T., Goubet, F., Refregier, G., Mouille, G., McCann, M., Rayon, C., Vernhettes, S., and Hofte, H. (2000). *PROCUSTE1* encodes a cellulose synthase required for normal cell elongation specifically in roots and dark-grown hypocotyls of Arabidopsis. Plant Cell **12,** 2409-2424.

Gifford, M.L., Robertson, F.C., Soares, D.C., and Ingram, G.C. (2005). ARABIDOPSIS CRINKLY4 function, internalization, and turnover are dependent on the extracellular crinkly repeat domain. Plant Cell **17,** 1154-1166.

Green, P.B. (1980). Organogenesis-a biophysical view. Annu. Rev. Plant Physiol. **31,** 51-82.

He, Z.-H., Fujiki, M., and Kohorn, B.D. (1996). A cell wall-associated, receptor-like protein kinase. J. Biol. Chem. **271,** 19789-19793.

Heim, D.R., Larrinua, I.M., Murdoch, M.G., and Roberts, J.L. (1998). Triazofenamide is a cellulose biosynthesis inhibitor. Pestic. Biochem. Physiol. **59,** 163-168.

Hématy, K., and Höfte, H. (2008). Novel receptor kinases involved in growth regulation. Curr. Opin. Plant Biol. **11,** 321-328.

Hématy, K., Sado, P.-E., Van Tuinen, A., Rochange, S., Desnos, T., Balzergue, S., Pelletier, S., Renou, J.-P., and Höfte, H. (2007). A receptor-like kinase mediates the response of Arabidopsis cells to the inhibition of cellulose synthesis. Curr. Biol. **17,** 922-931.

Humphrey, T.V., Bonetta, D.T., and Goring, D.R. (2007). Sentinels at the wall: cell wall receptors and sensors. New Phytol. **176,** 7-21.

Kieber, J.J., Rothenburg, M., Roman, G., Feldmann, K.A., and Ecker, J.R. (1993). *CTR1*, a negative regulator of the ethylene response pathway in *Arabidopsis*, encodes a member of the Raf family of protein kinases. Cell **72,** 427-441.

Kohorn, B.D., Kobayashi, M., Johansen, S., Riese, J., Huang, L.F., Koch, K., Fu, S., Dotson, A., and Byers, N.R. (2006). An Arabidopsis cell wall-associated kinase required for invertase activity and cell growth. Plant J. **46,** 307-316.

Kroiher, M., Miller, M.A., and Steele, R.E. (2001). Deceiving appearances: signaling by "dead" and "fractured" receptor protein-tyrosine kinases. Bioessays **23,** 69-76.

Lang, J., Eisinger, W., and Green, P. (1982). Effects of ethylene on the orientation of microtubules and cellulose microfibrils of pea epicotyl cells with polylamellate cell walls. Protoplasma **110,** 5-14.

Moore, B. (2004). Bifunctional and moonlighting enzymes: lighting the way to regulatory control. Trends Plant Sci. **9,** 221-228.

Morillo, S.A., and Tax, F.E. (2006). Functional analysis of receptor-like kinases in monocots and dicots. Curr. Opin. Plant Biol. **9,** 460-469.

Nakagawa, T., Suzuki, T., Murata, S., Nakamura, S., Hino, T., Maeo, K., Tabata, R., Kawai, T., Tanaka, K., Niwa, Y., Watanabe, Y., Nakamura, K., Kimura, T., and Ishiguro, S. (2007). Improved Gateway binary vectors: high-performance vectors for creation of fusion constructs in transgenic analysis of plants. Biosci. Biotechnol. Biochem. **71,** 2095-2100.

Paredez, A.R., Somerville, C.R., and Ehrhardt, D.W. (2006). Visualization of cellulose synthase demonstrates functional association with microtubules. Science **312,** 1491-1495.

Peng, L., Hocart, C.H., Redmond, J.W., and Williamson, R.E. (2000). Fractionation of carbohydrates in Arabidopsis root cell walls shows that three radial swelling loci are specifically involved in cellulose production. Planta **211,** 406-414.

Roberts, I.N., Lloyd, C.W., and Roberts, K. (1985). Ethylene-induced microtubule reorientations: mediation by helical arrays. Planta **164,** 439-447.

Roudier, F., Fernandez, A.G., Fujita, M., Himmelspach, R., Borner, G.H.H., Schindelman, G., Song, S., Baskin, T.I., Dupree, P., Wasteneys, G.O., and Benfey, P.N. (2005). COBRA, an Arabidopsis extracellular glycosyl-phosphatidyl inositol-anchored protein, specifically controls highly anisotropic expansion through its involvement in cellulose microfibril orientation. Plant Cell **17,** 1749-1763.

Scheible, W.R., Eshed, R., Richmond, T., Delmer, D., and Somerville, C. (2001). Modifications of cellulose synthase confer resistance to isoxaben and thiazolidinone herbicides in Arabidopsis *ixr1* mutants. Proc. Natl. Acad. Sci. USA **98,** 10079-10084.

Schindelman, G., Morikami, A., Jung, J., Baskin, T.I., Carpita, N.C., Derbyshire, P., McCann, M.C., and Benfey, P.N. (2001). COBRA encodes a putative GPI-anchored

protein, which is polarly localized and necessary for oriented cell expansion in Arabidopsis. Genes Dev. **15,** 1115-1127.

Sebastià, C.H., Hardin, S.C., Clouse, S.D., Kieber, J.J., and Huber, S.C. (2004). Identification of a new motif for CDPK phosphorylation in vitro that suggests ACC synthase may be a CDPK substrate. Arch. Biochem. Biophys. **428,** 81-91.

Shi, H., Kim, Y., Guo, Y., Stevenson, B., and Zhu, J.-K. (2003). The Arabidopsis *SOS5* locus encodes a putative cell surface adhesion protein and is required for normal cell expansion. Plant Cell **15,** 19-32.

Shiu, S.-H., and Bleecker, A.B. (2001). Receptor-like kinases from Arabidopsis form a monophyletic gene family related to animal receptor kinases. Proc. Natl. Acad. Sci. USA **98,** 10763-10768.

Somerville, C. (2006). Cellulose synthesis in higher plants. Annu. Rev. Cell. Dev. Biol. **22,** 53-78.

Steen, D.A., and Chadwick, A. (1981). Ethylene effects in pea stem tissue. Evidence for microtubule mediation. Plant Physiol. **67,** 460-466.

Taiz, L. (1984). Plant cell expansion: regulation of cell wall mechanical properties. Annu. Rev. Plant Physiol. **35,** 585-657.

Takahashi, H., Kawahara, A., and Inoue, Y. (2003). Ethylene promotes the induction by auxin of the cortical microtubule randomization required for low-pH-induced root hair initiation in lettuce (*Lactuca sativa L*.) seedlings. Plant Cell Physiol. **44,** 932-940.

Tatsuki, M., and Mori, H. (2001). Phosphorylation of tomato 1-aminocyclopropane-1-carboxylic acid synthase, LE-ACS2, at the C-terminal region. J. Biol. Chem. **276,** 28051-28057.

Vogel, J.P., Woeste, K.W., Theologis, A., and Kieber, J.J. (1998). Recessive and dominant mutations in the ethylene biosynthetic gene *ACS5* of *Arabidopsis* confer cytokinin insensitivity and ethylene overproduction, respectively. Proc. Natl. Acad. Sci. USA **95,** 4766-4771.

Wagner, T.A., and Kohorn, B.D. (2001). Wall-associated kinases are expressed throughout plant development and are required for cell expansion. Plant Cell **13,** 303-318.

Yamagami, T., Tsuchisaka, A., Yamada, K., Haddon, W.F., Harden, L.A., and Theologis, A. (2003). Biochemical diversity among the 1-amino-cyclopropane-1-carboxylate synthase isozymes encoded by the Arabidopsis gene family. J. Biol. Chem. **278,** 49102-49112.

Zimmermann, P., Hennig, L., and Gruissem, W. (2005). Gene-expression analysis and network discovery using Genevestigator. Trends Plant Sci. **10,** 407-409.

Figure 2.1. *fei1 fei2* mutants display conditional root anisotropic growth defects.

(A) Structures of the predicted FEI and ERECTA proteins. The percent identity between the kinase or LRR N-terminal domain of FEI1 and FEI2 or FEI2 and ERECTA is indicated. **(B)** Cartoon of *fei1*, *fei2-1* and *fei2-2* alleles. Boxes represent exons (blue area represents the kinase domain) and the triangles indicate the position of T-DNA insertions. **(C - D)** Phenotype of indicated seedlings grown on MS plus 1% sucrose **(C)** or plus 4.5% sucrose **(D)** for 9 days. Bars = 1 cm in top panels, and 1 mm in bottom. **(E)** RT-PCR analysis of *fei1* and *fei2* mutants. **Top:** Primers specific for the full-length ORF corresponding to the gene indicated on the right of the each photo (See Supplemental Table 1 online for the sequences of the primers used) were used to amplify the respective gene for 30 cycles from cDNA derived from the indicated line, or from wild-type genomic DNA (gDNA). The actin gene was amplified as control. **Bottom:** Primers specific for a portion of the *FEI1* gene 5' to the site of the T-DNA insertion (See Supplemental Table 1 online) were used in a PCR reaction for 30 cycles from cDNA derived from the indicated line. **(F)** Quantification of root growth after transfer to permissive or non-permissive conditions. The indicated seedlings were grown on MS media containing 0% sucrose for 4 days and then transferred to MS media containing either 0% or 4.5% sucrose as indicated. Root growth from the time of transfer until day nine is indicated on the Y-axis. Error bars show SE (n>30). **(G)** Kinetics of root elongation of wild-type and *fei1 fei2* mutant seedlings. Wild-type (WT) or *fei1 fei2* mutant seedlings were grown on MS media containing 0% sucrose for 4 days and then transferred to MS media containing either 0% or 4.5% sucrose as indicated. Root lengths were measured each day after transfer, and the amount of root growth that occurred each day after transfer then calculated. Error bars show SE (n>15). **(H)** Phloroglucinol staining for lignin (red color) of seedlings grown on MS media containing 0% sucrose for 4 days and then transferred to MS media containing 4.5% sucrose for 5 days. Bar = 0.5 cm.

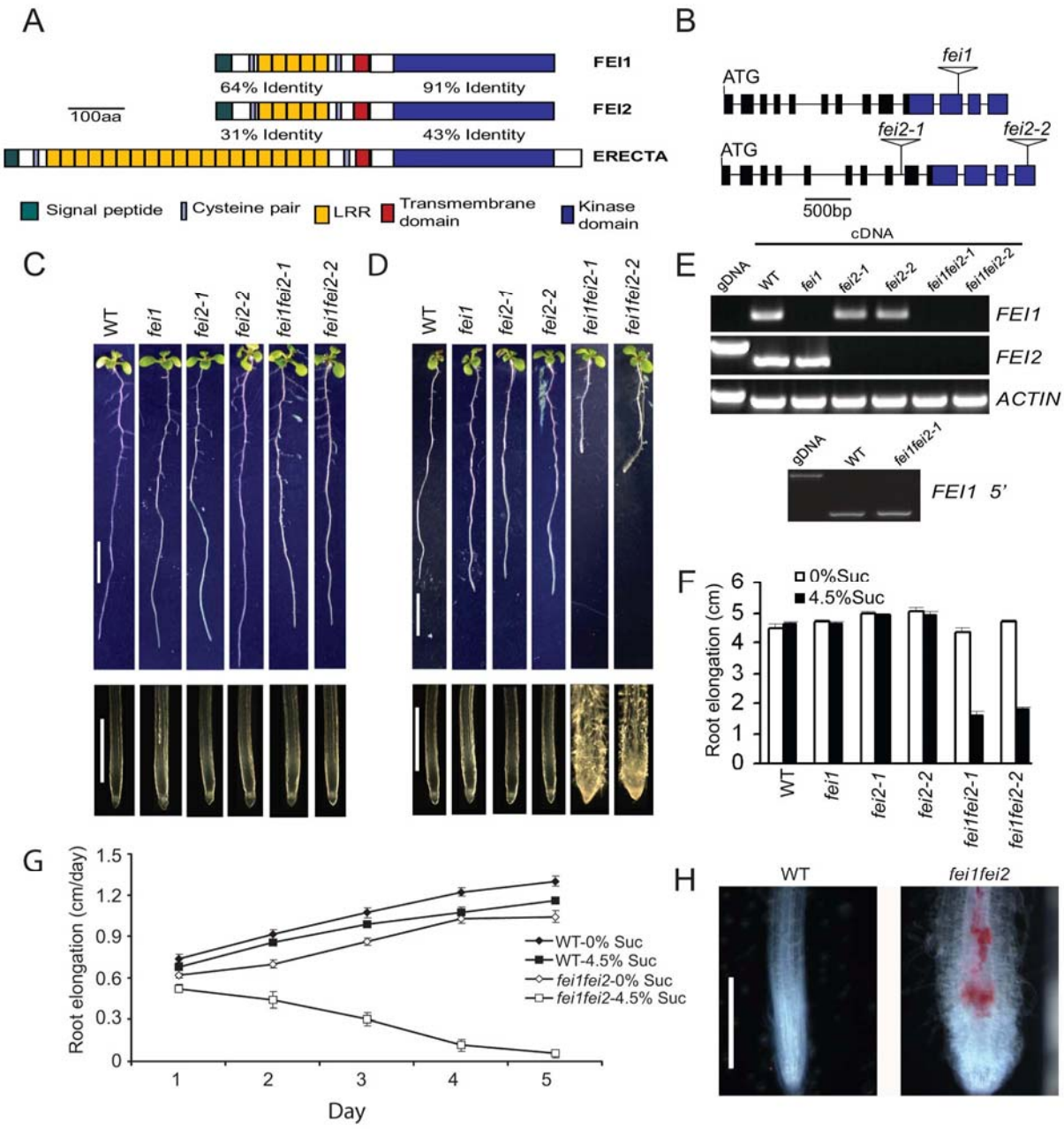
A
FEI1
64% Identity
91% Identity
FEI2
100aa
31% Identity
43% Identity
ERECTA
Signal peptide
Cysteine pair
LRR
Transmembrane domain
Kinase domain
B
fei1
ATG
fei2-1
fei2-2
ATG
500bp
C
WT
fei1
fei2-1
fei2-2
fei1fei2-1
fei1fei2-2
D
WT
fei1
fei2-1
fei2-2
fei1fei2-1
fei1fei2-2
E
cDNA
gDNA
WT
fei1
fei2-1
fei2-2
fei1fei2-1
fei1fei2-2
FEI1
FEI2
ACTIN
gDNA
WT
fei1fei2-1
FEI1 5'
F
0%Suc
4.5%Suc
Root elongation (cm)
0
1
2
3
4
5
6
WT
fei1
fei2-1
fei2-2
fei1fei2-1
fei1fei2-2
G
Root elongation (cm/day)
0
0.3
0.6
0.9
1.2
1.5
1
2
3
4
5
Day
WT-0% Suc
WT-4.5% Suc
fei1fei2-0% Suc
fei1fei2-4.5% Suc
H
WT
fei1fei2

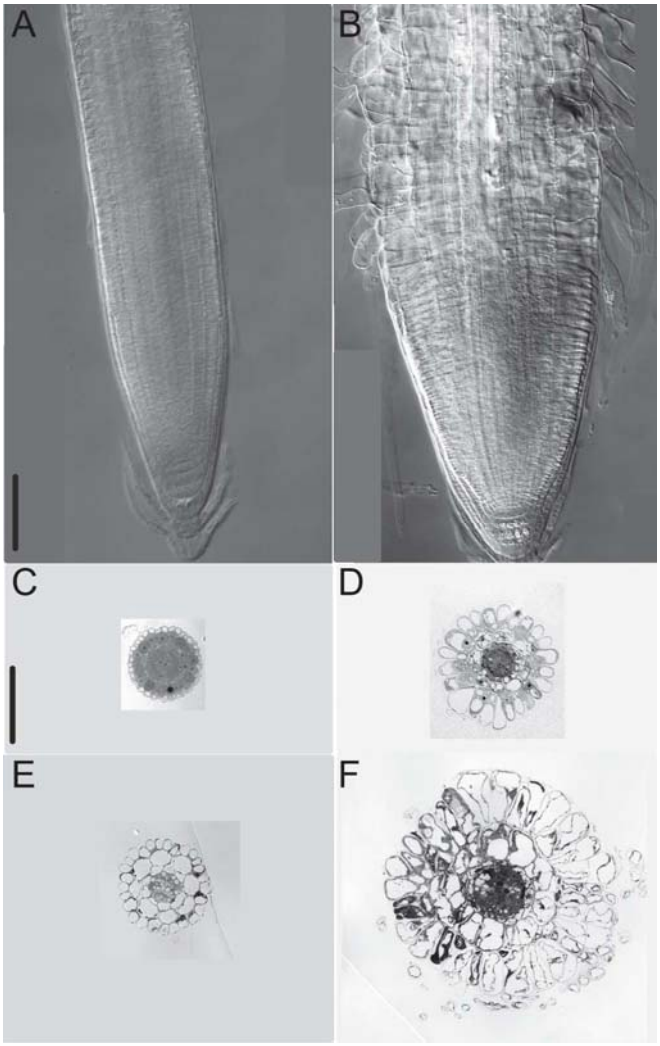

Figure 2.2. Analysis of wild-type and *fei1 fei2* mutant roots four days after transfer from media containing 0% sucrose to media containing 4.5% sucrose.

(A, B) Cleared whole-mount of wild-type **(A)** and *fei1 fei2* **(B)** root viewed with Normaski optics. Note that abnormal lateral expansion in the mutant root is most apparent in the epidermis. **(C, D)** Transverse section through the meristem of a wild-type **(C)** or a *fei1 fei2* **(D)** mutant root. **(E, F)** Transverse section through the elongation zone of a wild-type **(E)** or a *fei1 fei2* **(F)** mutant root. Scale bar (Lower left) = 100 μm.

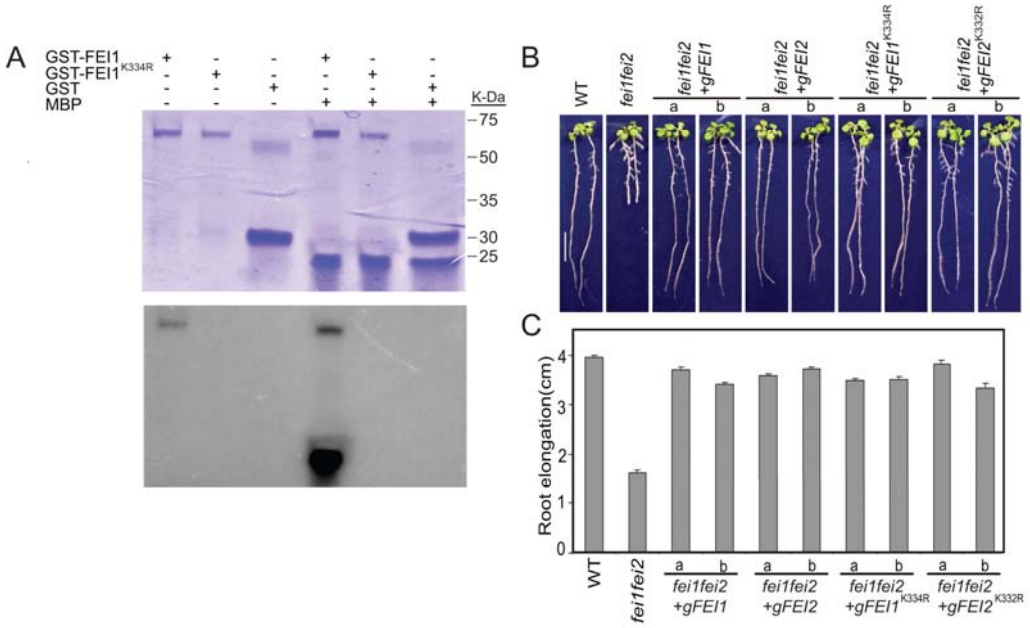

Figure 2.3. Intrinsic kinase activity is not required for FEI function.

(A) Kinase activity of FEI1. Wild-type or FEI1^{K334R} proteins were expressed in *E. coli* as glutathione S-transferase (GST) fusion proteins, purified by glutathione-affinity chromatography, and then subjected to an *in vitro* kinase assay and analyzed by SDS-PAGE. Purified GST was included as a control, and myelin basic protein (MBP) as a substrate. Top: Staining of the gel with Coomassie blue; Bottom: Autoradiograph of the gel. The positions of MW markers are shown on the right. **(B)** Complementation of *fei1 fei2* mutant phenotype by introduction of a wild-type (*gFEI1* or *gFEI1*) or kinase-inactive (*gFEI1*^{K334R} or *gFEI2*^{K332R}) version of *FEI1* or *FEI2*. Two independent lines ("a" and "b") are shown for each. Seedlings were grown for four days on MS media containing 0% sucrose and then transferred for four days to MS media containing 4.5% sucrose and representative seedlings photographed. **(C)** Quantification of root elongation from **(B)**. The mean (n>15) ± SE of seedling growth from days 4 to 8 is shown.

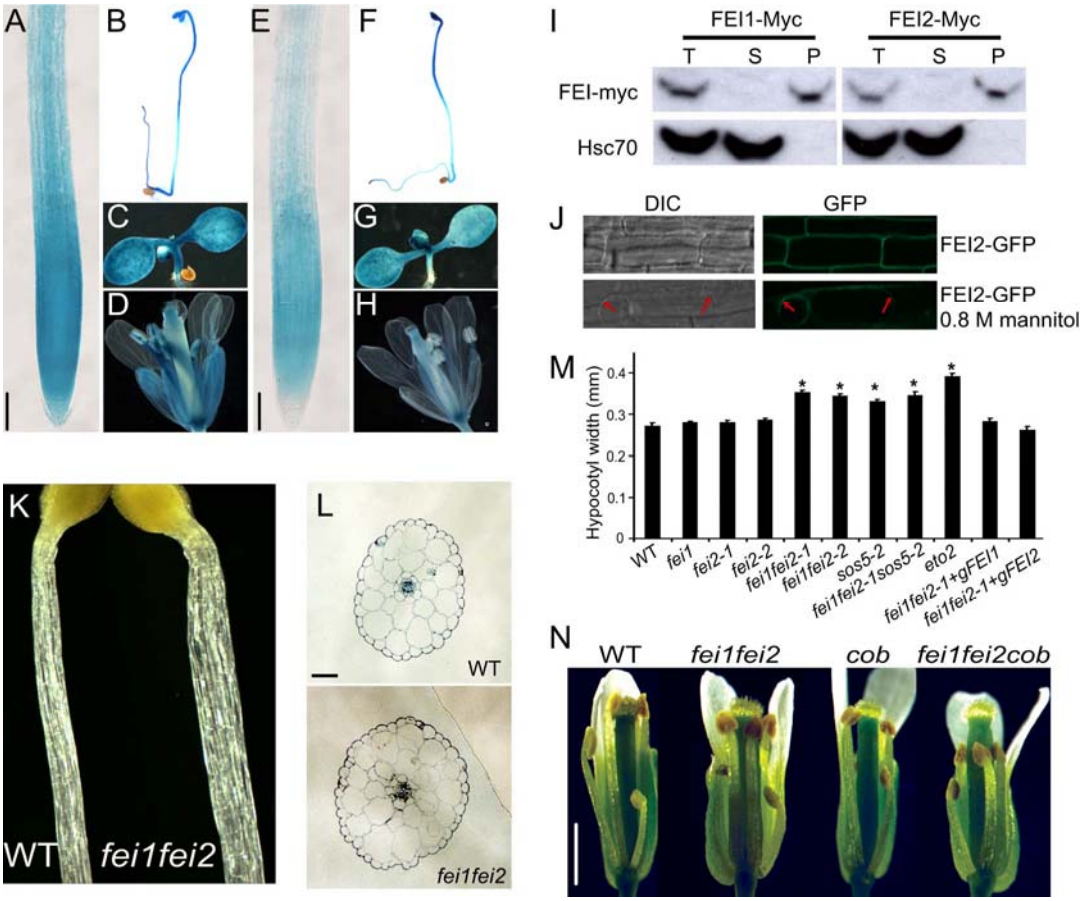

Figure 2.4. FEI1 and FEI2 expression, localization and function in hypocotyls and flowers.

(A-H) Staining (blue color) of transgenic lines harboring the promoter of *FEI1* **(A-D)** or *FEI2* **(E-H)** fused to GUS. **(A, C)** and **(E, G)** are from seedlings grown on MS media for seven days. **(B)** and **(F)** are three-day-old etiolated seedlings. **(D, H)** are flowers from plants grown in soil under long days for three weeks. Scale bars in **(A)** and **(E)** represent 100 µm. **(I)** Root tissue from plants expressing FEI1-myc or FEI2-myc was fractionated into soluble and microsome fractions. The total (T), soluble (S), and microsome (P) fractions were subjected to western blotting and probed with an anti-C-myc (top) or anti-Hsc70 (bottom) antibody. **(J)** Localization of FEI2-GFP fusion proteins. **Top**: DIC or GFP image of root cells from MS-grown seedlings; **Bottom**: image from seedlings plasmolyzed in 0.8 M mannitol. Red arrows indicate regions of membrane that has detached from the cell wall.**(K)** Image of hypocotyls from WT (left) and *fei1 fei2* mutant (right) three-day-old etiolated seedlings. Note that the *fei1 fei2* hypocotyls are thicker.**(L)** Transverse sections through hypocotyls of WT or *fei1 fei2* mutant etiolated three-day-old seedlings. Scale bar = 50 µm. **(M)** Quantification of hypocotyl widths from etiolated seedlings. Asterisks indicate a significant difference from wild type (Student's t-test $p < 0.05$, $n = 20$). Error bars show SE (n=20).**(N)** Stage 12 flowers from indicated genotypes. Several petals and sepals were removed from each flower to reveal the inner parts. Note that the *fei1 fei2 cob* triple mutants have shorter stamen filaments. Bar = 1 mm.

Figure 2.5. The *fei* mutants affect cell wall function.

(A) High sucrose or NaCl enhance the effect of isoxaben. Wild-type seedlings were grown on MS media containing 0% sucrose for 4 days and then transferred to the MS media plus the indicated supplement in the presence of 0 (control) or 1 nM isoxaben as indicated. 24 hours after transfer, root tips were imaged. Scale bar = 1 mm.**(B)** TEM of cell wall junctions from wild type or *fei1 fei2* mutant epidermal root cells from seedlings grown on 4.5% sucrose. Scale bar = 1 μm. **(C)** Response of indicated seedlings to isoxaben. Seedlings of the indicated genotype were grown on MS media containing 0% sucrose for 4 days and then transferred to media containing 1% sucrose and the indicated level of isoxaben. 24 hours after transfer, root tips were imaged. Bar = 1 mm.**(D)** Incorporation of ^{14}C glucose into acid soluble or insoluble fractions from excised root tips from wild-type or *fei* mutant seedlings grown in 0% sucrose for four days and then transferred to 0% or 4.5% sucrose as indicated for three days. The mean (n=3) ± SE is shown. Asterisks indicate a statistical difference between *fei1 fei2* and the respective WT sample (Student's t-test $p<0.05$).**(E)** Incorporation of ^{14}C glucose into acid soluble or insoluble fractions from excised roots from wild-type or *fei* mutants seedlings that were grown in 0% sucrose for four days and then transferred to 4.5% sucrose in the absence (control) or presence of AIB (1 mM) as indicated for three days. The mean (n=3) ± SE is shown. Asterisks indicate a statistical difference between *fei1 fei2* and the respective WT sample (Student's t-test $p<0.05$).

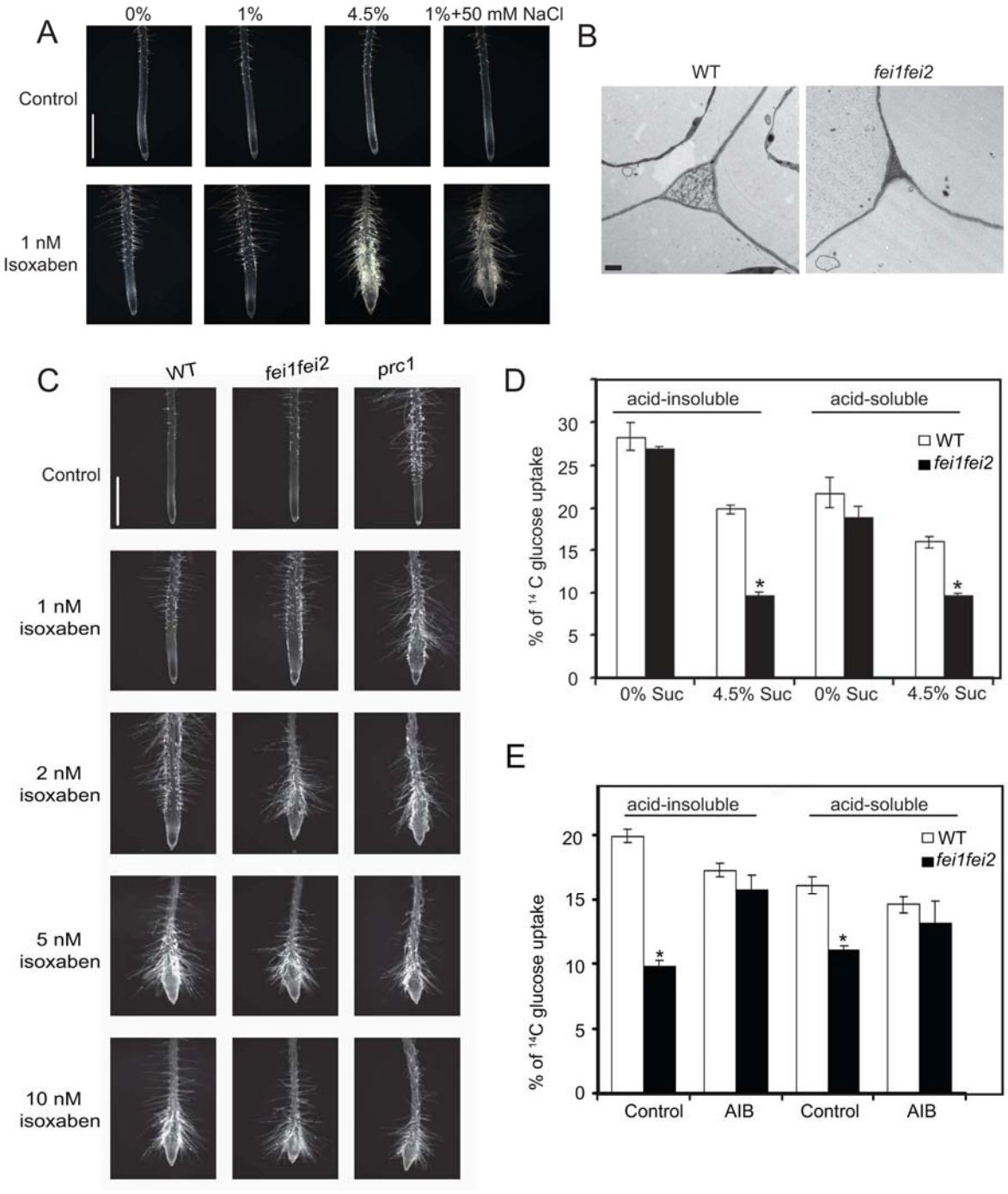
A
0%
1%
4.5%
1%+50 mM NaCl
Control
1 nM
Isoxaben
B
WT
fei1fei2
C
WT
fei1fei2
prc1
Control
1 nM
isoxaben
2 nM
isoxaben
5 nM
isoxaben
10 nM
isoxaben
D
acid-insoluble
acid-soluble
WT
fei1fei2
% of 14 C glucose uptake
0% Suc
4.5% Suc
0% Suc
4.5% Suc
E
acid-insoluble
acid-soluble
WT
fei1fei2
% of 14C glucose uptake
Control
AIB
Control
AIB

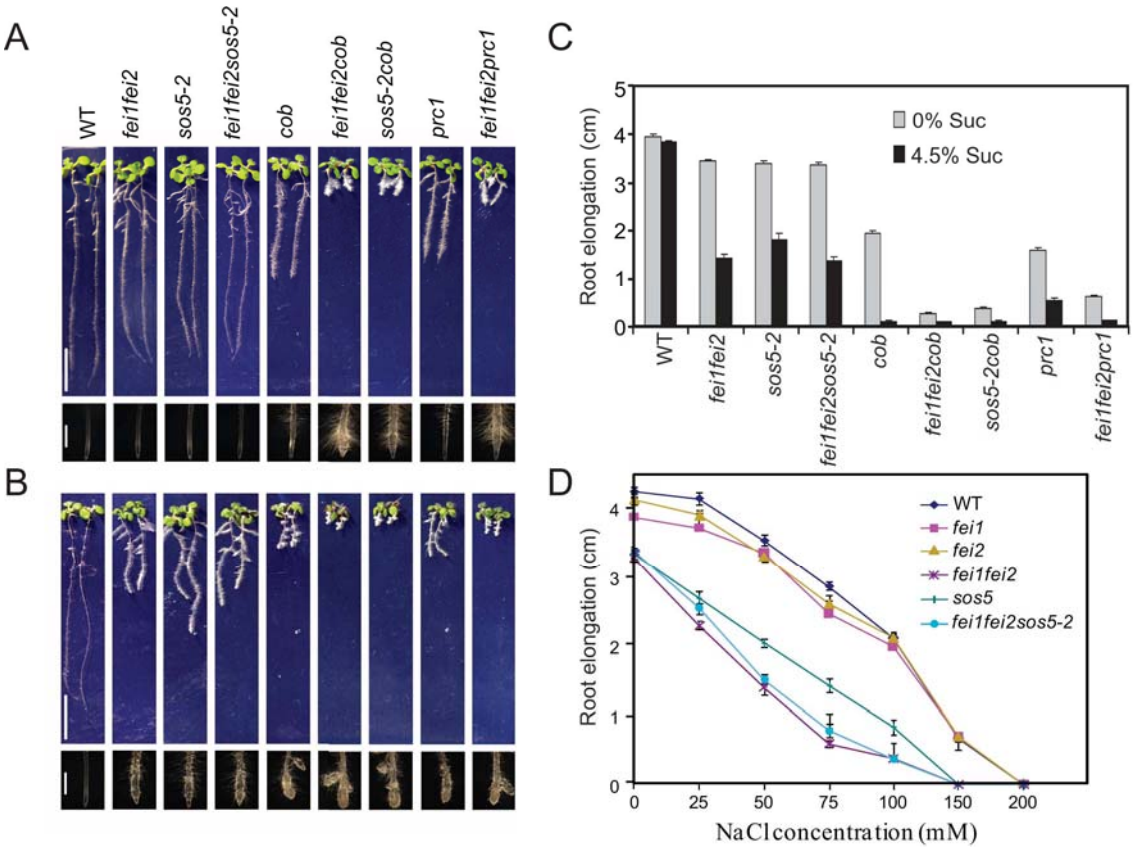

Figure 2.6. Genetic interaction of *fei1 fei2* with other mutants affecting cell elongation.

(A-B) Phenotype of wild-type and various mutant seedlings grown in media containing 0% sucrose for four days and then transferred to MS media containing no **(A)** or 4.5% **(B)** sucrose for four days. Top panel: Scale bar = 1 cm, Bottom panel, close-up of root tip, Scale bar = 1 mm. **(C)** Quantification of root elongation of various mutants grown and transferred as in **(A, B)**. Values represent the mean of growth four days after transfer to respective conditions. Error bars show SE (n>15). **(D)** Quantification of total root elongation of the indicated lines four days after transfer from MS media containing 1% sucrose to the same media with various levels of NaCl added. Error bars show SE (n > 15).

Figure 2.7. Role of ACC/ethylene on *fei* phenotype.

(A) Phenotypes of seedlings grown on MS media containing 0% sucrose for 4 days and then transferred to MS media containing 4.5% sucrose plus nothing, AOA (0.375 mM) or AIB (1 mM) as indicated. Scale bar = 1 cm. Note that the distribution of lateral roots in the *fei1 fei2* mutants in the presence of high sucrose is variable; the architecture of the *fei1 fei2 ein2* is not substantially different from the *fei1 fei2* parent.**(B)** Close-up of root tips from (A). Scale bar = 1 mm. **(C)** Yeast two-hybrid interactions among the FEIs and ACSs. Bait and Prey vectors containing the soluble kinase domains of WT or mutant FEI1 and FEI2 were cloned into a yeast two-hybrid bait vector were co-transformed into yeast with the indicated WT and *Eto* mutant ACS preys. Positive interactions result in Leu prototrophy (growth on –Leu). The soluble, kinase domain of ERECTA empty bait (pEG202) and prey (pJG4-5) vectors were used as controls.**(D)** FEI1 does not phosphorylate ACS5 *in vitro*. Top: Coomassie blue stained gel of purified GST-FEI and/or ACS5 protein. Bottom: autoradiograph following an *in vitro* kinase assay. The arrows indicate the position of ACS5.

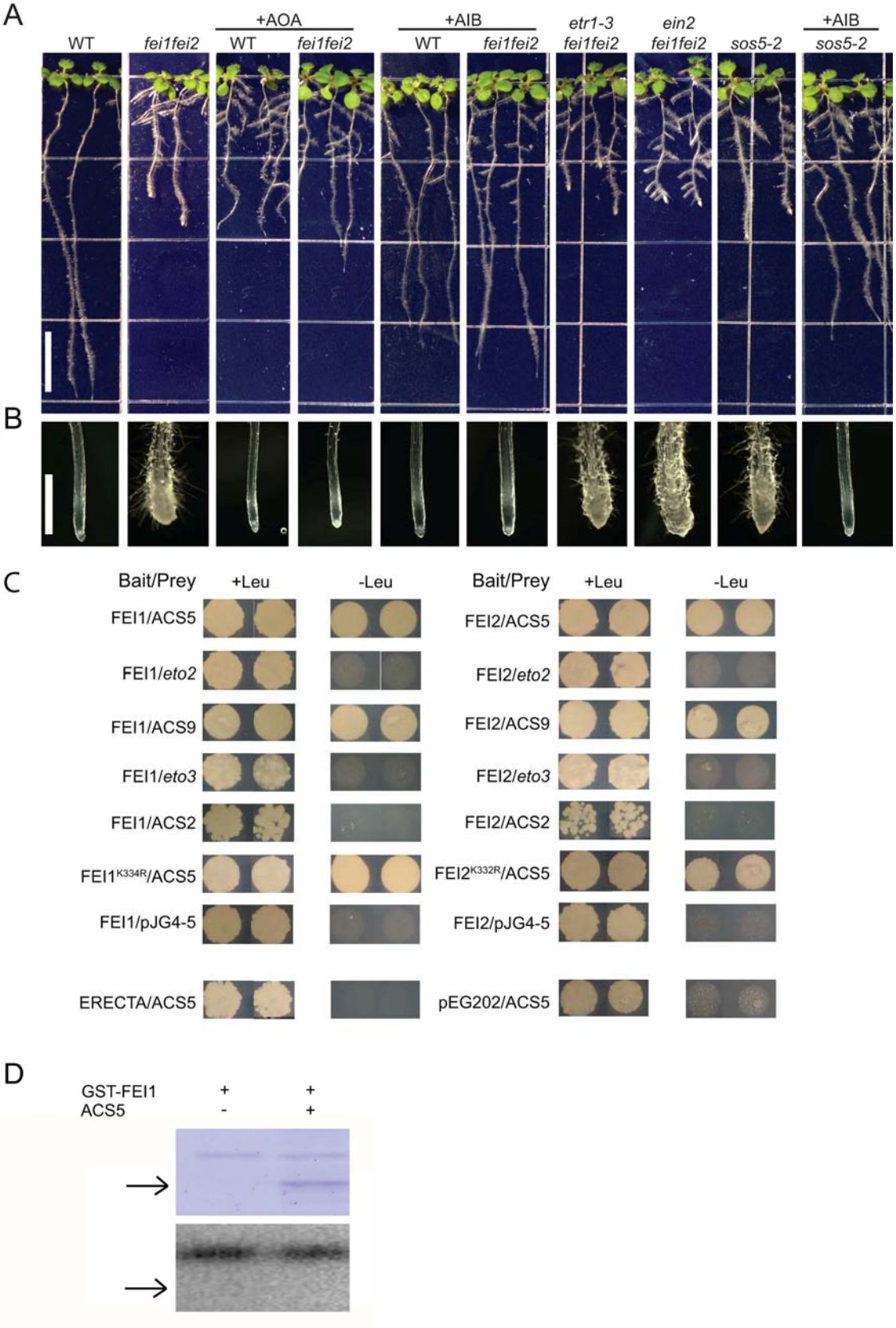
A
WT
fei1fei2
+AOA
WT
fei1fei2
+AIB
WT
fei1fei2
etr1-3 fei1fei2
ein2 fei1fei2
sos5-2
+AIB
sos5-2
B
C
Bait/Prey
+Leu
-Leu
FEI1/ACS5
FEI1/eto2
FEI1/ACS9
FEI1/eto3
FEI1/ACS2
FEI1K334R/ACS5
FEI1/pJG4-5
ERECTA/ACS5
Bait/Prey
+Leu
-Leu
FEI2/ACS5
FEI2/eto2
FEI2/ACS9
FEI2/eto3
FEI2/ACS2
FEI2K332R/ACS5
FEI2/pJG4-5
pEG202/ACS5
D
GST-FEI1
ACS5
+
-
+
+

Table 2.1. Root elongation in the absence or presence of ethylene inhibitors[a]

Genotype	Control[b]	+AIB[b]	$+Ag^{+}$ [b]	+MCP[b]
WT	4.63±0.07	3.67±0.05	4.42±0.05	4.03±0.12
fei1fei2	1.62±0.09	3.76±0.05	0.99±0.07	1.12±0.08
sos5-2	2.26±0.12	3.68±0.04	1.16±0.09	1.35±0.11
fei1fei2sos5-2	1.50±0.10	3.40±0.04	0.77±0.07	1.06±0.11
eto2	1.90±0.05	2.78±0.05	4.03±0.06	3.49±0.13
cob	0.12±0.01	0.13±0.01	0.12±0.01	nd
etr1-3fei1fei2	1.59±0.09	nd	nd	nd
ein2fei1fei2	0.98±0.06	nd	nd	nd
etr1-3	4.82±0.05	nd	nd	nd
ein2	4.84±0.12	nd	nd	nd

[a]values represent the mean of at least 15 roots (± standard error)
[b]root elongation in cm between day 4 and day 9.
nd: not determined.

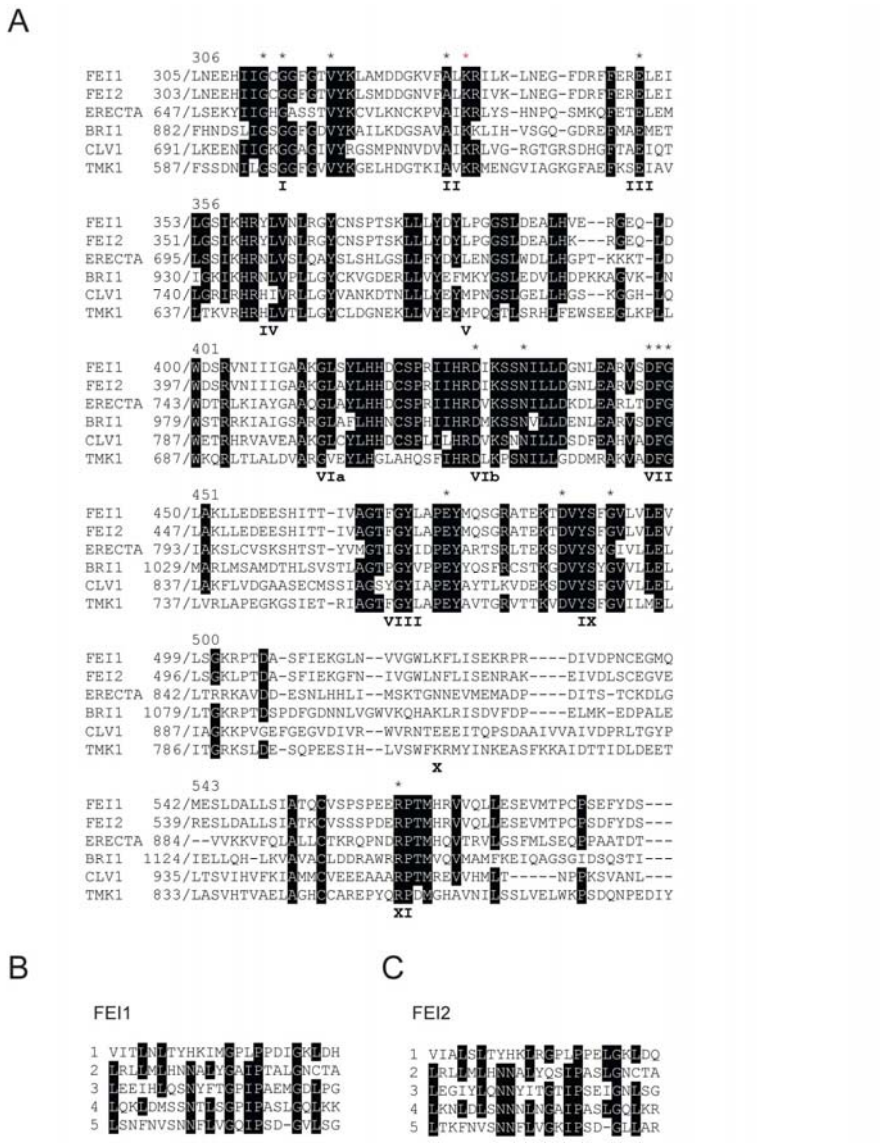

Figure S2.1. Structure of FEI1 and FEI2.

(A) Alignment of the cytoplasmic kinase domain of FEI1 and FEI2 with the kinase domains of ER, BRI1, CLV1 and TMK1, the four receptor-like kinases in plants. The 12 conserved protein kinase domains are indicated I to XI (Hanks and Quinn, 1991). Residues that are conserved among at least five of the compared sequences are boxed. The 15 invariant amino acids present in the all protein kinases are indicated by asterisks. The conserved lysine in domain II that is involved in ATP binding and which was mutated to create a kinase-dead version of FEI1 is indicated by red asterisk. **(B)** The alignment of LRR repeats in the FEI proteins. Residues that appear at each position at > 50% frequency are shown by black boxes. Numbers to the left of LRR domain indicate the specific LRR number.

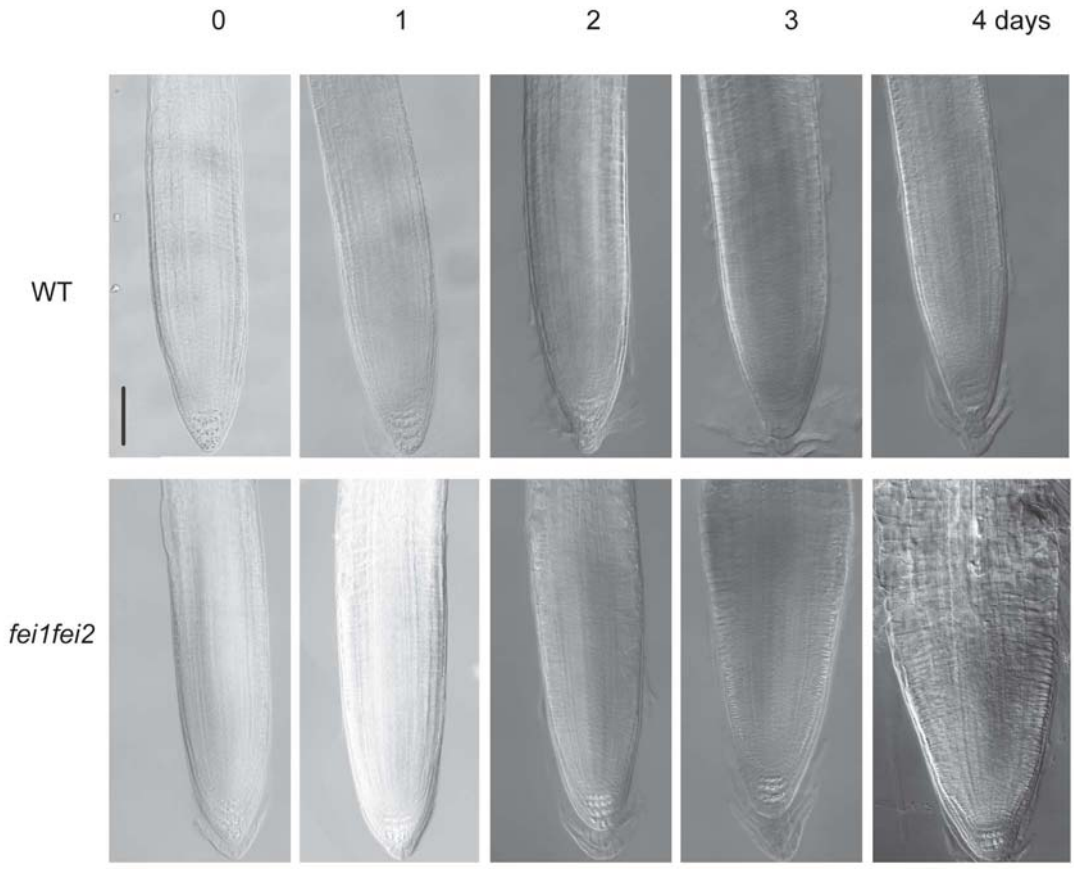

Figure S2.2. Time-course of root swelling following transfer from 0% to 4.5% sucrose media.

Wild-type and *fei1 fei2* root tips were imaged 0, 1, 2, 3, and 4 days after transfer. Bars=100 μm.

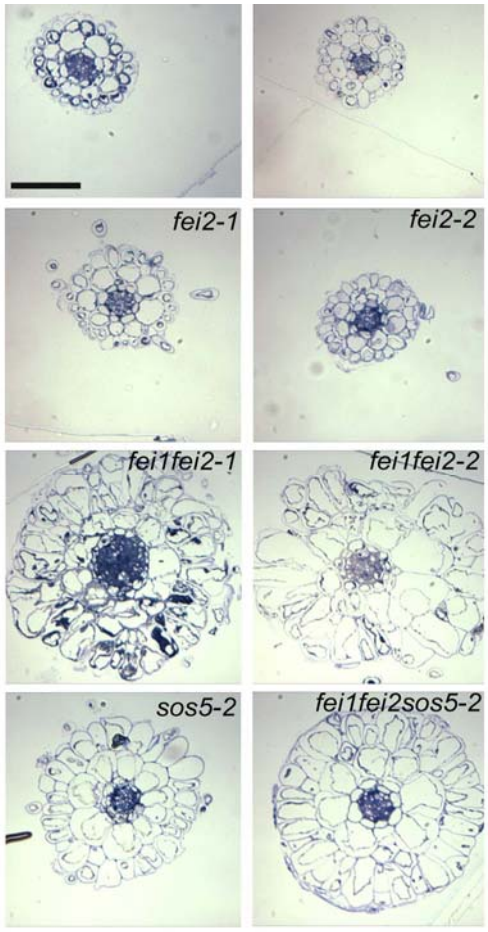

Figure S2.3. Transverse sections through the elongation zone of the root from the indicated mutants.

Bar =100 μm.

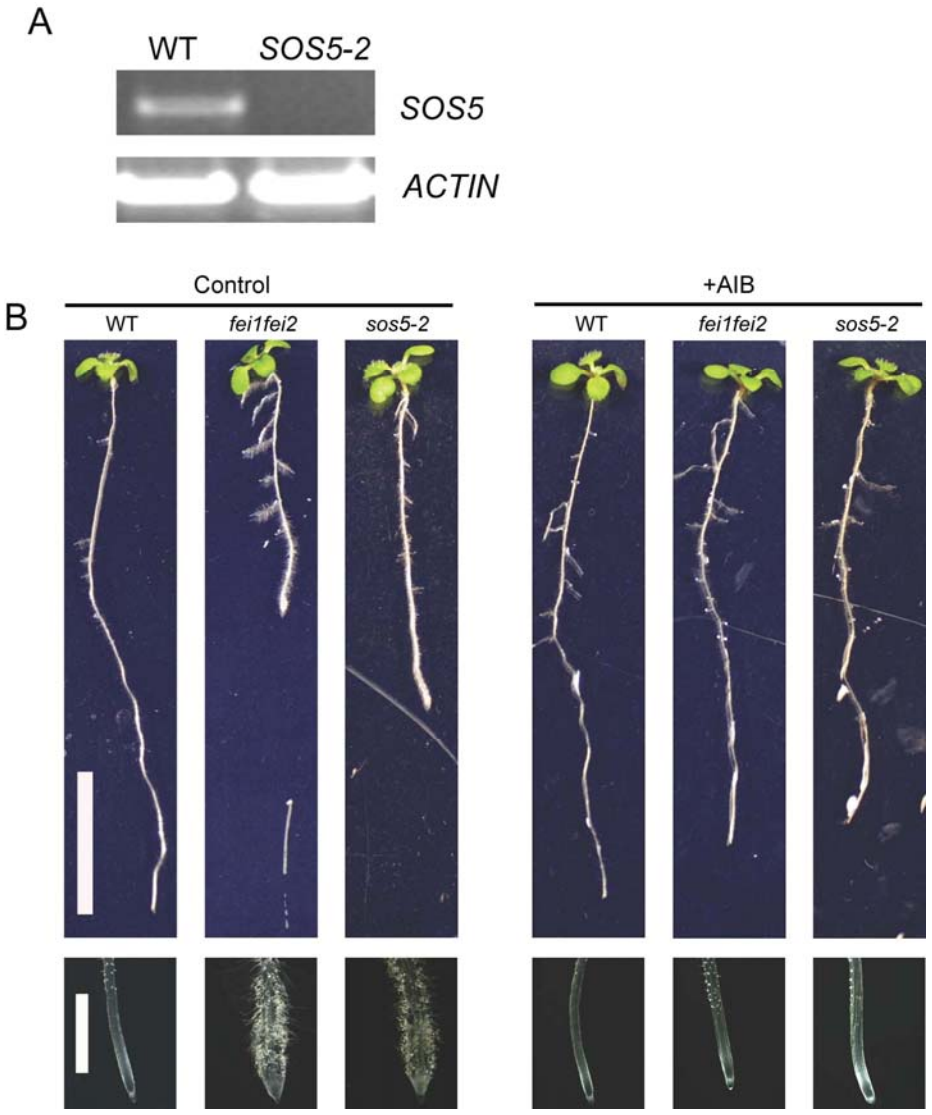

Figure S2.4. Analysis of *sos5-2* allele.

(A) RT-PCR analysis shows no full length transcript was detected in *sos5-2* mutant. The actin fragment was amplified as control. *SOS5* and *ACTIN* were amplified for 30 cycles. **(B)** Phenotype of seedlings of WT, *fei1fei2* and *sos5-2* four days after transferred to media containing 50 mM NaCl in the absence or presence of 2 mM AIB. Top bar = 1 cm; Bottom bar = 1 mm.

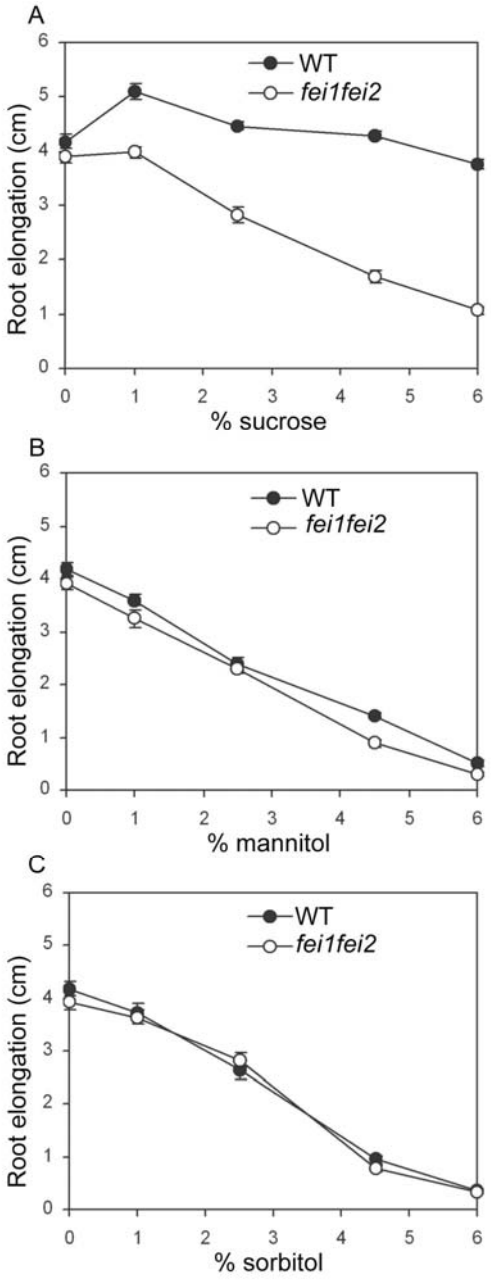

Figure S2.5. The *fei1fei2* mutant phenotype in response to sucrose is not the result of increased osmoticum.

Growth curve (days 4 – 8) of WT and *fei1fei2* after transfer to media containing the indicated amount of **(A)** sucrose; **(B)** mannitol; **(C)** sorbitol. Closed circles, wild type; Open circles, *fei1fei2*. Values shown are average ± se (n= 15).

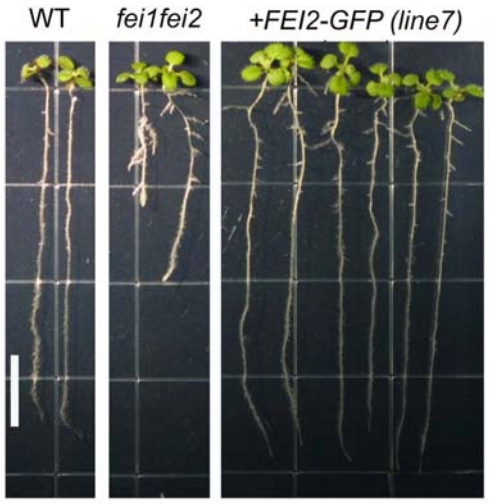

Figure S2.6. The FEI2-GFP fusion is functional. A 35S: *FEI2*-GFP genomic construct was introduced into the *fei1fei2* mutant.

Six seedlings from one of the transformed lines are shown. The WT, *fei1fei2* and transgenic seedlings were grown on MS media containing 4.5% sucrose for nine days.

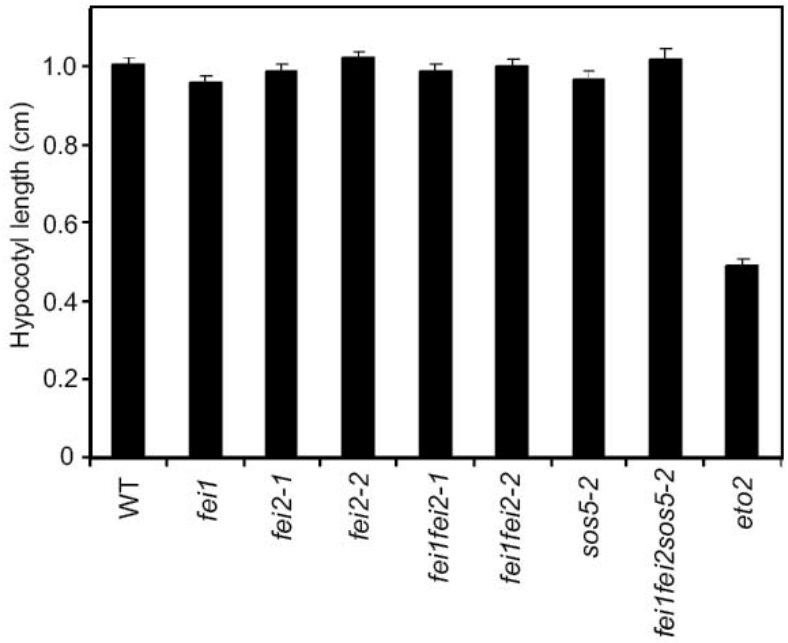

Figure S2.7. Hypocotyl length is not affected in the *fei* mutants.

Seedlings of the indicated genotype were grown for four days in the dark on MS media containing 1% sucrose and the hypocotyl length measured. The *eto2* mutant is included as a control. Data shown is the mean ± se (n= 15).

Figure S2.8. Phloroglucinol staining for lignin of the indicated seedlings grown on MS media for three days in the dark.

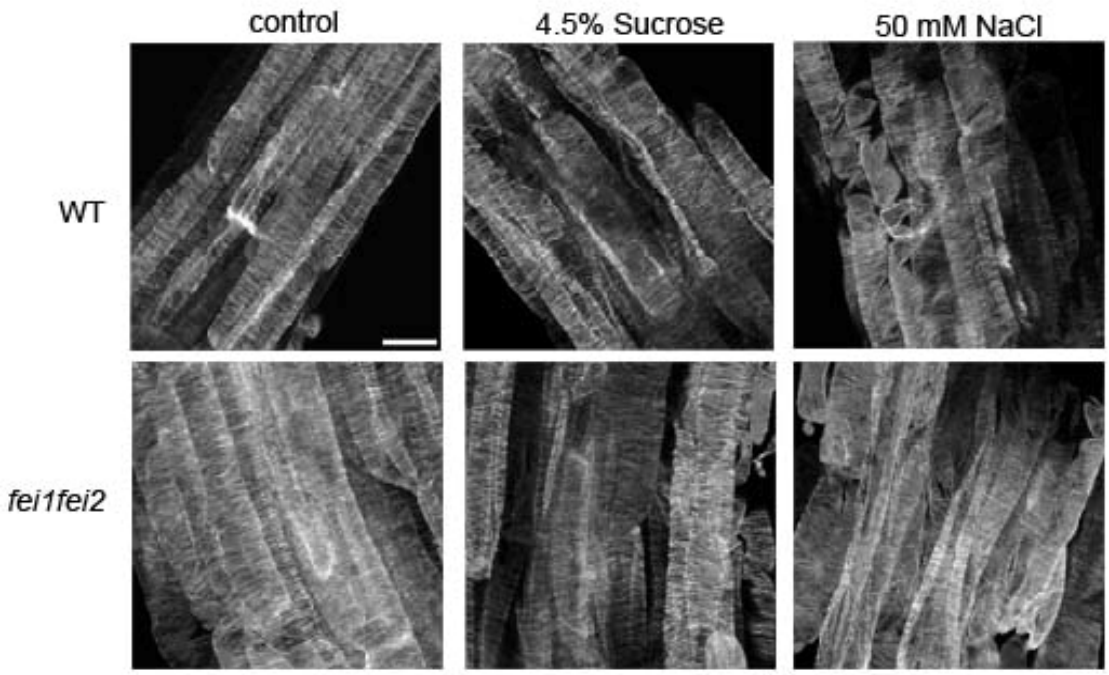

Figure S2.9. Organization of microtubules is not altered in the *fei1fei2* mutant.

Seedlings were grown on MS media containing 1% sucrose for four days and then transferred to media containing 1% sucrose (control), 4.5% sucrose, or 1% sucrose + 50 mM NaCl as indicated. Three days after transfer, seedlings were fixed and microtubules in the cells of the elongation zone were localized by immunocytochemistry. At this time, mutant roots had begun to swell but were not so swollen as to impede imaging. Similar treatment of *sos5-2* also showed no apparent disruption of the microtubules (not shown). Scale bar = 10 μm.

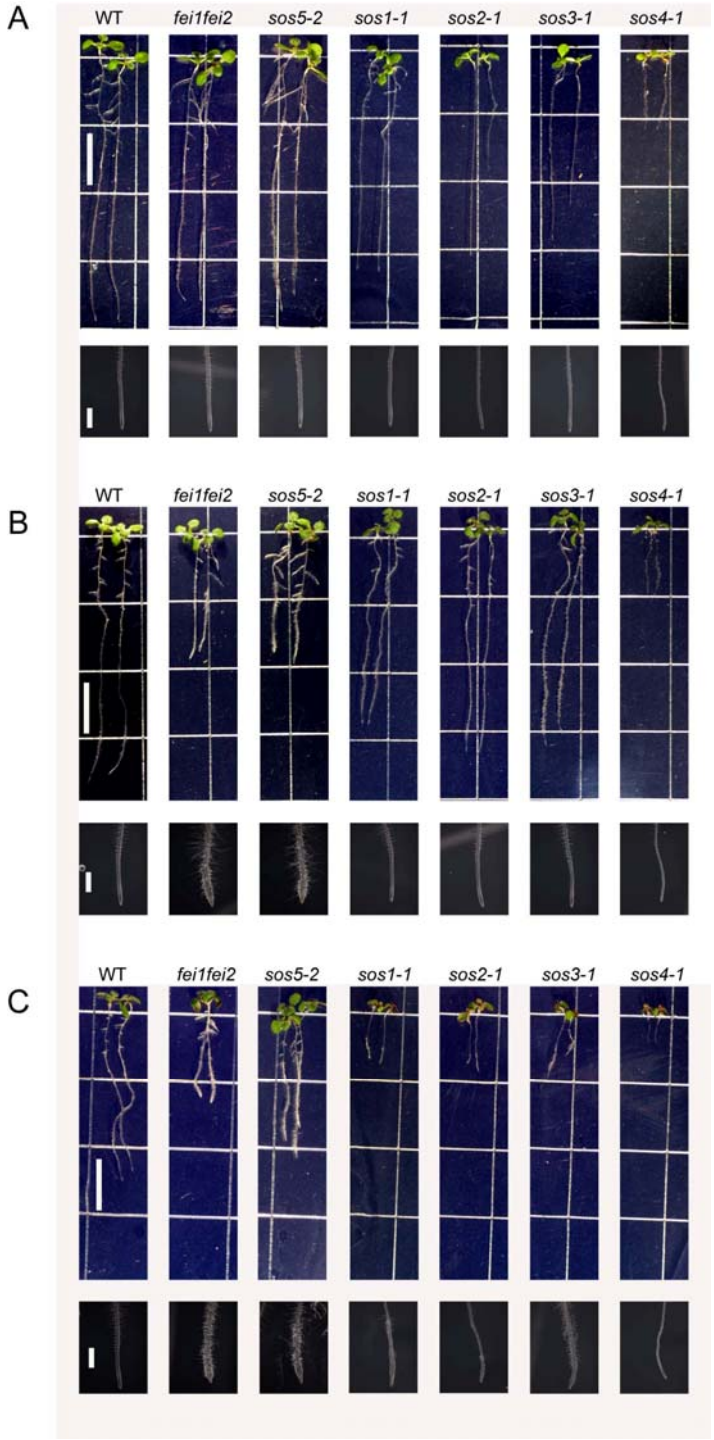

Figure S2.10. Growth in the presence of elevated sucrose does not affect other *sos* mutants.

The indicated seedlings were grown on MS media containing 0% sucrose for four days and then transferred for four days to MS media containing: **(A)** 0% sucrose; **(B)** 4.5% sucrose; **(C)** 1% sucrose and 75 mM NaCl.

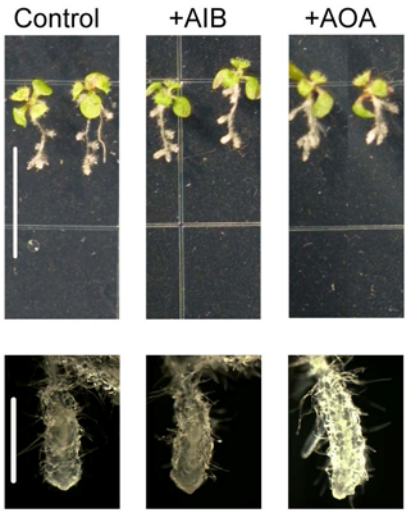

Figure S2.11. Effect of inhibition of ethylene biosynthesis on *cob* mutant.

Seedlings grown on MS media containing 0% sucrose for four days and then transferred to media containing 4.5% sucrose plus nothing (control and last two panels), AOA (0.375 mM) or AIB (1 mM). Scale bars: Top = 1 cm; Bottom = 1mm.

Table S2.1. Primers utilized in this study.

	Primers	Sequence
T-DNA characterization		
fei1	FEI1-Sense	5’ GAAGCTGGAAATGTTGAATGAAGA 3’
	FEI1-A5	5’ TTAATCAGAGCTGGAATCATAAAATTC 3’
	T-DNA left border primer-JMLB1	5' GGCAATCAGCTGTTGCCCGTCTCACTGGTG-3'
fei2-1	FEI2-S5	5’ ACAAATCGATATTGTGTGCAATGACAG 3’
	FEI1-A5	5’ TCAATCGGAGCTGGAGTCGTAGAAG 3’
	T-DNA left border primer	5' TTACCCAACTTAATCGCCTTGCAGCACAT3'
fei2-2	FEI2-S5	as above
	FEI2-A5	as above
	T-DNA left border primer-JMLB1	as above
sos5-2	SOS5-S2	5’ CACCATGGCCGCCGCAATTAACGTCACC 3’
	SOS5-A2	5’ GCCGGAAGAAACTATCTCACGC 3’
	T-DNA left border primer-JMLB1	as above
ein2	EIN2-S1	5 'GGTACATTGAGCTATACACAGCAAC 3'
	EIN2-A1	5' CATGAGAGACAAGTCAAGGACACG 3'
	T-DNA left border primer-JMLB1	as above
RT-PCR		
fei1 FL	FEI1-S9	5’ AAGCACTTCATGTAGAGAGAGG 3’
(for cDNA only)	FEI1-A2	5’GCGGCCGCATCAGAGCTGGAATCATAAAATTCG 3’
fei1 5’	FEI1-S4	5’ ATATGGAGCAATACCTACAGC 3’
	FEI1-A6	5’ TGATGCGCTAATCAGCAGCTTACCAG 3’
fei2	FEI2-S3	5’ GAAACTGGAATCTCTTAATGAAGAGC 3'
	FEI2-A2	5’GCGGCCGCATCGGAGCTGGAGTCGTAGAAG3’
sos5-2	SOS5-S1	5' CACCATGGCGAACGTAATCTCAATTTCC 3'
	SOS5-A1	5' TACCAAAACATAACAAAATGCTATAC 3'
ACTIN	Actin-S1	5’GTTGGGATGAACCAGAAGGA 3'
	Actin-A1	5’GAACCACCGATCCAGACACT 3'

Promoter: GUS		
FEI1:: GUS	FEI1-PROM-F1	5’ GTCGACTCGTCTTTAGAACAAGAAGCATTCA 3’
	FEI1-PROM-R1	5’ GCGGCCGCGGCACTGTCCAAGCATAATATAACT 3’
FEI2 :: GUS	FEI1-PROM-F2	5'CCATGG CTGGAAATGTTGGTTACTGAAGAGG 3
	FEI2-PROM-R2	5'GCGGCCGCTGGCACCGTTCAAGCATAATATAG 3
Complementation		
FEI1::*FEI1*-Myc	FEI1-S7	5’ CACCGGTGAAACAACGGACAACAATGGCTTC 3’
	FEI1-A3	5’ ATCAGAGCTGGAATCATAAAATTCG 3’
FEI2::*FEI2*-Myc	FEI2-S7	5’ CACCAGCTGAAAATACAAGAATTGTCCC 3’
	FEI2-A4	5’ ATCGGAGCTGGAGTCGTAGAAGTC 3’
35S::*FEI2*-GFP	FEI2-S8	5’ CACCATGGGCATCTGTCTAATGAAGCGCTGC 3’
	FEI2-A4	as above
Kinase assay		
Kinase domain of FEI1	FEI1-C2	5’ CACCATGAAAAAGCTTGGTAGAGTTGAG 3’
	FEI1-A5	as above
Kinase-inactive		
	Wild-type sequence of *FEI1*	5’ CTTTGCATTGAAGAGAATTCT 3’
Mutagenesis for FEI1	FEI1-M2F	5’ GGCAAAGTCTTTGCATTGAGGAGAATTCTAAAG 3’
	FEI1-M2R	5’ CTTTAGAATTCTCCTCAATGCAAAGACTTTGCC 3’
	Wild-type sequence of *FEI2*	5’ TTGCGCTGAAAAGAATTGTTAAG 3’
Mutagenesis for FEI2	FEI2-M2F	5’GGCAATGTTTTTGCGCTGAGAAGAATTGTTAAG 3’
	FEI2-M2R	5’ CTTAACAATTCTTCTCAGCGCAAAAACATTGCC 3’

Chapter 3

Isolation and characterization of *fei1 fei2* suppressors

Abstract

The plant cell wall is important for plants because the cell wall defines morphology of the cell and thus organ shape, and offers rigidity and strength. FEI1 and FEI2 are positive regulators of plant cell wall biosynthesis in Arabidopsis. The double mutant *fei1 fei2* displayed reduced root elongation and a swollen root tip in non-permissive condition as a result of defects in cellulose biosynthesis. To identify additional elements in the FEI pathway regulating cell wall biosynthesis, we screened for suppressors of *fei1 fei2.* The double mutant was mutagenized with EMS or T-DNA tagging and the M2 populations were screened for mutants with nearly wild-type root elongation in non-permissive condition. We identified nine extragenic suppressor mutations that we have named *shou1-shou8*, after the Chinese word for thin. We have cloned the gene corresponding to *shou1*. The restoration of root elongation and cell wall biosynthesis in *fei1fei2* mutations by the recessive *shou1* mutation indicates that wild-type SHOU1 may function as a negative regulator of cell wall biosynthesis. We cloned the *SHOU1* gene and found it encodes a pentatricopeptide repeat protein. In addition, we have identified two alleles of *shou2*, and we have mapped this mutation to a 47kb region on the upper arm of chromosome 1.

Introduction

The cell wall is central to plant growth and development. The plant primary cell wall is comprised of a polysaccharide network of cellulose microfibrils crosslinked by hemicelluloses in a pectin matrix, along with numerous proteins (Somerville, 2006). Cellulose microfibrils are the primary load bearing elements of the cell wall. The orientations of microfibrils determine both the direction and extent of cell expansion driven by turgor pressure (Darley et al., 2001). In growing cells, the cellulose microfibrils in the primary wall are deposited in an orientation perpendicular to the axis of elongation, similar to hoops around a barrel, thus constricting radial expansion (Baskin, 2005; Green, 1980; Taiz, 1984).

Much of our knowledge about cellulose synthesis in the primary cell wall has been derived from the identification of mutants in Arabidopsis. These mutants include those displaying tissue swelling, embryo lethality, and tolerance to inhibitors of cellulose biosynthesis or sensitivity to inhibitors of microtubules (Paredez et al., 2008; Somerville, 2006). The most extreme cellulose-deficient mutants, such as null alleles of cellulose synthase 1 (CESA1), cause embryo lethality (Beeckman et al., 2002). In homozygous CESA1 null mutant, the cells in the embryo are swollen; the primary cell walls are thin and frequently interrupted. Other less severe and conditional mutants have facilitated analysis of the effect of perturbations in the cellulose biosynthesis in more mature plants. It has been shown that the cortical microtubules, GPI-anchored proteins such as COBRA (COB) and SOS5, and KORRIGAN etc., are involved in regulation of cellulose biosynthesis (Cosgrove, 2005; Humphrey et al., 2007; Somerville, 2006; Taylor, 2008).

Previously, we identified FEI1 and FEI2 as regulators of cell wall biosynthesis. To further dissect components in the FEI pathway, we conducted a suppressor screen in the

fei1fei2 background to isolate mutants that restore wild-type root elongation in non-permissive conditions. These suppressors would most likely target genes that function downstream of FEI1/FEI2 or act in a parallel pathway. Here we report the isolation and characterization of eight suppressors, *SHOU1*-*SHOU8*. The *SHOU1* gene was cloned using a map-based approach and found to encode a pentracopeptide rich protein. *SHOU2* was mapped to a 47kb region on chromosome 1.

Results

Second-site mutants partially restore root growth in *fei1fei2*

The *fei1fei2* mutant shows reduced root elongation and a swollen root tip phenotype on media containing elevated sucrose as a result of defect in cellulose biosynthesis. To identify signaling components in the FEI pathway, we screened for suppressors of *fei1fei2*. We screened M2 seedlings of ethyl- methanesulfonate (EMS) mutagenized and T-DNA tagging populations of *fei1fei2* on high sucrose plates for individuals with long roots and non-swollen root tips. 30,000 homozygous *fei1fei2-1* seeds were mutagenized with ethyl methanesulfonate(EMS) and 5,000 independent T-DNA tagged lines were isolated . Approximately 200,000 M2 seedlings of the EMS population and 30,000 T-DNA tagging T2 seedlings were screened for mutant plants that suppressed *fei1fei2* phenotype. We identified nine extragenetic suppressor mutations which defined eight complementation groups (*shou1-shou8*, after the chinese word for thin).

Complementation analysis

All *shou1-shou8* mutants were crossed to the parental line *fei1 fei2*, and all the resulting F1 seedlings displayed swollen root tips on high sucrose media, indicating these suppressor mutations are recessive. Complementation analysis has revealed that these suppressors define eight complementation groups. *shou2,* represented by two alleles, has a root hair defective phenotype, but the remaining lines are wild-type in all aspects of growth and development.

Identification of the *shou1* mutant as a suppressor of *fei1fei2*

The *shou1* mutation was identified as a single allele from the EMS mutagenized population. The *shou1-1* mutation partially restores root elongation in the *fei1 fei2* background in non-permissive conditions (Figure 3. 1). The F2 progeny of a backcross of *shou1 fei1 fei2* to *fei1 fei2* plant segregated non-suppressed to suppressed plant in a 3:1 ratio (data not shown), consistent with a recessive mutation.

SHOU1* mutation partially restores cellulose biosynthesis in *fei1fei2

Previously, *theseus1 (the1)* was identified as a suppressor of the cellulose-deficient mutant *prc1* (Hématy et al., 2007). However, the cellulose biosynthesis was not restored in the *prc1-1 the1* double mutant, indicating that THE1 might mediate the response of growing plant cells to perturbation of cellulose synthesis. The *shou1* suppressor could either suppress the reduction of cellulose biosynthesis that occurs in the *fei1 fei2* mutant, or alternatively it could suppress the response to reduced cellulose of *fei1fei2* seedlings, similar to THE1. To distinguish these possibilities, we examined cellulose biosynthesis in the *shou1 fei1 fei2* triple mutant by analyzing *in vivo* incorporation of ^{14}C-glucose into the crystalline cellulosic

cell wall fraction of three-day-old roots after transfer to high sucrose. The *shou1* mutation significantly suppressed the defect in cellulose biosynthesis that occurs in the *fei1 fei2* mutant (Figure 3. 2). Thus, *shou1* suppresses the cell elongation defects in *fei1 fei2* by restoring near wild-type levels of cellulose biosynthesis.

Map-based Cloning of *SHOU1*

In order to map these suppressors using physical markers, we first introgressed the *fei1* and *fei2* mutations, which were originally identified in the Col ecotype, six times into a Ler genetic background. A line homozygous for *fei1* and *fei2* was obtained which we named *L6fei1fei2*. *L6fei1fei2*, also displayed short roots and a swollen tip in the presence of high sucrose, similar to the parental Columbia mutant line. We crossed *shou1* into this introgressed line and obtained an F2 mapping population. By using polymerase chain reaction-based markers, the *shou1* mutation was mapped to a ~ 109 kb region on the bottom arm of chromosome 5, between the markers F10E10-1 and MZA15-3 (Figure 3. 3). *shou1* was shown to be tightly linked to markers MZA15-2 (18.948 Mbp) and MZA15-3 (18.995Mbp), with no recombinants discovered among 519 progeny examined. Candidate genes in this region were sequenced and a single C to T point mutation in At5g46880 was found that is predicted to alter a serine residue to a leucine residue at position 12 in the protein encoding region. A transgene composed of a genomic fragment, including the entire At5g46880 open reading frame, its native promoter (1 kb upstream), and 700 base pairs (bp) of 3' DNA, was able to fully rescue the *shou1 fei1 fei2* triple to a *fei1 fei2* phenotype (Figure 3. 4), as the T1 transformants all displayed short roots and a swollen tip on high sucrose media. Taken together, these data indicate that At5g46880 indeed corresponds to *SHOU1*.

Sequence analysis of SHOU1

SHOU1 is predicted to encode a 468-amino acid polypeptide that is a member of the P subfamily of pentatricopeptide repeat (PPR)-containing proteins(Lurin et al., 2004). PPR proteins are characterized by having tandem repeats of a degenerate 35 amino acid signature motif that may form a nucleic acid binding groove (Small and Peeters, 2000). PPR family has undergone dramatic expansion in land plants, with ~450 and 447 members in Arabidopsis and rice, respectively (Lurin et al., 2004; O'Toole et al., 2008). Putative SHOU1 orthologs can be readily identified in grape (CAN63846) and rice (Os02g0793200). A majority of the PPR proteins are targeted to either mitochondria or plastids, where they have been proposed to function in RNA processing (splicing or cleavage), RNA editing, RNA stability, enhancing and blocking translation of RNA (Lurin et al., 2004) .

SHOU1 is not interrupted by introns and the predicted protein contains 12 PPR motifs consisting of a degenerate 35 amino-acid unit (Figure 3. 5). The SHOU1 protein does not have any signal peptide that would target it to mitochondria or chloroplasts. Homozygous T-DNA insertion lines were obtained and named *shou1-2* and *shou1-3* (Figure 3. 3). By PCR analysis, the insertions have been confirmed. The transcript level of *SHOU2* in *shou1-2* and *shou1-3* remains to be determined. *shou1-3* is very likely a null allele, as the insertion is in the early region of the open reading frame. We are currently in the process of obtaining *shou1-2 fei1 fei2* and *shou1-3 fei1 fei2* homozygous lines to determine if the putative null alleles also suppress *fei1 fei2*.

Examination of the public available expression data reveals that *SHOU1* is expressed in the root, with expression in all cell layers (Birnbaum et al., 2003), consistent with its suppression of the root phenotype of *fei1fei2*. In *Arabidopsis*, SHOU1 has a paralog (85%

similarity), however, there is no EST or any expression data for this homolog, and thus it is predicted to be a pseudogene.

shou2 mutations partially restore root growth in *fei1fei2shou2.*

We identified two alleles of the recessive suppressor *shou2*. Both *shou2-1 fei1 fei2* and *shou2-2 fei1 fei2* displayed long roots and a wild-type root tip in non-permissive condition (Figure 3.6 and data not shown for *shou2-2 fei1 fei2*). *shou2-1* and *shou2-2* were isolated from the EMS mutagenized population and the T-DNA activation tagged pool, respectively. Notably, the *shou2* mutations did not completely restore root elongation to wild-type levels.

In addition to their suppression of *fei1 fei2*, *shou2-1* and *shou2-2* also displayed root hair defects (Figure 3.7), as the root hairs are very short in the mutants. The root hair phenotype is not dependent on *fei1 fei2*, because F2 population generated from col and *shou2-1 fei1 fei2* crosses displayed wild-type root hair to defective root hair in a 1: 3 ratio, indicating root hair defects in *shou2* is caused by a monogenic recessive mutation.

Map-base cloning of *SHOU2*

The *shou2 fei1 fei2* mutant was crossed to *L6fei1fei2* and an F2 mapping population was obtained. Rough mapping of *SHOU2-1* showed high linkage to the markers F12K8 (7.954Mbp) and F13K9 (9.744Mbp). The *shou2-2* mutation showed the same linkage. Because both of these markers are close to FEI1 (at 11.249 Mbp) on chromosome 1, a second mapping population was obtained by crossing *shou2 fei1 fei2* to Ler. The root hair defect of *shou2* was used for the fine mapping. Using restriction fragment length polymorphisms

(RFLPs) and cleaved amplified polymorphic sequence markers (CAPS), the *shou2-1* mutation was mapped to a ~47-kilobase (kb) region delimited by recombination events between marker F3I6-D (8.552 Mbp) and F3I6-F (8.599Mbp) of chromosome 1 (Figure 3. 8). *shou2-1* was shown to be tightly linked to marker F3I6-H (8.570) with no recombinants discovered among 737 progeny examined. The genomic sequence of the ~47 kb region containing the *shou2* mutation contains eight candidate genes. We are in the process of sequencing of these eight candidate genes in the two *shou2* alleles.

shou2 suppresses other cellulose-deficient mutant phenotypes

To test if *SHOU2* may suppress other cellulose-deficient mutant, double mutant combinations of the *shou2-1* with various mutants affecting root growth were obtained and analyzed. *sos5* displayed the same sucrose-dependent root phenotype as *fei1 fei2,* and has previously been demonstrated to be in the same pathway as *fei1 fei2* (Xu et al., 2008). *shou2* also suppressed the *sos5* phenotype, as *shou2 sos5* double mutant seedlings displayed long roots and a wild-type appealing root tip. We are in the process of obtaining *cob shou2* double and *prc1 shou2* double mutants. In addition, *fei1 fei2* also has thicker hypocotyls than wild-type. s*hou2* does not suppress thickened hypocotyls in *fei1fei2* (data not shown).

Discussion

To identify additional regulators of cell wall biosynthesis and cell wall function that function in the FEI signaling pathway, a screen for suppressors of the *fei1fei2* short root

phenotype was performed. Mutations defining eight complementation groups that restore nearly wild-type root function were identified. The *SHOU1* gene was cloned and found to encode a putative pentatricopeptide repeat protein. The *shou1* mutation restores cellulose biosynthesis in the *fei1 fei2* mutant. This is distinguished from *the1*, which also suppresses a cellulose-deficient mutant *prc1-1*, as *the1* does not restore cellulose biosynthesis in *prc1-1*, even though it suppresses the short hypocotyl phenotype in *prc1-1* (Hématy et al., 2007). The complementation with At5g46680 restores the *shou1 fei1 fei2* to *fei1 fei2* phenotype, confirming that At5g46680 corresponds to SHOU1.

The pentatricopeptide repeat protein (PPR) family is characterized by having a degenerate 31-36 amino acid repeat in tandem array. In *Arabidopsis*, the PPR gene family contains 450 members, and many are predicted to be targeted to either the mitochondria or the chloroplast (Lurin et al., 2004; O'Toole et al., 2008). PPR proteins have been shown to be associated with various molecular events, mostly post-transcriptionally and bind to RNA specifically (Kotera et al., 2005; Koussevitzky et al., 2007). Recently, GUN1 has been shown to bind DNA and GUN1-GFP is associated with sites of active transcription on plastid DNA, suggesting GUN1 may function in regulation of gene transcription (Koussevitzky et al., 2007).

To date, our data provide the first evidence that a PPR protein is involved in cell wall biosynthesis. The possible mechanism by which SHOU1 acts in the FEI1/FEI2 pathway is unknown. We will determine the intracellular localization of SHOU1. We hypothesis that SHOU1 might regulate the expression of genes involved in cell wall biosynthesis. To dissect the role and possible target of SHOU1, we will first examine global gene expression in wild-

type, *fei1fei2*, and *fei1 fei2 shou1* roots. We hope that this will provide insight into the role of SHOU1 in regulating cell wall biosynthesis.

Tip growth and anisotropic growth difference and common.

The *shou2* mutation affects cell elongation in the root as well as the formation of the root hairs. These processes occur by two distinct modes of morphogenesis for plant cells: diffuse growth and tip growth. In diffuse growth, expansion of the cell surface is distributed over the whole cell (Castle, 1955; Green, 1963).This mode of morphogenesis is seen in most cells of multicellular plants, such as root cells in the elongation and differentiation zones. In contrast, in tip growth, the elongation of cell is restricted to a prolate dome where surface expansion takes place and cylindrical shape is achieved. The growth of root hairs occurs by tip growth, as does the growth of pollens tube and trichomes.

The cell wall is an important component of both tip growth and diffuse growth. Consistent with this, disruption of CESA1 (*rsw1*) results in an increased radial expansion in all cell types, including tip-growing cells such as trichomes and root hairs (Nicol and Höfte, 1998). However, other cellulose biosynthesis deficient mutants, such as *korrigan,* do not affect tip growth in root hairs, trichomes or pollen tubes (Nicol et al., 1998). Indeed, in the *fei1 fei2* mutant, we do not observe a defect in root hair formation or growth. KOJAK/AtCSLD3, a cellulose synthase-like protein, has been reported to be required for root hair cell morphogenesis in Arabidopsis (Favery et al., 2001). Distinct from other cellulose synthases that are localized in plasma membrane, KOJAK is localized in the endoplasmic reticulum. This localization suggests that KOJAK is required for the synthesis of noncellulosic wall polysaccharides. Other components, such as RhoGDP, and leucine-rich

repeat/extension cell wall protein LRX1 have been shown to be involved in root hair elongation (Baumberger et al., 2001; Carol et al., 2005). These mutants only have modest or no effects on root elongation (diffuse growth), suggesting that tip growth and diffuse growth share some common regulatory components but also have independent regulatory input.

SHOU2 appears to be involved in both modes of elongation, as the *shou2* mutation not only suppresses the anisotropic defects in *fei1 fei2*, but also result in root hair defects. This root hair defect is independent of *FEI1* and *FEI2*. Interesting, it is a paradox that *shou2* suppresses anisotropic defects but also inhibits the root hair expansion. If SHOU2 suppresses *fei1 fei2* anisotropic defects through restoring cellulose biosynthesis, then longer but not shorter root hair is expected in *shou2 fei1 fei2*.

The *shou2* mutation also suppresses the *sos5* mutant, consistent with SOS5 acting in the same pathway as FEI1/FEI2. It will be interesting to determine if *shou2* suppress other cellulose deficient mutants.

Methods

EMS mutagenesis of *fei1fei2*

Approximately 30,000 seeds (600mg) from Arabidodopsis thaliana (Columbia) plants homozygous for the *fei1 fei2-1* alleles and the *glabrous* allele (Xu et al., 2008) were mutagenized with 0.25 % ethyl methanesulfonate for 15 hours and sown in soil. M2 seeds were collected in approximately 150 pools.

The activation-tagging transgenic lines were generated in a *fei1 fei2-1 (gl)* (col ecotype) background with construct pSKI015 (Weigel et al., 2000) via floral dipping Agrobacterium-mediated transformation technique (Clough and Bent, 1998). M1 seedlings were grown on soil and 5000 lines were selected out on BASTA. M2 seeds were collected in 370 pools.

Growth conditions and measurement

For growth in soil, plants were grown at 23°C in ~75 μE constant light. For growth *in vitro*, seeds were surface sterilized and cold treated at 4°C for 3 days in the dark and then treated with white light for 3 h. Seedlings were grown on vertical plates containing 1X Murashige and Skoog salts (MS) , 0.6% phytagel (Sigma) at 22°C in ~100 μE constant light with sucrose as indicated in legend. For measurements of root elongation, seedlings were grown for 4 days on vertical plates containing no sucrose and then transferred to MS media supplemented with the indicated additions.

Isolation of *shou* mutant

Around 200,000 EMS M2 and 30, 000 T-DNA tagging M2 seeds were then grown on vertical Petri dishes for 10 days on MS media with 4.5% sucrose. Potential suppressor mutants were selected based of increased root length compared to that of *fei1fei2-1* and transferred to soil. Plants were allowed to self pollinate, and the M3 progeny was rescreened for the suppressor phenotype.

Mapping of *shou1* and *shou2*

fei1fei2-1 (Columbia, Col ecotype) were introgressed into Landsberg erecta (Ler) through back crossing with Ler six times and homozygous *fei1fei2-1* was obtained from F2 of the sixth backcross into Ler, which we named *L6fei1fei2*. Theoretically, after six backcrosses, approx 98.4% of the genome is Ler, with the exception of regions around the *fei1* and *fei2* mutation that remain Col. We tested 42 molecular markers across all 5 chromosomes and found only molecular markers F6N18, T10P12 near to *FEI1* and T1J8 near *FEI2* remained Col. All other 39 markers were Ler.

We crossed the triple mutant *shou1-1 fei1 fei2-1* (Col 0) with *L6fei1fei2* (Ler). 40 F2 *shou1-1fei1fei2-1* lines were selected for genotyping. The phenotype of these lines was verified in the F3 progeny. Linkage analysis with molecular marker distributed throughout the genome revealed, *shou1* was linked to MPL12 marker located at 18.758 on chromosome V. Fine mapping was carried out with a population of 519 *shou1fei1fei2-1* seedlings and we located the *shou1* mutation within a 109 Kb region between F10E10-1 (18.897, 1 recombinant) and MZA15-3 (19.006, 3 recombinant). This 109 Kb region contains 29 open reading frames (ORFs), which were subjected to sequencing.

The *shou2-1* and *shou2-2* mutants were identified in a screen for mutations induced by an ethylmethane-sulphonate-mutagenized population and T-DNA tagging using *fei1fei2-1*(*gl1*) respectively. Rough mapping of *SHOU2-1* showed high linkages to the markers F12K8 (7.954Mbp) and F13K9 (9.744Mbp). Rough mapping of *SHOU2-2* showed the same linkages. Because both of these markers are close to FEI1 (at 11.249 Mbp) on chromosome 1, a second mapping population by crossing *shou2 fei1 fei2* to Ler and F2 mapping population was obtained. Root hair defects phenotype of *shou2* was used for the fine mapping. Using restriction fragment length polymorphisms and cleaved amplified polymorphic sequence markers, the *shou2-1* mutation was mapped to a ~47-kilobase (kb) region delimited by recombination events between marker F3I6-D (8.552 Mbp) and F3I6-F (8.599Mbp) of chromosome 1. *shou2-1* was shown to be tightly linked to marker F3I6-H (8.570) with no recombinants discovered among 737 progeny examined. The genomic sequence of the ~47 kb region containing the *shou2* mutation contains eight candidate genes.

SHOU1 constructs and transgenic plants

The *SHOU1* genomic DNA, including the entire At5g46880 open reading frame, its native promoter (1 kb upstream), and 700 base pairs (bp) of 3' DNA, was amplified from wild-type Col genomic DNA using Pfu DNA polymerase as described by the manufacturer (Stratagene; La Jolla, CA). The PCR fragment was cloned into pENTR-TOPO-D (Invitrogen Corporation, Carlsbad, CA, USA). The resultant entry plasmid was used in an LR reaction as described by the manufacturer (Invitrogen Corporation, Carlsbad, CA) to introduce the respective genes into the binary pGWB1 (Nakagawa et al., 2007) vector for complementation. The resulting constructs were transformed into *Agrobacterium tumefaciens*, strain GV3101. Transgenic

plants were generated by the floral dip method (Clough and Bent, 1998)and selected on MS medium containing 50 mg/l kanamycin and 30 mg/l hygromycin. All destination binary vectors were kindly provided by Dr. Tsuyoshi Nakagawa from the Research Institute of Molecular Genetics, Matsue, Japan.

Cellulose synthesis assays

Cellulose synthesis was determined by ^{14}C-glucose labeling as described (Fagard et al., 2000) with the following modifications. Seedlings were grown on 0% sucrose MS plates for 4 days and then transfer to MS media containing various supplements three days. 1.5 cm root tips were cut and washed three times with 3 ml of glucose-free MS media. 40 root tips were then incubated in 1 ml MS media containing ^{14}C-glucose (NEN Research, Boston, MA), 0.1 $\mu Ci.ml^{-1}$ for 1 hr in the dark at 22°C in glass tubes. After treatment, the roots were washed three times with 3 ml of glucose-free MS medium. Next, the roots were extracted 3X with 3 ml of boiling absolute ethanol for 20 min, and total aliquots were collected ("ethanol-soluble fraction"). Roots were then resuspended in 3 ml of chloroform/methanol (1:1 v/v), extracted for 20 min at 45°C, and finally resuspended in 3 ml of acetone for 15 min at room temperature with gentle shaking. The remaining material was resuspended in 500 µl of an acetic acid/nitric acid/water solution (8:1:2 v/v/v), for 1 hr in a boiling water bath. Acid-soluble material and acid-insoluble material were separated by glass microfiber filters (GF/A; 2.5cm diameter; Whatman, Maidstone, UK) after which the filters were washed with 5 ml of water. The acid wash and water wash constitute the acid-soluble fraction. The filters yield the acid-insoluble fraction. The amount of label in each fraction was determined by scintillation

counting using liquid scintillation fluid (Scintiverse^{TM} BD cocktail, Fisher SX 18-4). The incorporation in the cellulosic fraction was calculated per seedling.

Reference

Baskin, T. I. (2005). Anisotropic expansion of the plant cell wall. Annu Rev Cell Dev Biol **21**, 203-222.

Baumberger, N., Ringli, C., and Keller, B. (2001). The chimeric leucine-rich repeat/extensin cell wall protein LRX1 is required for root hair morphogenesis in Arabidopsis thaliana. Genes Dev **15**, 1128-1139.

Beeckman, T., Przemeck, G. K. H., Stamatiou, G., Lau, R., Terryn, N., De Rycke, R., Inze, D., and Berleth, T. (2002). Genetic complexity of cellulose synthase A gene function in Arabidopsis embryogenesis. Plant Physiol **130**, 1883-1893.

Birnbaum, K., Shasha, D. E., Wang, J. Y., Jung, J. W., Lambert, G. M., Galbraith, D. W., and Benfey, P. N. (2003). A gene expression map of the Arabidopsis root. Science **302**, 1956-1960.

Carol, R., Takeda, S., Linstead, P., Durrant, M., Kakesova, H., Derbyshire, P., Drea, S., Zarsky, V., and L., D. (2005). A RhoGDP dissociation inhibitor spatially regulates growth in root hair cells. Nature **438**, 1013-1016.

Castle, E. (1955). The mode of growth of epidermal cells of the Avena coleoptile. Proc Natl Acad Sci **41**, 197-199.

Clough, S. J., and Bent, A. F. (1998). Floral dip: a simplified method for Agrobacterium-mediated transformation of *Arabidopsis thaliana*. Plant J **16**, 735-743.

Cosgrove, D. J. (2005). Growth of the plant cell wall. Nat Rev Mol Cell Biol **6**, 850-861.

Darley, C. P., Forrester, A. M., and McQueen-Mason, S. J. (2001). The molecular basis of plant cell wall extension. Plant Mol Biol **47**, 179-195.

Favery, B., Ryan, E., Foreman, J., Linstead, P., Boudonck, K., Steer, M., Shaw, P., and Dolan, L. (2001). KOJAK encodes a cellulose synthase-like protein required for root hair cell morphogenesis in Arabidopsis. Genes Dev **15**, 79-89.

Green, P. (1963). Cell walls and geometry of plant growth. Brookhaven Symposia in Biology **16**, 203-217.

Green, P. B. (1980). Organogenesis-a biophysical view. Annu Rev Plant Physiol ***31***, 51-82.

Hématy, K., Sado, P.-E., Van Tuinen, A., Rochange, S., Desnos, T., Balzergue, S., Pelletier, S., Renou, J.-P., and Höfte, H. (2007). A receptor-like kinase mediates the

response of Arabidopsis cells to the inhibition of cellulose synthesis. Curr Biol **17**, 922-931.

Humphrey, T. V., Bonetta, D. T., and Goring, D. R. (2007). Sentinels at the wall: cell wall receptors and sensors. New Phytol **176**, 7-21.

Kotera, E., Tasaka, M., and Shikanai, T. (2005). A pentatricopeptide repeat protein is essential for RNA editing in chloroplasts. Nature **433**, 326-330.

Koussevitzky, S., Nott, A., Mockler, T., Hong, F., Sachetto-Martins, G., Surpin, M., Lim, J., Mittler, R., and, Chory, J. (2007). Signals from chloroplasts converge to regulate nuclear gene expression. Science **316**, 715-719.

Lurin, C., Andrés, C., Aubourg, S., Bellaoui, M., Bitton, F., Bruyère, C., Caboche, M., Debast, C., Gualberto, J., Hoffmann, B., *et al.* (2004). Genome-wide analysis of Arabidopsis pentatricopeptide repear proteins reveals their essential role in organelle biogenesis. . Plant Cell **16**, 2089-2103.

Nicol, F., His, I., Jauneau, A., Vernhettes, S., Canut, H., and Höfte, H. (1998). A plasma membrane-bound putative endo-1,4-beta-D-glucanase is required for normal wall assembly and cell elongation in Arabidopsis. EMBO J **17**, 5563-5576.

Nicol, F., and Höfte, H. (1998). Plant cell expansion: scaling the wall. Curr Opin Plant Biol **1**, 12-17.

O'Toole, N., Hattori, M., Andres, C., Iida, K., Lurin, C., Schmitz-Linneweber, C., Sugita, M., and Small, I. (2008). On the expansion of the pentatricopeptide repeat gene family in plants. Mol Biol Evol **25**, 1120-1128.

Paredez, A., Persson, S., Ehrhardt, D., and Somerville, C. (2008). Plant Physiol. Genetic evidence that cellulose synthase activity influences microtubule cortical array organization **147**, 1723-1734.

Small, I., and Peeters, N. (2000). The PPR motif: a TRP-related motif prevalent in plant organeller proteins. Trends Biochem Sci **2**, 46-47.

Somerville, C. (2006). Cellulose synthesis in higher plants. Annu Rev Cell Dev Biol **22**, 53-78.

Taiz, L. (1984). Plant cell expansion: regulation of cell wall mechanical properties. Annu Rev Plant Physiol **35**, 585-657.

Taylor, N. G. (2008). Cellulose biosynthesis and deposition in higher plants. New Phytol **178,** 239-252.

Weigel, D., Ahn, J. H., Blazquez, M. A., Borevitz, J. O., Christensen, S. K., Fankhauser, C., Ferrandiz, C., Kardailsky, I., Malancharuvil, E. J., Neff, M. M., *et al.* (2000). Activation tagging in Arabidopsis. Plant Physiol **122**, 1003-1013.

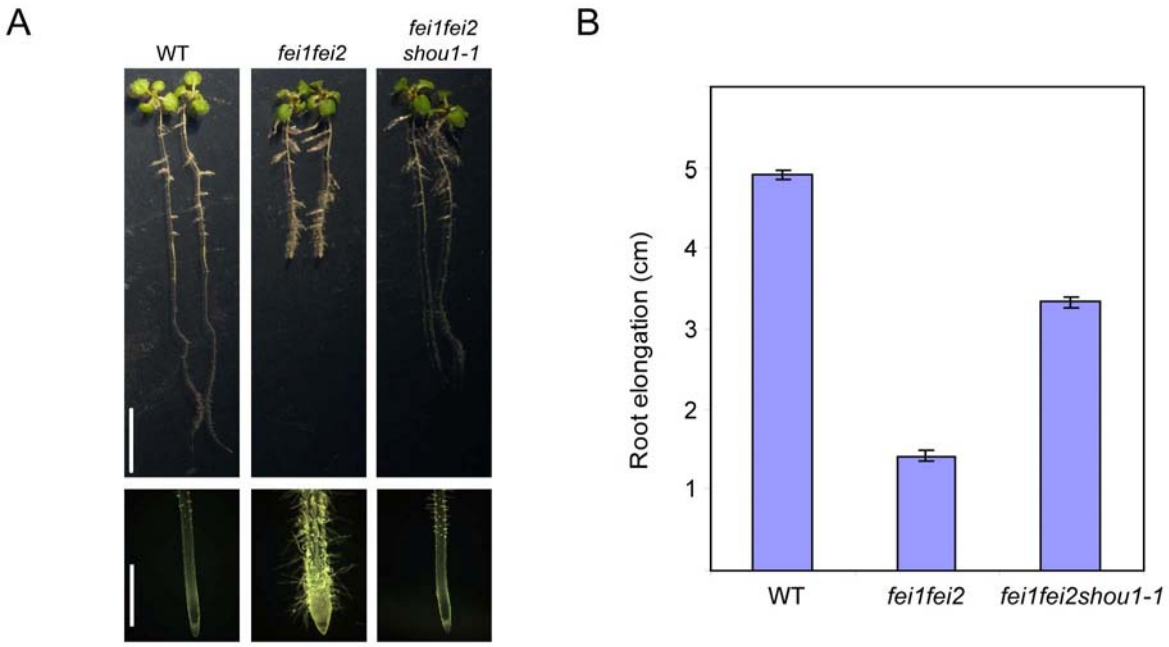

Figure 3.1. Identification of the *shou1-1* mutant as a suppressor of *fei1fei2*.

(A) Seedling phenotype of wild type, *fei1fei2* and *fei1fei2shou1-1* were grown on MS media containing 0% sucrose for 4 days and then transferred to MS media containing 4.5% sucrose for 5 days. Top panel: Scale bar=1cm, Bottom panel, close-up of root tip, scale bar=1mm. **(B)** Quantification of root elongation of wild type, *fei1fei2* and *fei1fei2shou1-1* and transferred as in **(A)**. Values represent the mean of the growth of 5 days after transfer to 4.5% sucrose MS plates. Error bars show SE (n>15).

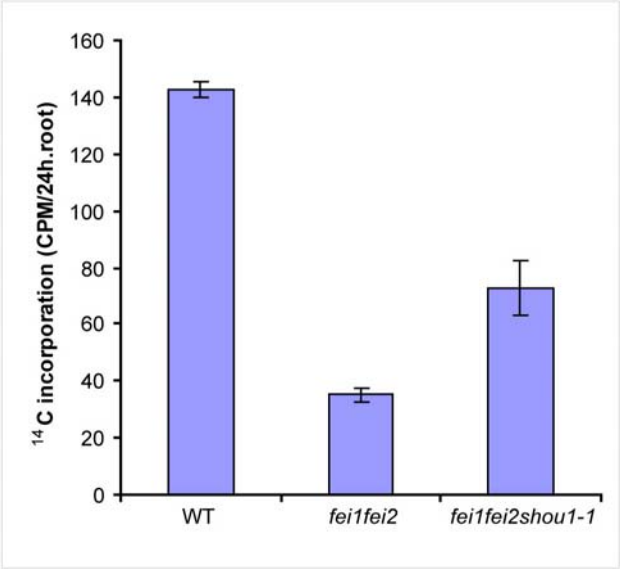

Figure 3.2. *shou1-1* partially restore cellulose biosynthesis in *fei1fei2*.

Cellulose accumulation as measured by (^{14}C)-D-glucose incorporation into acid-insoluble cell wall fraction expressed per root.

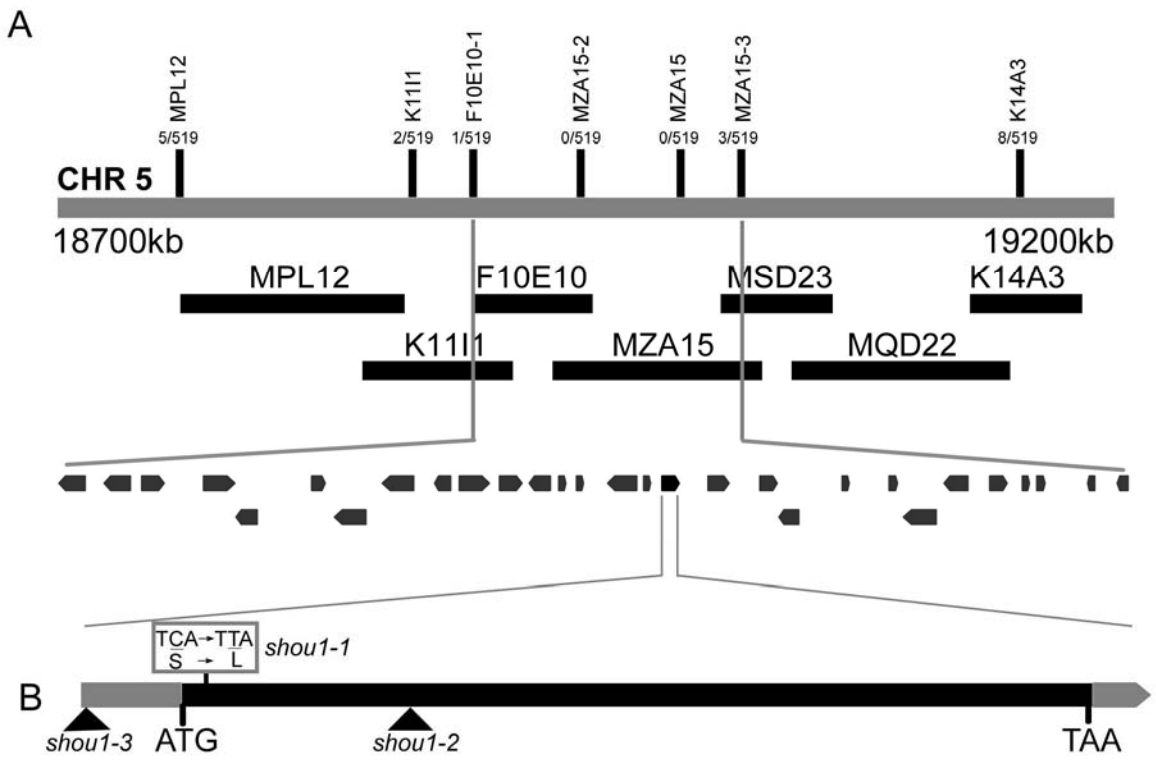

Figure 3.3. Positional cloning of the *SHOU1* Gene.

(A) *SHOU1* is located on the low arm of chromosome 5. The SSLP and DCAPS markers for fine genetic mapping and the number of recombinant from 519 suppressors for the respective markers are indicated on the top. The contigs and putative genes were assembled based on information in the Arabidopsis database (http://www.arabidopsis.org). **(B)** *SHOU1* is an intronless gene. The *shou1-1* mutation is indicated. *shou1-2* and *shou1-3* T-DNA insertion are indicated.

Figure 3.4. Complementation of *SHOU1* restore *fei1fei2* root phenotype.

T1 transgenetic *shou1fei1fei2* plants harboring wild-type genomic SHOU1 was selected on MS media plates containing 0% sucrose with kanamycin and hygromycin for 5 days and then transferred to 4.5% sucrose MS plates. Wild-type, *fei1fei2*, *fei1fei2shou1-1* were grown on MS plates containing 0% sucrose plates and then transferred to the same 4.5% sucrose MS plates. Pictures were taken 4 days after transfer.

Figure 3.5. Structure of SHOU1.

Comparison of structure of the predicted SHOU1 to other PPR proteins.

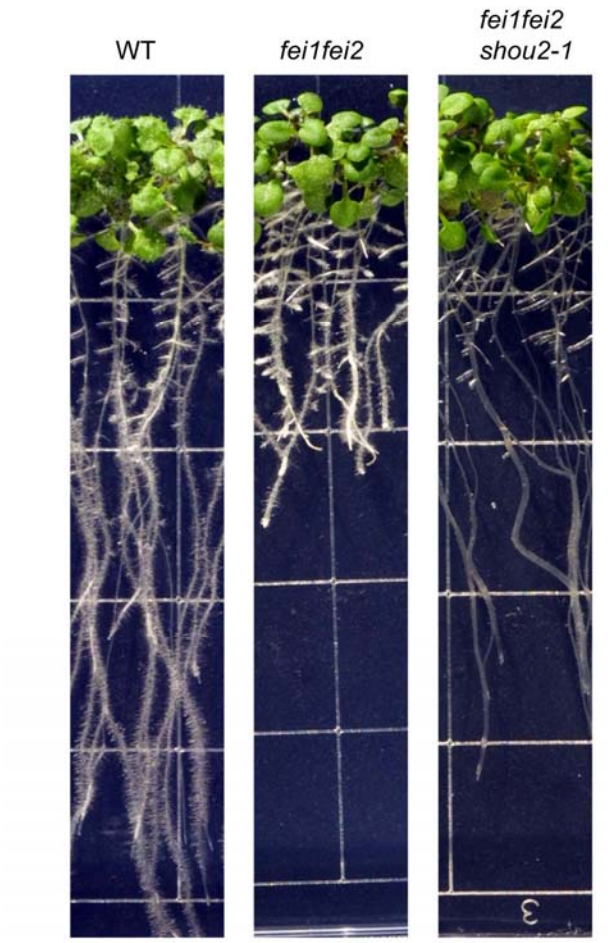

Figure 3.6. Identification of the *shou2-1* as a suppressor of *fei1fei2*.

Seedlings of wild-type, *fei1fei2-1* and *shou2-1* grown on MS plates with 4.5% sucrose for 10 days.

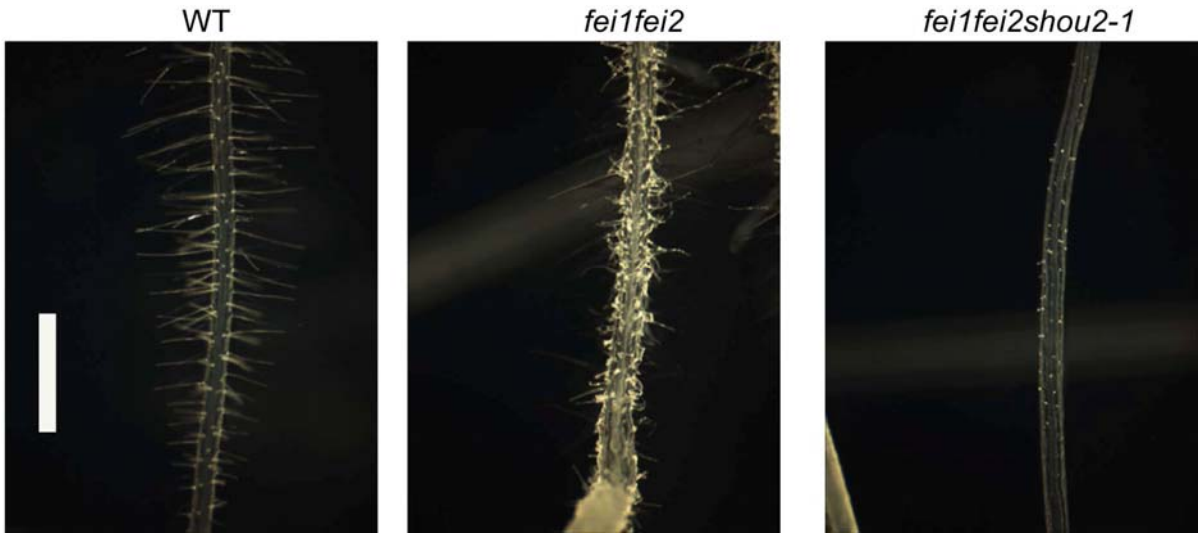

Figure 3.7. *fei1fei2 shou2-1* has root hair defects.

Pictures of root hair in elongation zone of wild-type, *fei1fei2* and *fei1fei2shou2-1*. Seedlings were grown on MS plates with 0% sucrose for 4 days and transfer to MS plates with 4.5% sucrose for 5 days. Scale bar=1mm.

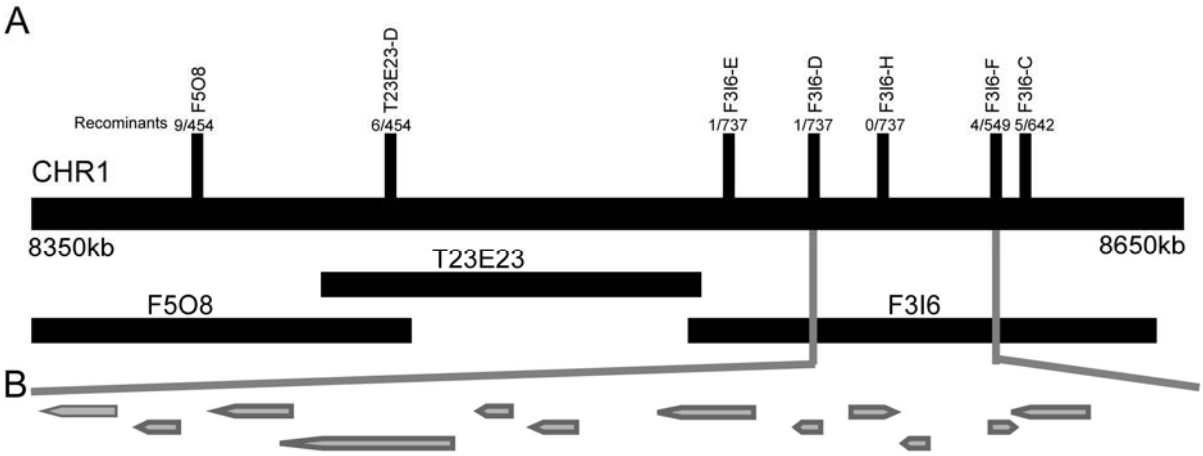

Figure 3.8. Map-based cloning of *SHOU2*.

(A). Genetic map of the *SHOU2* region with positions of linked markers above the line. *SHOU2* was mapped to the upper arm of chromosome 1. The fraction of recombinant plant detected in the mapping population is indicated. **(B).** Candidate genes identified in the sequenced region delimited by the closest linked recombinant events.

Table S3.1: Primers utilized in *shou1* mapping

Marker	Chr	Position	Col.	Ler	primers	Restriction Enzyme
MPL12	5	18.758	319	-26	GTCCCCAAAACCAATCATAAG TCCGAGTGAGAAGAGAGTTTG	
K11I1	5	18.868	175	-17	GAAACACAAAGACCCCGAAA TTGACTTAATCACGGCCACA	
F10E10-1	5	18.897	545	130+415	CCTGATTCCGGATCGTAGAA CGGTCTAGGCATTGGGATAA	CAPS: Bgl II
MZA15-2	5	18.948	531	265+265	AGAAACAGAGAAGGCCGGTT AACAAGGGAGATGGACGAAA	CAPS: Dde I
MZA15	5	18.995	258	-11	CCAAAGCTCGTAAGGAGCAC ATGGAAACGTTTTGTCGTCC	
MZA15-3	5	19.006	285	190+95	TCCATTGGTCCACCGTATTT TGAGAGGTCAAATGGAAGGG	CAPS: Dde I
K14A3	5	19.156	182	-18	AACTCATGCAATGCGACATC CCCGTCCATGATCTGTTTCT	

Table S3.2. Primers used in *SHOU2* mapping.

Marker	Chr.	Position	Col.	Ler	Primers	Restriction Enzyme
					CTTGCAAACTATTGGTTGCTCT	
F28C11	1	8.304	177	-26	CATATTTTCGTCTGATCTTTGCC	
					CCAGTTGTTCAGGAAATGGAA	
F5O8	1	8.392	145+251	396	TGACGAATGTATTGCAACCG	
					GTGATCTTGCGCCAGAAGTA	CAPS:
T23E23D	1	8.442	537	346+191	CAACCTGATTGTCTGCCTCA	Bsp1286I
					CCGAACCAACCTTGAATTTG	
F3I6-E	1	8.530	320	134+186	TTGGTGTGCCGATAAAAACA	
					TGCCATGTCGTAAATTCCTG	CAPS:
F3I6-D	1	8.552	215+35+23	250+22	GCAGAATAAGCCATCGTGGT	MseI
					TTCAGTTCACGATTAAAATTGCAAT	dCAPS:
F3I6H	1	8.570	173	-20	TCTTCTCAGCTGTTTCGTCG	BsrDI
					GGGACCTCGTTACCCAAAAT	CAPS:
F3I6F	1	8.599	524	195+329	GCTTCAACACTCCTCCAAATC	BsrDI
					TTGTCGAAGGGACAGTGTTG	
F3I6-C	1	8.607	197	-15	GTGGTCTGCTCTCAGCCTCT	
					TGCTCAATTGCTCATAATGAAA	
T24P13	1	9.203	330	-49	AGTTGCGTACTTGGAATGGG	

Chapter 4

Conclusions and future experiments

Much progress has been made in our understanding of the biosynthesis of the plant cell wall last 20 years. In 1980, Mueller and Brown discovered hexameric rosette structures (terminal complexes) of approximately 25-30 nm in diameter by freeze fracture analysis of corn and mung bean plasma membranes (Mueller and Brown, 1980). Subsequently, using a cellulose synthase antibody, these rosette structures were demonstrated to contain cellulose synthase (Kimura et al., 1999). Biochemistry studies on cellulose synthase resulted in little success: plant cellulose synthases are recalcitrant to purify because they are large (~1000 amino-acid) and membrane localized (eight transmembrane domains); and cellulose synthase activity is also very difficult to measure in extracts from higher plants. A major breakthrough came with cloning and characterization of Arabidopsis mutants with a swollen root phenotype, especially the mutant *rsw1*. Compelling evidence that CESA1 was indeed in the cellulose synthase rosette came from studies of a temperature sensitive allele of *rsw1*(*cesa1*), in which it was found that the rosette structure dissociated into individual lobes in non permissive condition (Arioli et al., 1998). Subsequently, other mutants were isolated and characterized based on embryo lethality, swelling of the root, hypocotyl or embryo, altered vascular structure, or altered responses to inhibitors of cellulose biosynthesis or microtubules (Somerville, 2006; Taylor, 2008).

A combination of expression analysis, genetic studies, and co-immunoprecipation experiments has defined roles for the various *CESA* genes. CESA1, CESA3 and CESA6 interact with each other to form a class of rosettes that function in primary cell wall biosythesis. CESA4, CESA7 and CESA8 comprise distinct rosettes that function in

secondary cell wall biosynthesis (Desprez et al., 2007; Persson et al., 2007; Persson et al., 2005). Other mutants with reduced cellulose biosynthesis were characterized and identified a number of elements that play important roles in regulating cellulose biosynthesis, including KORRIGAN, COBRA, and KOBITO. However, the mechanisms by which these proteins act in cell wall biosynthesis is unclear (Somerville, 2006; Taylor, 2008).

My graduate work focused mainly on two receptor-like kinases FEI1 and FEI2, which were originally identified by our lab as interactors with ACC synthase. Single and double mutants of *fei1* and *fei2* were made, and the double mutants were found to display short roots and a swollen root tip phenotype on high sucrose MS media, with the most prominent expansion in epidermal cells. This phenotype is reminiscent of that of weak cellulose-deficient mutants such as *cellulose synthase 6* (*prc1*), *cobra* and *sos5*. The *fei1 fei2* mutant was more sensitive to the cellulose biosynthesis inhibitor isoxaben, similar to *prc1*. Consistent with this, cellulose biosynthesis was significantly reduced in the *fei1 fei2* double mutant. In addition, *fei1 fei2* displayed an additive phenotype with *cob* and *prc1*, but not with *sos5*, indicating FEI1 /FEI2 may act in the same pathway as SOS5, but in a different pathway from COB and PRC1. In conclusion, we have begun to discern the function of two receptor-like kinases, *FEI1* and *FEI2,* involved in cellulose biosynthesis and have connected FEIs to ACC and/or ethylene biosynthesis. This raises many interesting questions that remain to be addressed.

Are there other receptor kinase/ or kinase redundant with FEI1 and FEI2 in regulating cell wall biosynthesis?

The *fei1 fei2* mutant displays a conditional phenotype. Even in non-permissive condition, the phenotype of the *fei1 fei2* mutant phenotype is relatively weak as compared to other conditional mutants, such as *cob-1* and *prc1*. While weak *cob* alleles affect only the root, a null mutant of *cob* displays striking defects in anisotropic expansion in many developing organs, including roots, hypocotyls, cotyledons and leaves. The only phenotype of *fei1 fei2* in the shoot is slightly thicker hypocotyls in etiolated seedlings. Combination *fei1 fei2* with a weak *cob* allele reveals a role for the FEI genes in floral development. Thus, FEI1 and FEI2 act primarily in the root and their phenotype is weaker than other cellulose deficient mutants, suggesting that the *fei1 fei2* mutants only partially disrupt cellulose biosynthesis.

It is possible that FEI1 and FEI2 interact with other receptor-like kinases to regulate cell wall biosynthesis, and combining loss of function mutations in these other RLKs with *fei1 fei2* could result in an enhanced phenotype. The observation that a FEI1 kinase-inactive protein still complements the *fei1 fei2* phenotype suggests that the FEIs might indeed heterodimerize with a 2nd RLK that transphosphates FEI1. Using a yeast two-hybrid screen, we identified a distinct RLK that interacts with the FEIs. This receptor kinase has a highly similar paralog in Arabidopsis. We have obtained loss-of-function alleles of these kinases and are currently examining the genetic interactions among these genes. A second approach to identify genes that act redundantly with the FEIs is to use an enhancer screen. To this end, I have made a T-DNA activation tagging population of *fei1fei2*. This represents a useful tool for future analysis.

FEI1/FEI2 downstream factors or parallel pathway

To isolate components of FEI/FEI2 mediated pathway in cellulose biosynthesis, I performed a suppressor assay. The suppressor screening to isolate *fei1 fei2* suppressors will predicted to yield four types of mutants: 1) mutants in restoring cellulose biosynthesis. This is the class in which *shou1* falls. 2) mutations in a parallel pathway that might compensate for the FEI1/ FEI2 defect; 3) mutations in the cell wall signaling pathway in response to perturbations in cell wall biosynthesis such as Theuseus1; 4) Mutations in a putative ACC signaling pathway.

The weak phenotype of *fei1 fei2* makes it a good candidate for a suppressor screen to isolate components in FEI1/FEI2 pathway. I performed the suppressor screen and identified nine extragenetic suppressors that belong to eight complementation groups, *shou1-shou8*. Previously, a suppressor screen using *prc1* mutant identified *theseus1* (*the1*) (Hématy et al., 2007). The *the1* mutation suppresses *prc1* and other cellulose-deficient mutants, but does not restore cellulose biosynthesis in *prc1*. Unlike *the1*, the cellulose biosynthesis is partially restored in the *shou1 fei1 fei2* mutant. It will be interesting to explore exactly how *SHOU1* functions in the *fei1 fei2* mutants to restore cellulose biosynthesis.

Some SHOU suppressors might act as sensors of cell wall defects, similar to *the1*. *the1* has been shown to partially restore hypocotyl elongation in *prc1 the1*. However, *the1* does not restore root elongation in *prc1 the1*, even though *THE1* is expressed in the root and inhibits the lignin accumulation in *prc1 the1*. This suggests either lignin accumulation and growth inhibition define distinct pathways in the response of roots, or that *THE1* acts redundantly with other receptor kinases in the root. Alternately, *THE1* might not be involved in growth inhibition in response to cell wall defects in the root, but rather there is a distinct RLK in the root that senses the cell wall integrity. Cloning and characterization of the *SHOU*

mutants should help elucidate how cellulose biosynthesis is regulated and how plants respond to cell wall defects.

In addition, I have also isolated the *shou2* mutant which suppresses *fei1 fei2* anisotropic growth defects. This *shou2* mutation also suppresses root hair elongation. So far, there are only several mutants that are defective in root hair elongation and none of them maps to the position of *shou2*. It will be very interesting to identify and characterize *SHOU2*, as it is involved in both diffuse and tip growth.

Conclusion

Despite many years of research on cell wall biosynthesis, the mechanisms and components in involved in this process still remain largely unknown. Using genetic screening, we are isolating components that are involved in cellulose biosynthesis and are attempting to identify genes involved in cell wall signaling pathway. Our research will contribute to the understanding of these processes.

Reference

Arioli, T., Peng, L., Betzner, A., Burn, J., Wittke, W., Herth, W., Camilleri, C., Höfte, H., Plazinski, J., Birch, R., *et al.* (1998). Molecular analysis of cellulose biosynthesis in Arabidopsis. Science **279**, 717-720.

Desprez, T., Juraniec, M., Crowell, E., Jouy, H., Pochylova, Z., Parcy, F., Höfte, H., Gonneau, M., and Vernhettes, S. (2007). Organization of cellulose synthase complexes involved in primary cell wall synthesis in Arabidopsis thaliana. Proc Natl Acad Sci U S A **104**, 15572-15577.

Hématy, K., Sado, P.-E., Van Tuinen, A., Rochange, S., Desnos, T., Balzergue, S., Pelletier, S., Renou, J.-P., and Höfte, H. (2007). A receptor-like kinase mediates the response of Arabidopsis cells to the inhibition of cellulose synthesis. Curr Biol **17**, 922-931.

Kimura, S., Laosinchai, W., Itoh, T., Cui, X., Linder, C., and Brown, R. J. (1999). Plant Cell. Immunogold labeling of rosette terminal cellulose-synthesizing complexes in the vascular plant vigna angularis **11**, 2075-2086.

Mueller, S., and Brown, R. J. (1980). Evidence for an intramembranous component associated with a cellulose microfibril synthesizing complex in higher plants. J Cell Biol **84**, 315-326.

Persson, S., Paredez, A., Carroll, A., Palsdottir, H., Doblin, M., Poindexter, P., Khitrov, N., Auer, M., and Somerville, C. (2007). Genetic evidence for three unique components in primary cell-wall cellulose synthase complexes in Arabidopsis. Proc Natl Acad Sci U S A **104**, 15566-15571.

Persson, S., Wei, H., Milne, J., Page, G., and Somerville, C. (2005). Identification of genes required for cellulose synthesis by regression analysis of public microarray data sets. Proc Natl Acad Sci U S A **102**, 8633-8638.

Somerville, C. (2006). Cellulose synthesis in higher plants. Annu Rev Cell Dev Biol **22**, 53-78.

Taylor, N. G. (2008). Cellulose biosynthesis and deposition in higher plants. New Phytol **178**, 239-252.